

5-3-2008

Design and Construction of a Liquid-Cooled Solid-State Digital Television Transmitter

Geoffrey Ewald Carter

Follow this and additional works at: <https://scholarsjunction.msstate.edu/td>

Recommended Citation

Carter, Geoffrey Ewald, "Design and Construction of a Liquid-Cooled Solid-State Digital Television Transmitter" (2008). *Theses and Dissertations*. 1291.
<https://scholarsjunction.msstate.edu/td/1291>

This Graduate Thesis - Open Access is brought to you for free and open access by the Theses and Dissertations at Scholars Junction. It has been accepted for inclusion in Theses and Dissertations by an authorized administrator of Scholars Junction. For more information, please contact scholcomm@msstate.libanswers.com.

DESIGN AND CONSTRUCTION OF A LIQUID-COOLED
SOLID-STATE DIGITAL TELEVISION TRANSMITTER

By

Geoffrey Ewald Carter

A Thesis
Submitted to the Faculty of
Mississippi State University
In Partial Fulfillment of the Requirements
For the Degree of Master of Science
in Engineering
in the Department of Electrical and Computer Engineering

Mississippi State, Mississippi

May 2008

Copyright by
Geoffrey Ewald Carter
2008

DESIGN AND CONSTRUCTION OF A LIQUID-COOLED
SOLID-STATE DIGITAL TELEVISION TRANSMITTER

By

Geoffrey Ewald Carter

Approved:

J. Patrick Donohoe
Professor of Electrical and
Computer Engineering
(Director of Thesis)

W. Glenn Steele
Acting Dean of the Bagley College
of Engineering

Nicholas Younan
Professor of Electrical and
Computer Engineering
(Graduate Program Director and
Committee Member)

Erdem Topsakal
Assistant Professor of Electrical
and Computer Engineering
(Committee Member)

Name: Geoffrey Ewald Carter

Date of Degree: 2 May, 2008

Institution: Mississippi State University

Major Field: Electrical Engineering

Major Professor: J. Patrick Donohoe

Title of Study: DESIGN AND CONSTRUCTION OF A LIQUID-COOLED
 SOLID-STATE DIGITAL TELEVISION TRANSMITTER

Pages in Study: 158

Candidate for Degree of Master of Science

With the advent of terrestrial digital broadcasting, new and improved digital transmitter technologies are required since existing analog transmitter technology is, for the most part, unable to adequately transmit a decodable digital television signal. This study focuses on the design and construction of a solid-state, liquid-cooled UHF digital television transmitter. Emphasis is placed on the design of the amplifier module including the amplifier card, Wilkinson splitter and combiner, input and output matching circuits, DC bias network and the system mask filter. The results of this research are also presented for two television transmitters that are installed and continue to be in use today, including analyses of specific failures that have occurred while in the field.

The overall objective of this study is to document the research that is behind the design of this system and to document the construction of the transmitter for reference as a basis for future designs.

Key words: transmitter, Wilkinson combiner, amplifier, solid-state, DTV, digital, television, liquid-cooled

DEDICATION

I wish to dedicate this work to my family. To my wife and children, Jeri, Jonathan, Austin, Brooks and Bremen, for their patience and unending support. To my mother and grandmother, Gisa and Margarete, for raising me to have the strength and courage to tackle a project of this magnitude. To my sister Margot, for allowing me to disassemble all her toys to figure out how they worked, and for not getting mad when I reassembled them with a small number of leftover parts. To my grandfather Ewald Kothe, for without his wisdom and steady hand I would not be the engineer that I am today.

ACKNOWLEDGEMENTS

The author wishes to express his sincere gratitude to the many people for whom without their selfless assistance this work would not be possible. First, sincere thanks are due Dr. J. Patrick Donohoe for his time, effort and support in the writing of this thesis, his guidance in the thesis program, and his willingness to help me complete my degree via email and the internet. Thanks are also due the other members of my thesis committee, Dr. Nick Younan and Dr. Erdem Topsakal for the guidance and aid provided by them. Finally the author wishes to thank Mr. Frank K. Spain for his guidance and financial support that made this project and thesis possible.

TABLE OF CONTENTS

DEDICATION		ii
ACKNOWLEDGEMENTS		iii
LIST OF TABLES		vi
LIST OF FIGURES		vii
CHAPTER		
I. INTRODUCTION		1
II. REVIEW OF THE LITERATURE		4
ATSC Digital Television Transmission Standard		4
Six dB Power Ratio		5
Signal Distortion		6
III. DEVELOPMENT OF THE SYSTEM HARDWARE		10
Modulator		11
Amplifier Card		13
Wilkinson Combiner and Splitter		45
Cold Plate		55
Intermediate Power Amplifier		59
Power Amplifier		61
Mask Filter		63
Cooling System		84
Control System		88
AC and DC Power Distribution		96
IV. TRANSMITTER PERFORMANCE EVALUATION		100
Power Measurement		101
Peak-to-Average Ratio		104
8VSB Constellation		105
Signal-to-Noise Ratio and Modulus Error Ratio		110

Error Vector Magnitude.....	111
Transmitter Measurements	111
Modulator	112
Intermediate Power Amplifier	114
Power Amplifier	116
Overdriven Power Amplifier	119
System Performance of WLOV and KTFL	121
V. CONCLUSIONS AND RECOMMENDATIONS	124
REFERENCES	127
APPENDIX	
A. MSMRF INC. UHF-4DTV TRANSMITTER BILL OF MATERIALS	131
B. MOTOROLA PRF-377 (MRF-377) DATA SHEET	141
C. K-TECH TELECOMMUNICATIONS VSB-ENC-200 DATA SHEET	149
D. MINICIRCUITS ZHL-3010 DATA SHEET	151
E. ARTICHILL REFRIGERATED LIQUID CHILLER DATA SHEET ..	153
F. ANAREN 3A325 BALUN DATA SHEET	156

LIST OF TABLES

3.1	Source and Load Impedance of the PRF377 Transistor	16
3.2	Amplifier Card Microstrip Line Requirements.....	17
3.3	Calculated Microstrip Line Widths and Lengths	23
3.4	Element Values for 0.01dB Ripple Tchebyscheff Filter.....	70
3.5	Calculated Values for End-Coupled Cavity Irises	74
3.6	Calculated Values for Side-Coupled Cavity Irises	75
3.7	PLC Slot Assignments	90
4.1	Map of 8VSB Constellation Points [45].....	106

LIST OF FIGURES

3.1	Transmitter System Block Diagram.....	11
3.2	K-Tech 8VSB Modulator Block Diagram	13
3.3	Measured S-Parameter Data for the 3A325 Balun	15
3.4	Broadband Input Matching Network Simulation Results.....	17
3.5	Broadband Input Matching Network Design.....	18
3.6	25 Ω , 22 Ω , 14.5 Ω and 12.5 Ω Microstrip Line Widths on 0.762mm Substrate	19
3.7	Input Matching Network Microstrip Layout.....	24
3.8	Simulation Results for the Narrowband Input Matching Network.....	26
3.9	Channel 16 Narrowband Input Matching Network Design	26
3.10	M21 Data for the Broadband Input Match Over the UHF DTV Band.....	28
3.11	SWR Data for the Broadband Input Match Over the UHF DTV Band.....	28
3.12	M21 Data for the Broadband Input Match for Channel 16.....	29
3.13	SWR Data for the Broadband Input Match for Channel 16.....	29
3.14	Simulated vs. Measured M21 Data for the Narrowband Input Match.....	30
3.15	Simulated vs. Measured SWR Data for the Narrowband Input Match.....	30
3.16	Output Matching Network Microstrip Layout.....	31
3.17	Simulation Results for the Broadband Output Matching Network.....	32
3.18	Broadband Output Matching Network Design	32

3.19	Simulation Results for the Narrowband Output Matching Network	34
3.20	Channel 16 Narrowband Output Matching Network Design	34
3.21	M21 Data for the Broadband Output Match Over the UHF DTV Band	36
3.22	SWR Data for the Broadband Output Match Over the UHF DTV Band	36
3.23	M21 Data for the Broadband Output Match for Channel 16	37
3.24	SWR Data for the Broadband Output Match for Channel 16	37
3.25	Simulated vs. Measured M21 Data for the Narrowband Output Match	38
3.26	Simulated vs. Measured SWR Data for the Narrowband Output Match	38
3.27	Amplifier Bias Filter Network	41
3.28	Simulation Results for the Input Bias Filter Network	42
3.29	Complete Amplifier Gate Bias Supply	43
3.30	Complete Amplifier Card Block Diagram	44
3.31	Microstrip Implementation of a Wilkinson Splitter / Combiner	45
3.32	70.7 Ω and 50 Ω Line Widths on a 1.524mm Rogers RT/duroid 6002 Substrate	47
3.33	Microstrip Layout for the Channel 16 Splitter Card	50
3.34	Microstrip Layout for the Channel 16 Input / Combiner Card	51
3.35	Wilkinson Splitter Combiner Test Setup	52
3.36	Wilkinson Splitter and Combiner Test over the Entire DTV Band	53
3.37	Wilkinson Splitter and Combiner Test over Channel 20	54
3.38	Mitered Corner for the Microstrip Splitter and Combiner	55
3.39	Amplifier Cold Plate Mechanical Design	57
3.40	Intermediate Power Amplifier RF Block Diagram	60

3.41	Power Amplifier RF Block Diagram	62
3.42	Final Amplifier Assembly with Power Distribution Card Removed.....	62
3.43	Complete Power Amplifier Module.....	63
3.44	FCC DTV Emission Mask	64
3.45	Graphical Comparison of 0.01 dB Ripple Tchebyscheff Filter Characteristics	66
3.46	Assembly Diagram of the Folded Waveguide Filter	68
3.47	Location of d_1 and d_2 on the Coupling Iris	71
3.48	Shop Drawing for the Mask Filter Panels Qe(a) and Qe(b).....	72
3.49	Partially Assembled Filter Cavity.....	73
3.50	Shop Drawing for the Inter-Cavity Filter Panels K12, K23, K34, K45, K56, K78 and K89	76
3.51	Results of the Initial Tuning for the Folded Waveguide Filter.....	77
3.52	Final Tuning Results for the Channel 16 Mask Filter.....	78
3.53	Folded Waveguide Filter Front during Assembly	79
3.54	Folded Waveguide Filter Rear during Assembly.....	80
3.55	Complete Folded Waveguide Filter	81
3.56	Coax-to-Waveguide Transition.....	83
3.57	Refrigerated Chiller Installed at KTFL-TV in Flagstaff, Arizona.....	85
3.58	Cooling System Schematic	87
3.59	Control System Block Diagram.....	92
3.60	Transmitter Control System Operator Menu	95
3.61	AC and DC Power Distribution	99

4.1	<i>Kt</i> for Ethylene-Glycol/Water Mixtures vs. Temperature [39].....	102
4.2	Flowmeter Correction Factor for Fluid Temperature and Density [40]	103
4.3	Typical Distribution of Peak Power for 8VSB Transmission [41].....	104
4.4	I-Q Diagram for an 8VSB Signal.....	105
4.5	Ideal 8VSB Constellation Diagram [46].....	107
4.6	8VSB Constellation Diagram with Noise Effects [47].....	108
4.7	8VSB Constellation Diagram with Clipping Effects or AM/AM Conversion Error [48].....	109
4.8	8VSB Constellation Diagram with Phase Effects or AM/PM Conversion Error [49].....	110
4.9	Transmitter System Test Setup	112
4.10	8VSB Constellation Diagram of the Transmitter Measured at the Output of the Modulator with the Transmitter Operating at 400 Watts with One Amplifier Module and I_{DQ} set to 1.8A.....	113
4.11	8VSB Constellation Diagram of the Transmitter Measured at the Output of the Intermediate Power Amplifier with the Transmitter Operating at 400 Watts with One Amplifier Module and I_{DQ} set to 1.8A.....	115
4.12	8VSB Constellation Diagram of the Transmitter Measured at the Output of the Driver Card on The Power Amplifier with the Transmitter Operating at 400 Watts with One Amplifier Module and I_{DQ} set to 1.8A.....	116
4.13	8VSB Constellation Diagram of the Transmitter Measured at the Output of the Power Amplifier with the Transmitter Operating at 400 Watts with One Amplifier Module and I_{DQ} set to 1.8A.....	117
4.14	Cumulative Distribution of Peak Power Measured at the Output of the Power Amplifier with the Transmitter Operating at 400 Watts with One Amplifier Module and I_{DQ} set to 1.8A.....	118

4.15	8VSB Constellation Diagram of the Transmitter Measured at the Output of the Power Amplifier with the Transmitter Operating at 450 Watts with One Amplifier Module and I_{DQ} set to 1.8A.....	119
4.16	Cumulative Distribution of Peak Power Measured at the Output of the Power Amplifier with the Transmitter Operating at 450 Watts with One Amplifier Module and I_{DQ} set to 1.8A.....	120
4.17	UHF-4DTV Transmitter Installed for WLOV Television in West Point, Mississippi.....	122
4.18	UHF-4DTV Transmitter Installed for KTFL Television in Flagstaff, Arizona.....	122
5.1	Eight-Way Gysel Combiner Layout for High-Power Combiner	126

CHAPTER I

INTRODUCTION

With a United States Congressional mandate, the Federal Communications Commission (“FCC”) has required all United States full power television stations transmit an 8VSB digital signal at full authorized power by June 2006. The reason for adopting a new transmission standard is twofold, giving the consumer access to a much higher quality picture with a clearer signal, higher resolution images and bolder colors while allowing for a revised bandplan, reducing the number of over the air broadcast channels available from 82 to 50 (channels 2 through 51), but allowing multiple data streams per channel, with the possibility of four or more standard definition video streams per channel. The Advanced Television Systems Committee (“ATSC”) has recommended standard practices that are required and enforced by the FCC, encompassing all technical specifications for digital television transmission including the 8VSB standard, the method by which has been developed and patented by Zenith Corporation. The new digital transmission standards require that all stations upgrade their studio facilities and build new transmission plants, including the Studio-To-Transmitter microwave link, transmitter, transmission line and antenna.

The core of the new digital transmission facility is the transmitter itself which requires a complete redesign of fifty year old technology. It would have been desirable for the broadcaster to convert his existing transmitter to digital operation, but this proved to be impractical for two reasons. First, the older transmitters, although linear enough to carry the approximately 4.5 MHz of video bandwidth required for analog operation with linearity correction, were not linear enough to properly handle the full 6 MHz bandwidth required for 8VSB transmission. Second, the broadcaster is required to operate both digital and analog operation for several years, and converting a transmitter over to digital operation would preclude the operation on analog.

A new reliable digital television transmitter is required to fill the need of the broadcaster during the transition period. This transmitter should be capable of cost effective low power operation as well as expansion to full power operation at the end of the transition period. The UHF-4DTV transmitter was specifically designed for this purpose. With versatility in mind, the transmitter was designed with a modular approach so amplifier trays could be added or removed to meet the customer's power requirements, or so that multi-tray systems could have one or more of the amplifier trays removed for servicing without completely shutting the transmitter down.

All work on this transmitter system was performed at and funded by Microwave Service Manufacturing, Incorporated, a spinoff company from Microwave Service Company of Mississippi. Microwave Service Company was formed approximately fifty years before this writing. Their mission was to design, manufacture and maintain microwave equipment for the broadcast and telephone industries with a wide range of

products in the six and seven gigahertz bands. With the advent of the terrestrial digital broadcast conversion, Microwave Service Manufacturing, Inc. (MSM, Inc.) was formed with the sole vision to build low, medium and high power digital broadcast transmitters, with its most popular and versatile system, the UFH-4DTV four kilowatt, solid-state, liquid-cooled digital television transmitter.

This thesis is focused on the design and construction of a liquid-cooled solid-state digital transmitter. The requirements for 8VSB digital transmitters are discussed in Chapter 2. A discussion of the development of the hardware used in the water cooled digital transmitter is presented in Chapter 3. Transmitter performance is outlined and discussed in Chapter 4. The work encompassed by this thesis is summarized and further research recommendations are reviewed in Chapter 5.

CHAPTER II

REVIEW OF THE LITERATURE

This chapter presents an overview of the new standards by which all television broadcast transmitters must adhere to be in compliance with Federal Communications Commission regulations.

ATSC Digital Television Transmission Standard

At the time of this writing, the Advanced Television Systems Committee (ATSC) standard for digital television, designated A/53, had been adopted by Canada, South Korea, Taiwan, Argentina and the United States Federal Communications Commission [1]. This standard is the result of many years of work by leading government and industry experts and is intended to be the defacto standard for terrestrial television broadcasting for many years to come. The A/53 standard describes system operating protocol and characteristics and their subsystems required for originating, encoding, transmitting, receiving and decoding of video by terrestrial broadcast systems. This system is intended to replace the National Television Standards Committee (NTSC) analog transmission standards with the new ATSC transmission standard while maintaining the 6 MHz channel allocation system currently in use in the United States.

The ATSC A/53 standard specifies a system to transmit digital video, digital audio and data of various data rates through a system at 19.39 megabits per second(Mb/s). The standard does not mandate at what data rates the individual components be encoded, but does require that the sum of all components with payload and overhead be 19.39 Mb/s. This flexibility allows the broadcaster to make his own decision as to the quality of video to be transmitted, if at all. At the time of this writing, the FCC requires that all existing television broadcasters use their primary stream to co-transmit their current analog programming, but the quality of this signal is yet undefined and could be in either standard definition or high definition, with a variety of encoding rates for each. This gives the broadcaster the option to use most of his allotted bandwidth for a high definition video program, or the same bandwidth for four standard definition programs, or using the same bandwidth for a single standard definition video program and a high speed data channel.

Six dB Power Ratio

In digital communication systems like the 8VSB ATSC system, the signal is random and noise-like, therefore digital systems have a well defined average power, but a statistically defined peak envelope power. It is well documented [2] that the average power of an 8VSB system will be 6.5 dB below the peak power 99.9% of the time. This 6.5 dB peak-to-average power ratio is critical in all aspects of transmission system performance. The amplifiers in an 8VSB transmitter must be rated to operate four times the measured average power; therefore, a transistor rated for an FM power level of 250

watts is only capable of operating at 56 watts for ATSC television. The entire transmitter system must be designed to operate at four times the actual average output power because at any moment the instantaneous power may be four times the average power and all the system components must be capable of handling the peak power. If an attempt is made to operate an amplifier without 6.5 dB of peak-to-average headroom, a seriously degraded signal will occur, resulting in possibly a total loss of picture at the receiver. It is critical that all components are able to be operated linearly up to the peak power levels of the transmitter.

Signal Distortion

There are two major interrelated sources of non-linear distortion in a wide-band digital transmitter system: over-driving the amplifier into the non-linear region of operation and intermodulation distortion. Both of these can be the cause or result of the other and both can have serious implications on the quality of the transmitter signal. Intermodulation distortion (IMD) occurs when mixing of various signals within the amplifier occurs producing unwanted signals both in and outside the band or channel edge. Excessive IMD can consume more power than the wanted signals within a band which results in a serious drop in the transmitter signal-to-noise ratio [3]. A signal-to-noise ratio of 27 dB is absolute minimum [4] for a transmitted signal for broadcast DTV. For every 0.25 below the 27 dB SNR threshold, there will be a corresponding ¼ mile reduction in the coverage area from the transmission point [5], even though there will be no reduction in transmitted power.

IMD can also be emphasized when an amplifier is operated beyond the non-linear region. In this case, the fundamentals will be compressed or limited but there is still room for spectral growth from the IMD products. This condition will not only cause a serious reduction of the signal-to-noise ratio, but will also drastically increase the symbol error rate since the peak signals are being compressed into erroneous data. An 8VSB digital amplifier operating at the 1 dB compression point will clip considerably and AM/PM conversion will become uncorrectable [6].

Intermodulation distortion produced in a solid-state amplifier is measured as IP₃, or the third-order intercept point. This is the point at which the third order IMD products would intercept and then overtake the fundamentals in output power [7]. This point is usually beyond the saturation point of the transistor and cannot be practically realized, but makes an excellent benchmark for the operation of an amplifier. It has been shown that the ratio of the slope of the IP₃ power to the fundamental power is at least 2:1 [8] for a class A amplifier. In this design a class AB amplifier is used to achieve greater efficiency, but IMD products of much higher orders with greater slopes can greatly reduce the performance of a class AB amplifier over the more linear class A amplifier [9]. Class A amplifiers can only achieve efficiencies of 10% or less, and are therefore only desirable for operation at lower power or pre-amplifier levels. Efficiencies approaching 30% or greater are achievable with a class AB amplifier while keeping the spectral regrowth at or below -30 dB [10].

The design of this transmitter is based on a solid-state balanced amplifier design that takes into consideration the linear operation of the amplifier as well as the non-linear distortions produced by the amplifier including intermodulation distortion. Without proper control of IMD, the system would operate inefficiently with a poor signal-to-noise ratio and a high symbol error rate. In addition, high IMD will cause spectral regrowth outside the channel edge, which will be wasted energy reflected back to the amplifier from the mask filter. It is of utmost importance that the design limits the system non-linearities and the intermodulation distortion while maximizing the power produced and the signal-to-noise ratio. The higher the power and better the SNR, the better the quality of signal will be at the receiver, and since this is digital television, the consumer will not be satisfied with a marginal signal. Unlike analog television, a marginal DTV signal will not produce a picture at all. In comparison, NTSC video has performance considered marginal at 34 dB above the noise floor, while an 8VSB signal would have to drop below 15 dB above the noise before any signal degradation is noticed [11].

Signal-to-noise ratio or SNR (or S/R) refers to post detection signal-to-power noise ratio and is defined as the average power of the ideal symbol values divided by the noise power, or the difference between the ideal signal and the actual signal as demodulated along the in-phase real axis [12]:

$$SNR = \frac{Power(I_{IDEAL})}{Power(I_{IDEAL} - I_{ACTUAL})} \quad (2-1)$$

The ATSC recommends that the SNR of a transmitter be at least 27 dB and is standard industry practice [13]. The higher the SNR the better the quality of the transmitter signal, and the better the coverage of the transmitter [14]. This figure was selected because with a 27 dB SNR, the receiver threshold will degrade approximately 0.25 dB. If the SNR is increased by 5 dB to 32 dB the margin increases to only 0.15 dB, but if the SNR is decreased by only 2 dB to 25 dB, the reception margin decreases to 0.45 dB [15]. Clearly, any SNR increase above 27 dB has little improvement on the transmitted signal, while SNR changes below 27 dB will rapidly degrade the signal. Therefore, 27 dB is the target operation point for 8VSB transmitters and a SNR less than 27 dB quickly becomes a marginal signal at the receiver.

CHAPTER III

DEVELOPMENT OF THE SYSTEM HARDWARE

The UHF-4DTV transmitter consists of three major subsystems, each of which can be further divided into individual components. The first major subsystem is the 8VSB modulator. The modulator accepts a SMPTE-310 transport stream input and modulates it on channel per the ATSC 8VSB standard. The modulator also has a linear and non-linear precorrection circuit and firmware that constantly monitors a feedback signal from the output transmission line. This feedback signal is analyzed to produce an error correction signal that is then combined with the original 8VSB signal to produce a corrected signal compensated for linear and non-linear errors in the amplifiers and filters.

The second subsystem is the amplifier. The amplifier consists of a computerized control and monitoring system, cooling system, power supplies and several amplifiers connected in series with increasing gain so that the combined output is up to 4 kW average power per amplifier cabinet. Most of the design work for this transmitter and the emphasis of this work is on the basic amplifier card, the intermediate power amplifier (IPA) and the final power amplifier (PA).

The last subsystem before the transmission line and the antenna is the filter system. For digital broadcast transmitters, two are required, a mask filter to limit the bandwidth prior to the harmonic filter, which eliminates the transmission on odd

multiples of frequencies above the intended channel. The mask filter is especially important during the analog-to-digital transition period during which there will be twice the number of television stations operating in the United States than were originally allocated and some channels will be operating within close proximity of the next adjacent channel. The mask filter will help to prevent overlap onto the adjacent channels and minimize interference during the transition period. The complete system block diagram is shown in Figure 3.1.

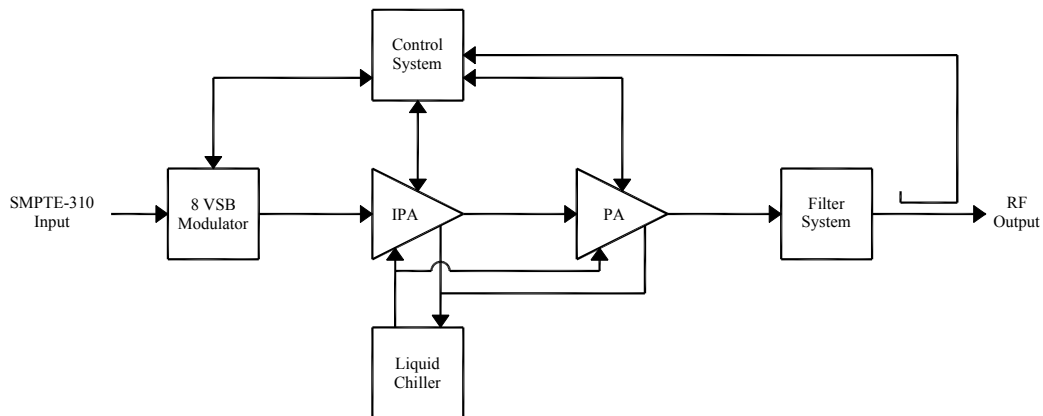


Figure 3.1 Transmitter System Block Diagram

Modulator

After a series of trials, the K-Tech Telecommunications VSB-ENC-200 8VSB Modulator was chosen as the modulator for the UHF-4DTV Transmitter. This unit was selected for a number of reasons including its versatility and ability to adapt to a wide variety of operating conditions with only soft programming changes. The K-Tech modulator was also proven to be very stable and have a faster response time than all the

competition when adapting its linear and non-linear tables to changes in the operating environment, while other units tested often took hours to adapt to these changes. MSMrf, Inc. felt it was very important for a transmitter to quickly adapt to changes in the operating environment since some changes can occur very quickly. For example, a UHF transmitting antenna installed at 1500 feet above ground level can be completely covered in ice during a winter storm, thus changing the entire system from a linear system over the channel bandwidth to a very non-linear system in just a matter of minutes requiring rapid system pre-correction in order for the viewer at home to keep the received bit error rate low enough to maintain a viewable picture.

A block diagram of the K-Tech Modulator is shown in Figure 3.2. For more information regarding the technical specifications of the K-Tech modulator, refer to Appendix C.

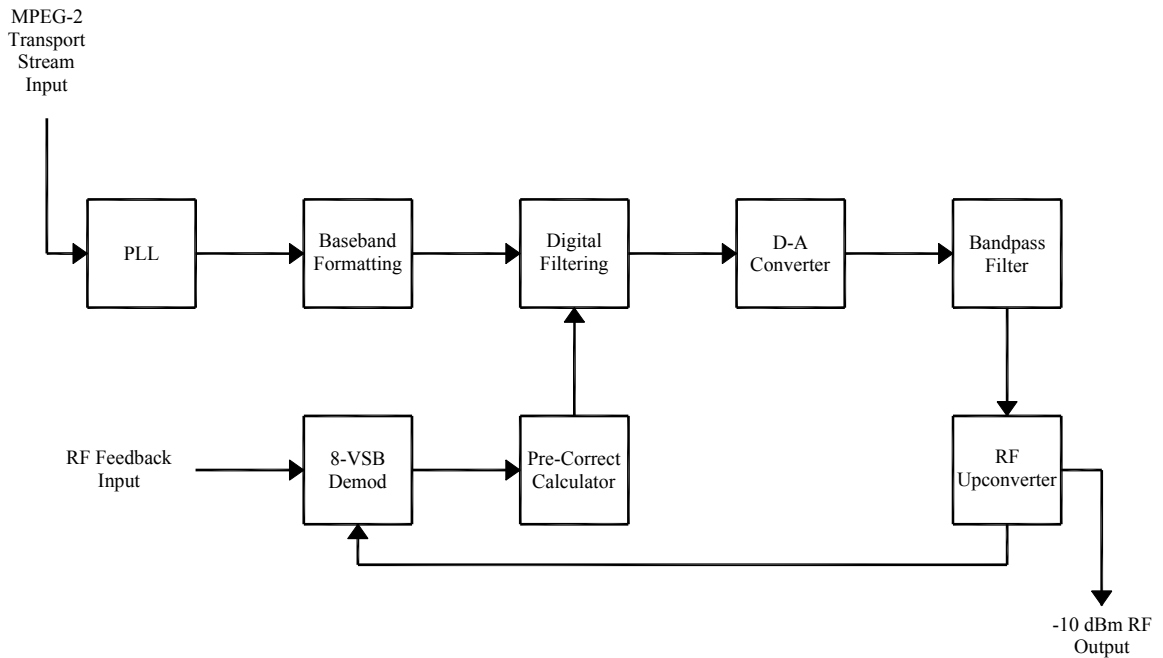


Figure 3.2 K-Tech 8VSB Modulator Block Diagram

Amplifier Card

The entire transmitter system was built around a single amplifier card that is used in both the intermediate power amplifier and the power amplifiers, and in both the preamplifiers and main amplifiers in each unit. This was done to minimize the use of different parts to minimize design, maintenance and inventory costs. After an exhaustive search, the Motorola PRF377 (MRF377) was selected as the transistor for the amplifier cards. The PRF377 was selected based on its ability to operate over the entire UHF

television band, or 470 to 860 MHz, with a very flat gain over the entire range of operation. The PRF377 has high gain with high power handling capability with low third order intercept (IP3) and is packaged in a Class AB matched transistor package. Specific details on the PRF377 can be seen in the Motorola data sheet in Appendix B.

In addition, the Anaren 3A325 balun transformer was selected to split and combine the power into and out of the transistors and provide the 180 degree phase shift between the two transistors. The 3A325 was selected based on its frequency range of operation, high power handling capability, and flat response over the UHF frequency band. The 3A325 is manufactured in a small surface mount package, making automated manufacturing of the amplifier cards feasible. Figure 3.3 shows plots of the 3A325 SWR vs. frequency along with a plot of M21 vs. frequency where M21 is the power measured from the input port to one of the output ports with the second input port terminated into 25 ohms.

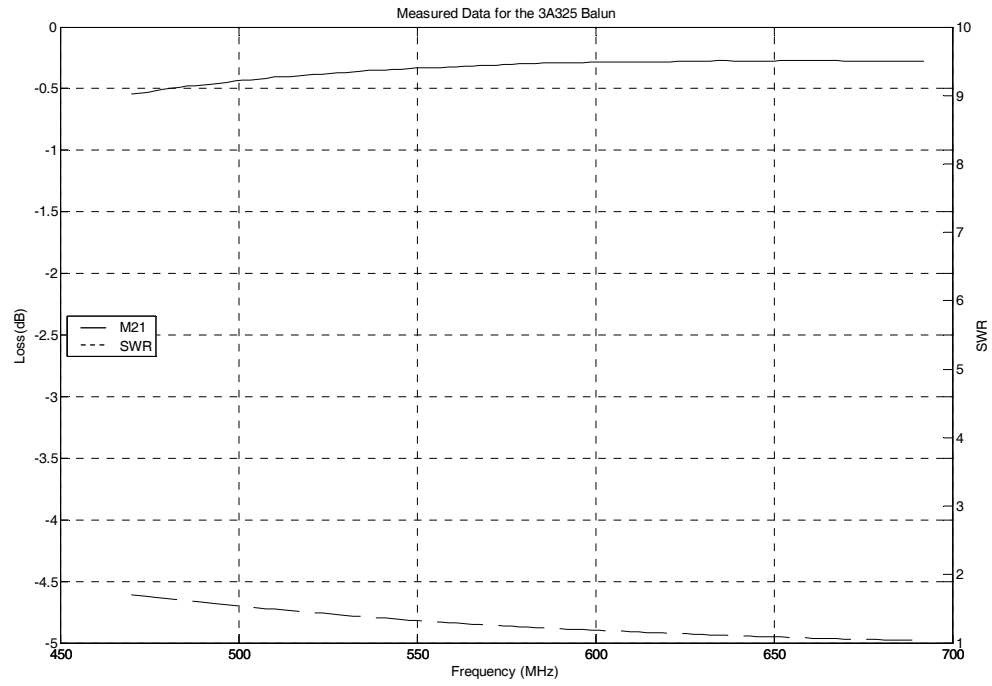


Figure 3.3 Measured S-Parameter Data for the 3A325 Balun

With the transistor, balun and substrate selected, the matching network was designed for the input and output of the transistor. The transistor impedances used for the matching network design are shown in Table 3.1.

Table 3.1

Source and Load Impedances of the PRF377 Transistor

Frequency (MHz)	Source Impedance (Ω)	Load Impedance (Ω)
470	5.79 - j2.40	6.21 - j1.69
560	6.63 - j2.63	5.66 - j1.12
660	6.57 - j4.03	6.76 - j1.00
760	6.67 - j 4.55	6.57 - j1.91
860	5.34 - j6.28	7.37 - j5.45

With input from the Motorola Engineering Group and the PRF377 datasheet, the input and output matching transformers were designed and simulated using Link [16] software. The input section starts with a 50 ohm unbalanced input which is then converted to 50 ohm balanced through an Anaren balanced-unbalanced transformer (balun). The 50 ohm balanced output of the balun, which is in fact 25 ohms to ground, then passes through a three section matching transformer that consists of a 22 Ω section, a 14.5 Ω section, a 12.5 Ω section and then steps to the input impedance of the transistor which is approximately 6 Ω . This configuration provides a broadband match across the DTV band with a typical VSWR of less than 5:1 without any additional reactive components. Table 3.2 lists the required matching section impedances and line lengths.

Table 3.2

Amplifier Card Microstrip Line Requirements

Required Impedance (Ω)	Required Length (Wavelength)	Required Length (Degrees)
25.0	-	-
22.0	0.0454	16.344
14.5	0.0046	1.667
12.5	0.0316	11.376

The simulation results for the broadband input matching network are shown in Figure 3.4 and the input circuit block diagram can be seen in Figure 3.5.

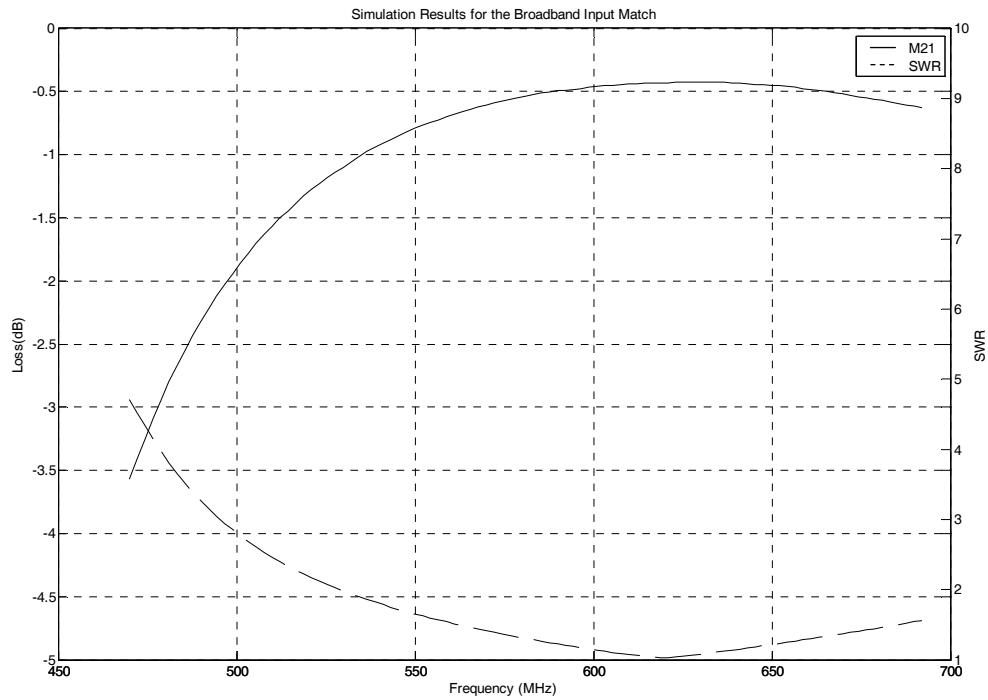


Figure 3.4 Broadband Input Matching Network Simulation Results

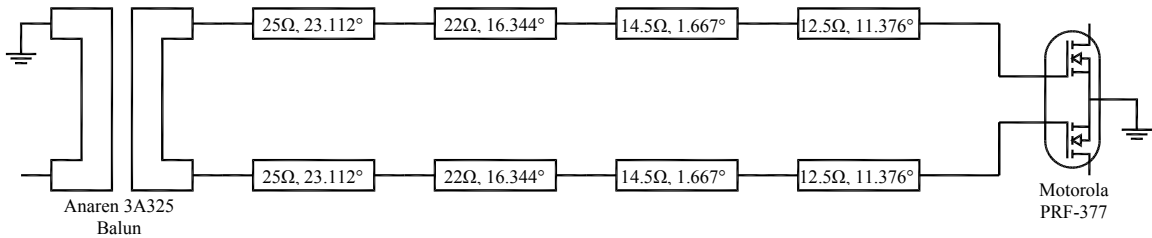


Figure 3.5 Broadband Input Matching Network Design

The amplifier cards are constructed in microstrip form using Rogers RO3003 substrate 0.030in (0.762mm) thick with 1oz. (35 μ m) rolled copper on both sides of the material. This material has a dielectric constant, ϵ_r , of 3.00. Based on a material thickness of 0.762mm, it is estimated that a W/d ratio will be greater than two for the 25 Ω , 22 Ω , 14.5 Ω and 12.5 Ω lines where W is the width of the upper microstrip conductor and d is the separation distance between the upper conductor and the ground plane, as shown in Figure 3.6.

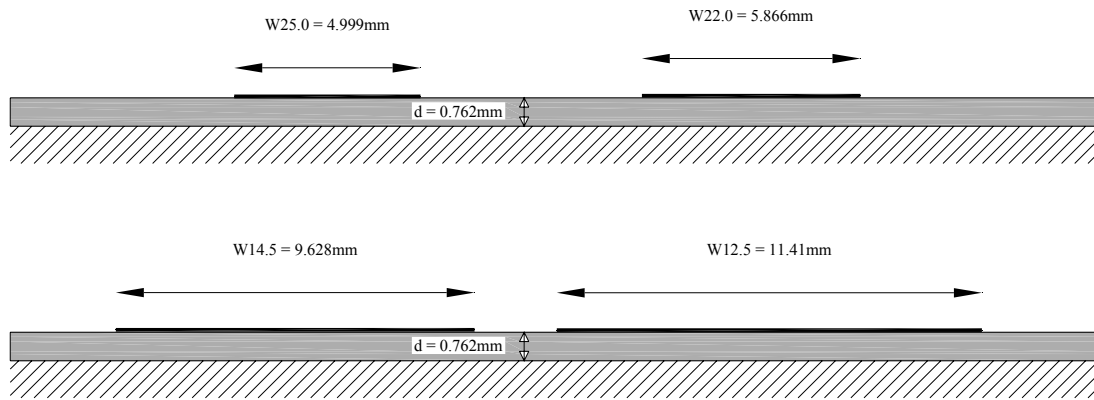


Figure 3.6 25Ω, 22Ω, 14.5Ω and 12.5Ω Microstrip Line Widths on 0.762mm Substrate

With $W/d > 2$ it is possible to calculate the line width required for the 25Ω, 22Ω, 14.5Ω and the 12.5Ω lines and the line lengths required using [17]:

$$\frac{W}{d} = \frac{2}{\pi} \left[B - 1 - \ln(2B - 1) + \frac{\epsilon_r - 1}{2\epsilon_r} \left\{ \ln(B - 1) + 0.39 - \frac{0.61}{\epsilon_r} \right\} \right] \quad (3-1)$$

$$\epsilon_e = \left(\frac{120\pi}{Z_0 [W/d + 1.393 + 0.667 \ln(W/d + 1.444)]} \right)^2 \quad (3-2)$$

$$\ell = \frac{\phi(\pi/180)}{\sqrt{\epsilon_e} k_0} \quad (3-3)$$

$$k_0 = \frac{2\pi f}{c} \quad (3-4)$$

$$B = \frac{377\pi}{2Z_0 \sqrt{\epsilon_r}} \quad (3-5)$$

Where:

- Z_0 = characteristic impedance
- ϕ = phase shift in degrees
- $\frac{W}{d}$ = width to depth ratio of the microstrip line
- ϵ_e = effective relative permittivity of the material
- ℓ = length of the microstrip transmission line at impedance and frequency
- k_0 = the free space or air wavenumber

By substituting in for the known values, the width of the 25.0Ω line is found:

$$B_{25.0} = \frac{377\pi}{2(25)\sqrt{3.00}} = 13.667 \quad (3-6)$$

$$\frac{W_{25.0}}{d} = \frac{2}{\pi} \left[\frac{13.667 - 1 - \ln(2(13.667) - 1) + \frac{3.00 - 1}{2(3.00)} \left\{ \ln(13.667 - 1) + 0.39 - \frac{0.61}{3.00} \right\}}{\frac{3.00 - 1}{2(3.00)}} \right] = 6.560 \quad (3-7)$$

$$W_{25.0} = 6.560(0.762mm) = 4.999mm \quad (3-8)$$

For the 22.0Ω line:

$$B_{22.0} = \frac{377\pi}{2(22.0)\sqrt{3.00}} = 15.541 \quad (3-9)$$

$$\frac{W_{22.0}}{d} = \frac{2}{\pi} \left[\frac{15.541 - 1 - \ln(2(15.541) - 1) + \frac{3.00 - 1}{2(3.00)} \left\{ \ln(15.541 - 1) + 0.39 - \frac{0.61}{3.00} \right\}}{\frac{3.00 - 1}{2(3.00)}} \right] = 7.698 \quad (3-10)$$

$$W_{22.0} = 7.698(0.762mm) = 5.866mm \quad (3-11)$$

The 16.344° length of 22Ω line at band center or 581MHz:

$$\epsilon_{e_{22.0}} = \left(\frac{120\pi}{22.0[7.698 + 1.393 + 0.667 \ln(7.698 + 1.444)]} \right)^2 = 2.631 \quad (3-12)$$

$$k_{0.581} = \frac{2\pi 581 \times 10^6 \text{ Hz}}{2.998 \times 10^8 \text{ m/s}} = 12.177 \text{ m}^{-1} \quad (3-13)$$

$$\ell_{0.0454\lambda_{581}} = \frac{16.344(\pi/180)}{\sqrt{2.631}(12.177)} = 14.44 \text{ mm} \quad (3-14)$$

For the 14.5Ω line:

$$B_{14.5} = \frac{377\pi}{2(14.5)\sqrt{3.00}} = 23.579 \quad (3-15)$$

$$\frac{W_{14.5}}{d} = \frac{2}{\pi} \left[\frac{23.579 - 1 - \ln(2(23.579) - 1) + \frac{3.00 - 1}{2(3.00)} \left\{ \ln(23.579 - 1) + 0.39 - \frac{0.61}{3.00} \right\}}{\right] = 12.636 \quad (3-16)$$

$$W_{14.5} = 12.636(0.762mm) = 9.628mm \quad (3-17)$$

The 1.667° length of 14.5Ω line at band center or 581MHz:

$$\varepsilon_{e_{14.5}} = \left(\frac{120\pi}{14.5[12.636 + 1.393 + 0.667 \ln(12.636 + 1.444)]} \right)^2 = 2.710 \quad (3-18)$$

$$l_{0.0046\lambda_{581}} = \frac{1.667(\pi/180)}{\sqrt{2.710}(12.177)} = 1.451mm \quad (3-19)$$

For the 12.5Ω line:

$$B_{12.5} = \frac{377\pi}{2(12.5)\sqrt{3.00}} = 27.352 \quad (3-20)$$

$$\frac{W_{12.5}}{d} = \frac{2}{\pi} \left[\frac{27.352 - 1 - \ln(2(27.352) - 1) + \frac{3.00 - 1}{2(3.00)} \left\{ \ln(27.352 - 1) + 0.39 - \frac{0.61}{3.00} \right\}}{2(3.00)} \right] = 14.974 \quad (3-21)$$

$$W_{12.5} = 14.974(0.762mm) = 11.410mm \quad (3-22)$$

The 11.376° length of 12.5Ω line at band center or 581MHz:

$$\varepsilon_{e_{12.5}} = \left(\frac{120\pi}{12.5[14.974 + 1.393 + 0.667 \ln(14.974 + 1.444)]} \right)^2 = 2.736 \quad (3-23)$$

$$\ell_{0.0316\lambda_{581}} = \frac{11.376(\pi/180)}{\sqrt{2.736}(12.177)} = 9.858mm \quad (3-24)$$

The results of the above calculations are shown in tabular form in Table 3.3 and Figure 3.7 shows the layout of the microstrip realization of the input matching network.

Table 3.3

Calculated Microstrip Line Widths and Lengths

Required Impedance (Ω)	Required Length (Wavelength)	Required Length (Degrees)	Calculated Width (mm)	Calculated Length (mm)
25.0	-	-	4.999	-
22.0	0.0454	16.344	5.866	14.44
14.5	0.0046	1.666	9.628	1.45
12.5	0.0316	11.376	11.41	9.858

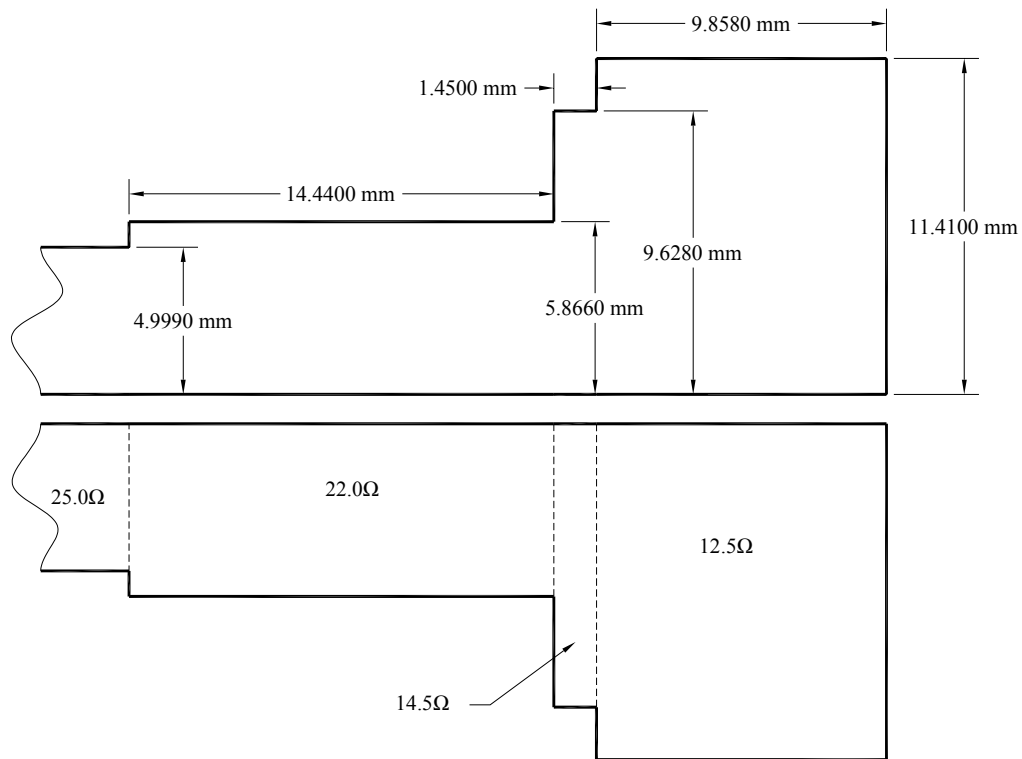


Figure 3.7 Input Matching Network Microstrip Layout

A broadband solution was investigated with the intention that a single amplifier card could be used anywhere within the UHF television band, but this proved to be somewhat impractical since the amplifiers could be made much more efficient by tuning them for narrowband operation. Since the amplifiers are needed for only a 6MHz portion of the DTV band, they were tuned to specific DTV channels with the addition of passive reactive components to improve the performance for that specific channel. The balanced broadband design was converted into a single ended design and implemented in the WinSmith software package [18]. Capacitors were added one at a time starting at the

load end of the match and working towards the source. After each capacitor was added, the circuit was fine tuned by adjusting the value of the capacitor and the position along the microstrip until the input was as close to $50 + j0\Omega$ as possible at channel center (485 MHz for channel 16). This process was repeated until a good match was achieved. The circuit was then converted back to a balanced design and re-simulated using the Link software package [19]. The circuit was fine tuned in Link for maximum flatness, tilt and gain across the 6 MHz wide channel, while SWR was minimized. By adding capacitors to the input matching network, the single channel performance for channel 16 (482-488 MHz) improved from a maximum SWR of 4:1 to 1.2:1 across the channel, and the loss through the network was reduced from 2.8 dB to 0.3 dB. The simulation results for the narrowband input match for channel 16 can be seen in Figure 3.8 and the narrowband input block diagram in Figure 3.9

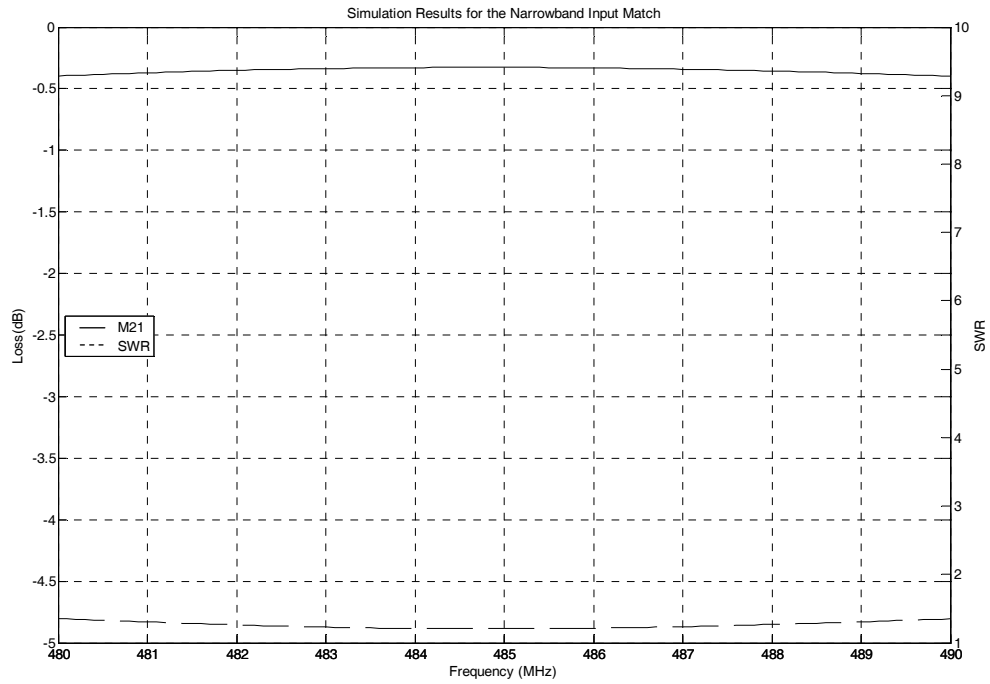


Figure 3.8 Simulation Results for the Narrowband Input Matching Network

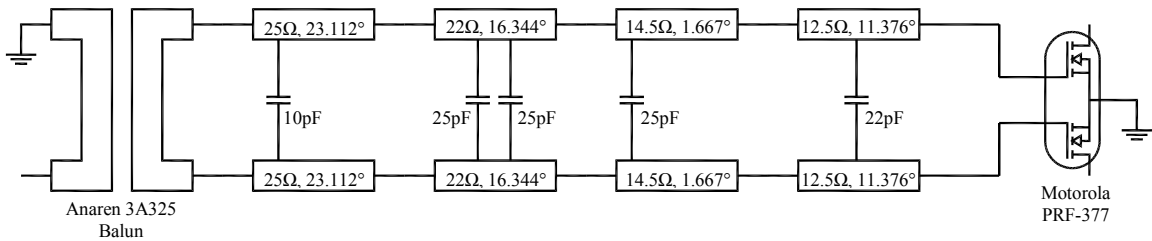


Figure 3.9 Channel 16 Narrowband Input Matching Network Design

To verify the input match design, the simulations for both the broadband and narrowband cases were repeated with the transistor removed from the circuit and replaced

with a ground on one leg of the balanced match and a 50 ohm load on the other leg. This is necessary to simulate the circuit being terminated by a network analyzer as in the measurement connection of the transistor. Figure 3.10 shows the wideband case for the input match loss through the circuit and 3.11 shows the SWR, with both the simulated and measured results over the UHF DTV band. Figures 3.12 and 3.13 show the same data but over channel 16 only and Figures 3.14 and 3.15 represent the simulated vs. actual results for the narrowband match again for channel 16. In all cases, the dashed line represents the simulated results.

It is interesting to note that the measured broadband results seem to fall off above 550 MHz, which is near the design center of 581 MHz. However, even with this degradation, the measured results are still within 1 dB of the simulated results. It is also interesting that the narrowband measured results were over 2 dB better than the simulated results. This improvement can be attributed to the fact that the losses in the physical realization of the design were not accounted for in the simulation and that this circuit was tuned for the test configuration while no further tuning was performed on the simulation.

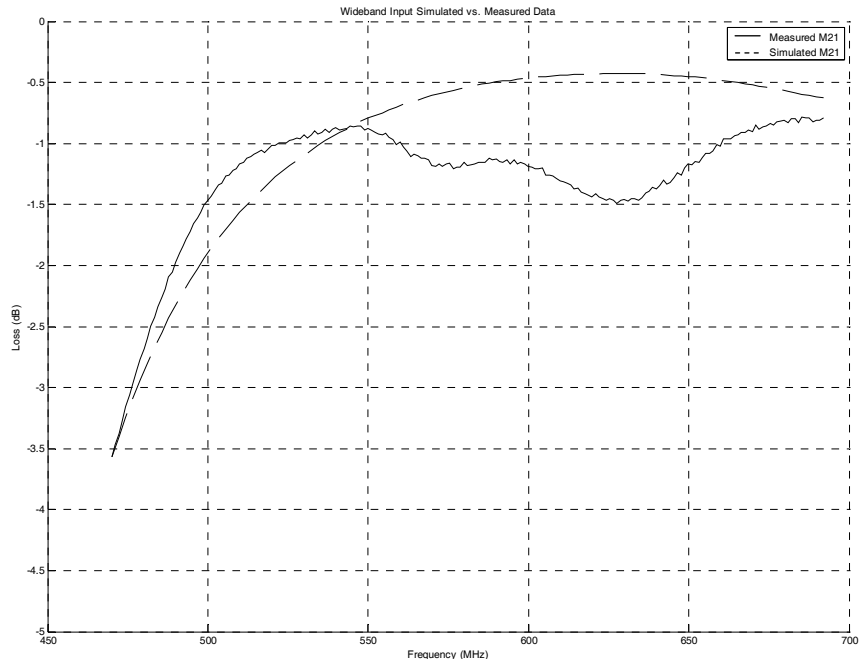


Figure 3.10 M21 Data for the Broadband Input Match Over the UHF DTV Band

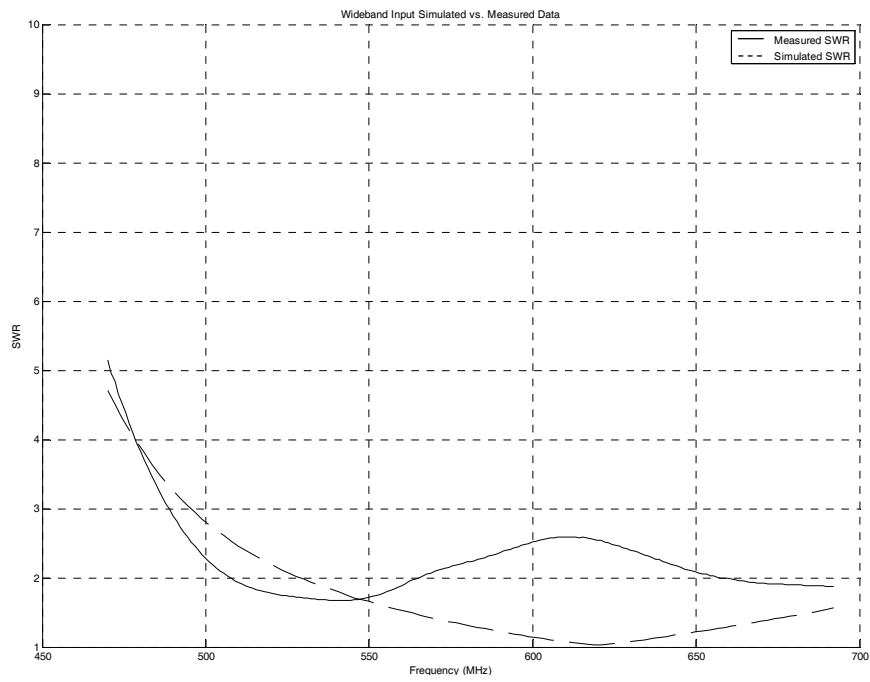


Figure 3.11 SWR Data for the Broadband Input Match Over the UHF DTV Band

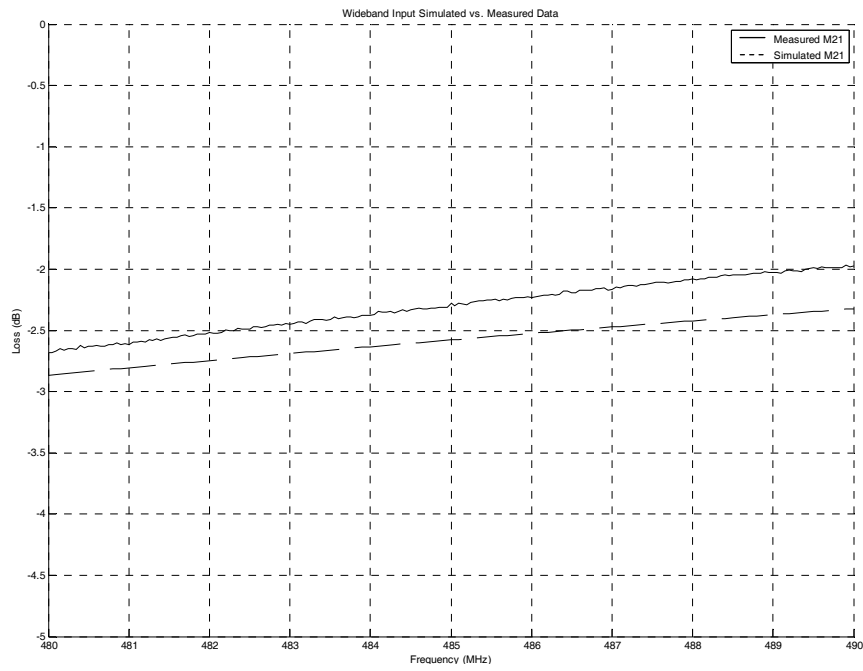


Figure 3.12 M21 Data for the Broadband Input Match for Channel 16

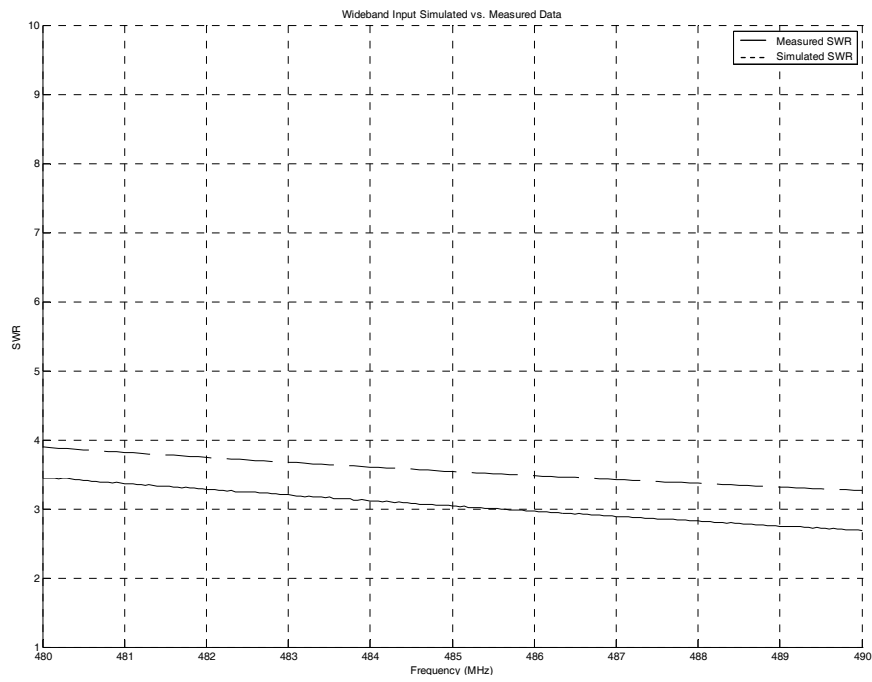


Figure 3.13 SWR Data for the Broadband Input Match for Channel 16

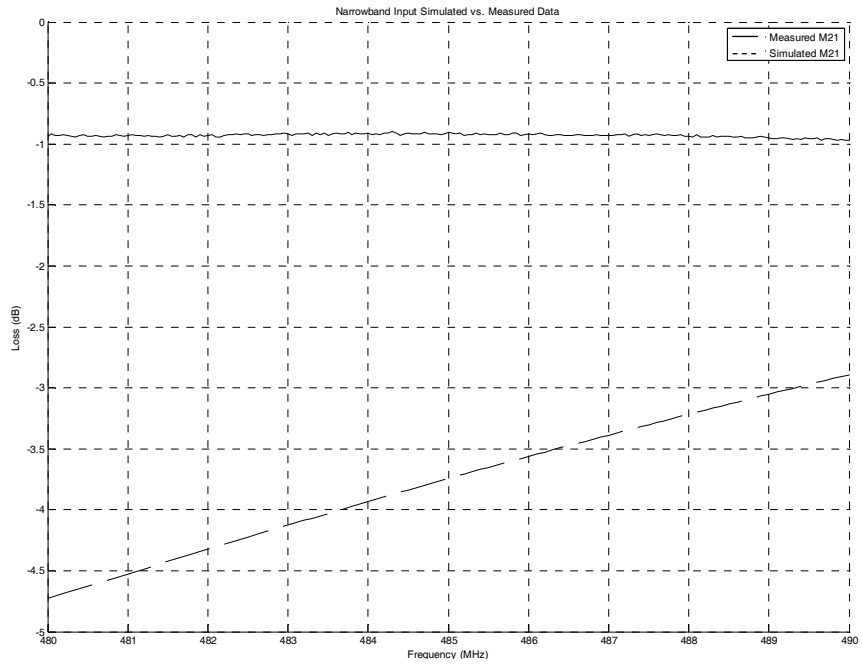


Figure 3.14 Simulated vs. Measured M21 Data for the Narrowband Input Match

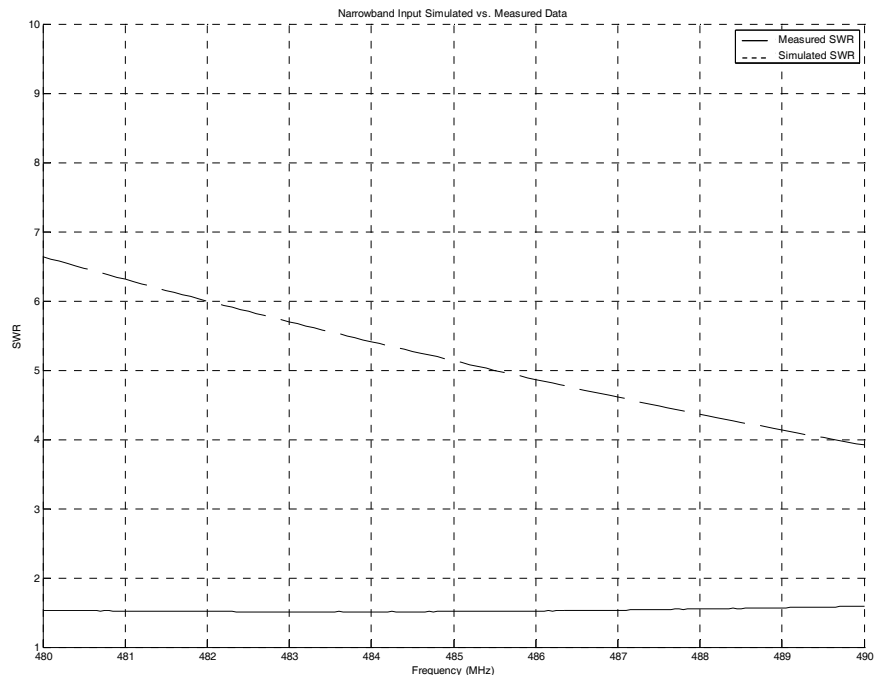


Figure 3.15 Simulated vs. Measured SWR Data for the Narrowband Input Match

The output matching section is essentially the input match in reverse as is shown in Figure 3.16. The output impedance of the transistor is approximately 6Ω that steps to the 12.5Ω section of the match, which then feeds the 14.5Ω section and the 22Ω section. The last transition is to 25Ω to feed the balun transformer which converts the 50Ω (25Ω to ground) balanced input to a 50Ω unbalanced output.

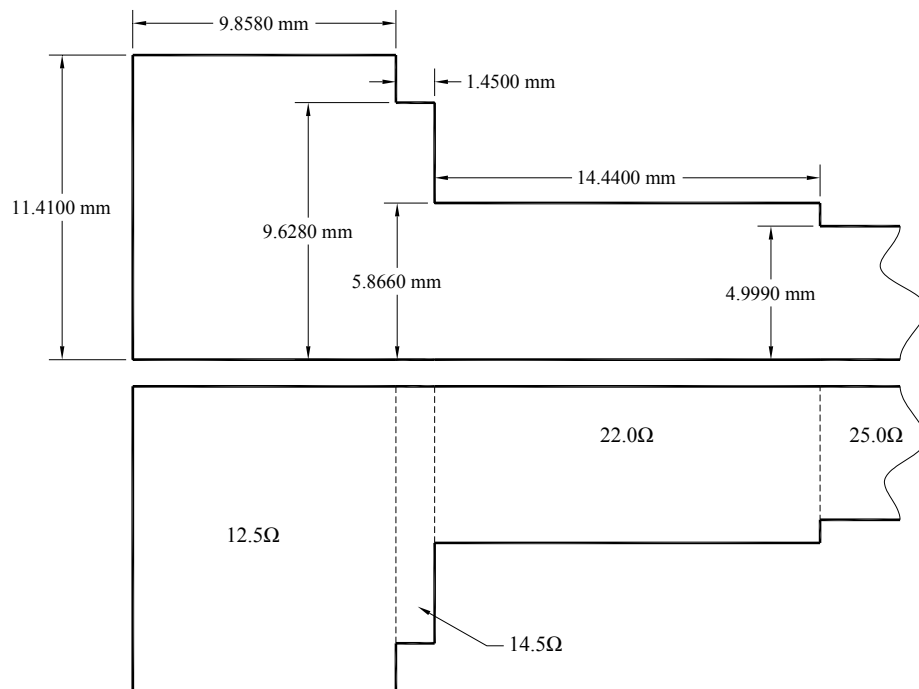


Figure 3.16 Output Matching Network Microstrip Layout

The simulation results for the broadband output matching network are shown in Figure 3.17 and the output matching network block diagram, in Figure 3.18.

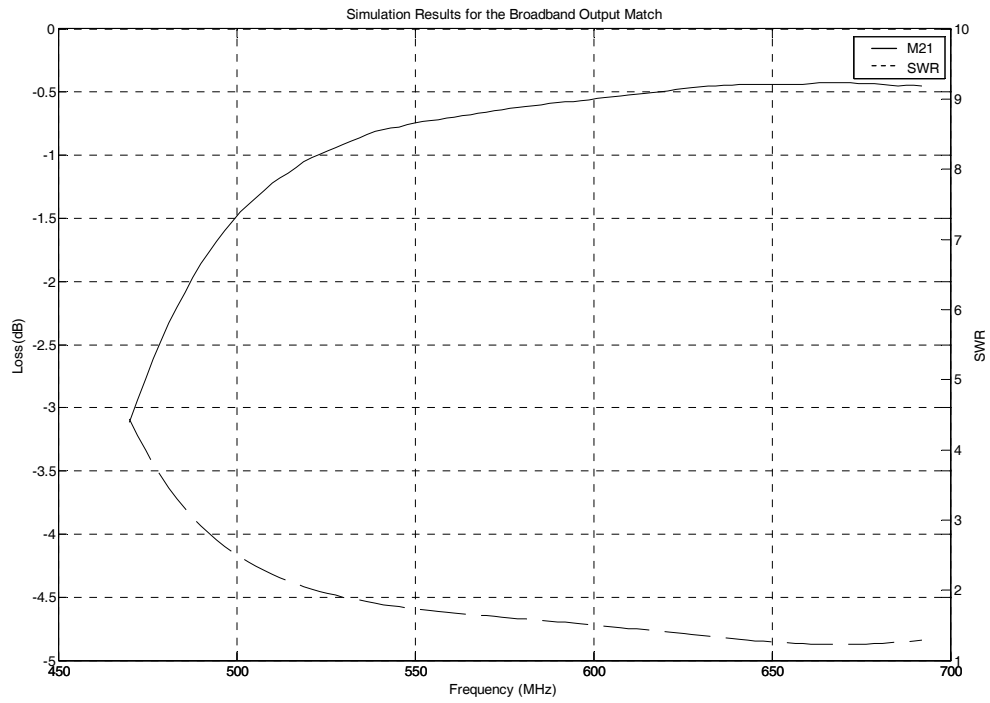


Figure 3.17 Simulation Results for the Broadband Output Matching Network

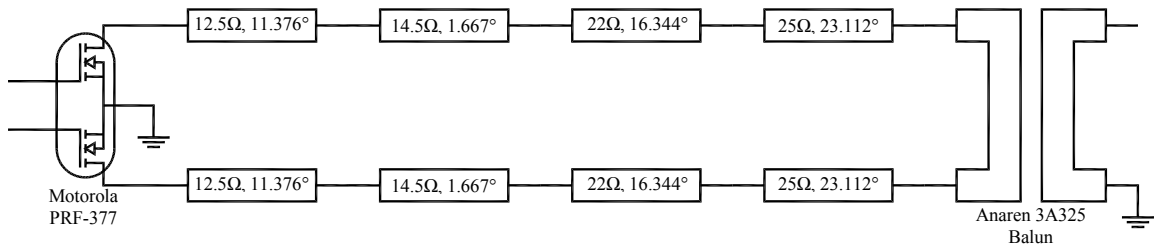


Figure 3.18 Broadband Output Matching Network Design

This configuration also provides a broadband match over the DTV band, but passive components are again added to make the amplifier channel specific. Once again, the design was simulated using the WinSmith and Link software packages and by adding capacitors and inductors to the matching sections, the amplifier efficiency and linearity was improved at the band edges. Although the broadband amplifier cards worked well on any channel over the entire DTV band without the addition of any components, the decision was made to narrowband the cards to specific channels to maximize performance for that particular system. By tuning the amplifier card output narrowband, the SWR over a single channel improved from 4.4:1 to 1.5:1, and the loss through the matching network improved from 3.1 dB to 0.4 dB as can be seen in Figure 3.19. Figure 3.20 shows the narrowband output match for channel 16.

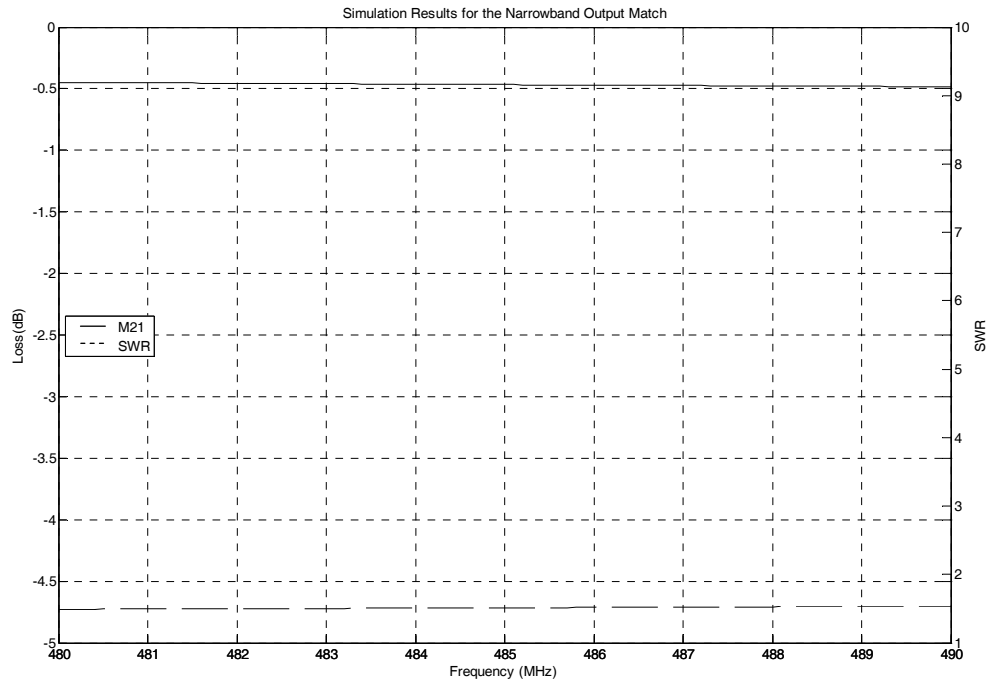


Figure 3.19 Simulation Results for the Narrowband Output Matching Network

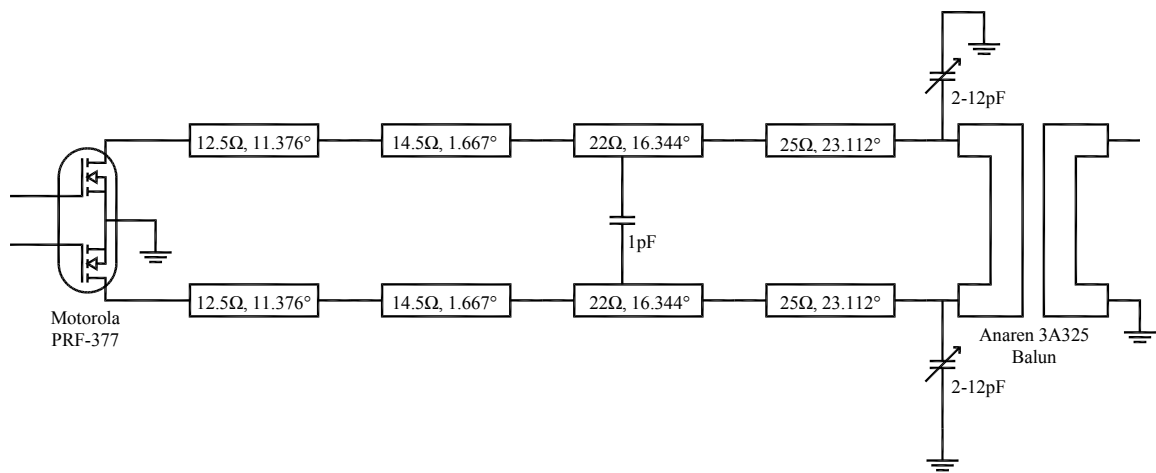


Figure 3.20 Channel 16 Narrowband Output Matching Network Design

To verify the output match design, the simulations were once again repeated for the broadband and narrowband cases with the transistor removed and replaced with a ground on one leg of the balanced match and a 50 ohm source on the other leg to simulate the measurement circuit with the connection of the network analyzer as opposed to the transistor. Figure 3.21 shows the broadband case for the output match loss and Figure 3.22 shows the SWR, with both the simulated and measured results over the UHF DTV band. Figures 3.23 and 3.24 show the same data but over channel 16 only and Figures 3.25 and 3.26 show the simulated vs. actual results for the narrowband match over channel 16.

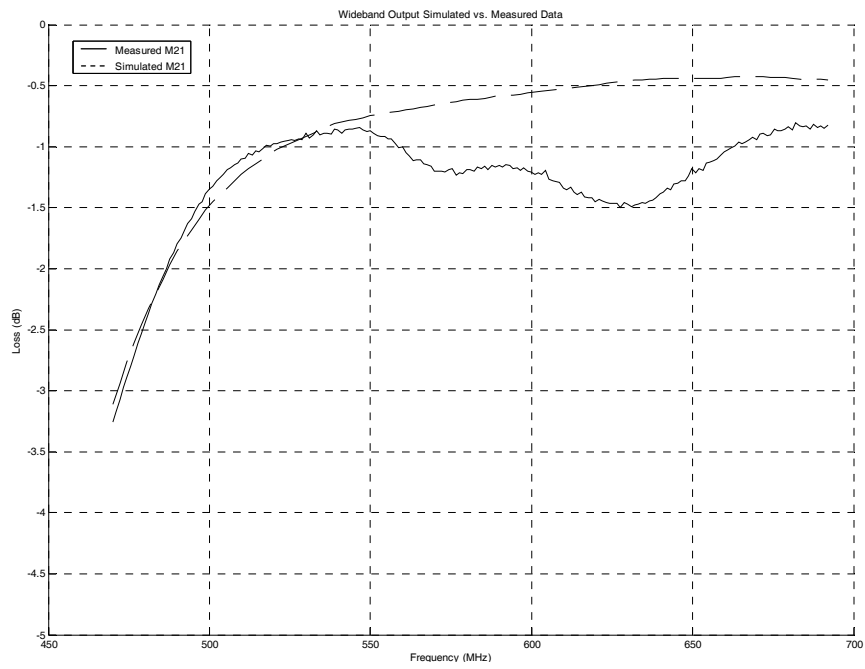


Figure 3.21 M21 Data for the Broadband Output Match Over the UHF DTV Band

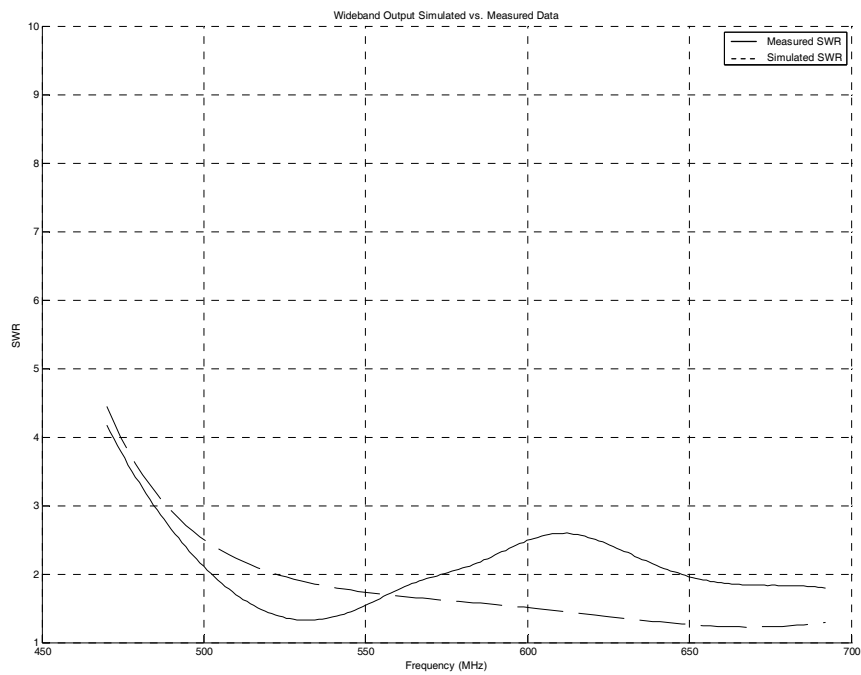


Figure 3.22 SWR Data for the Broadband Output Match Over the UHF DTV Band

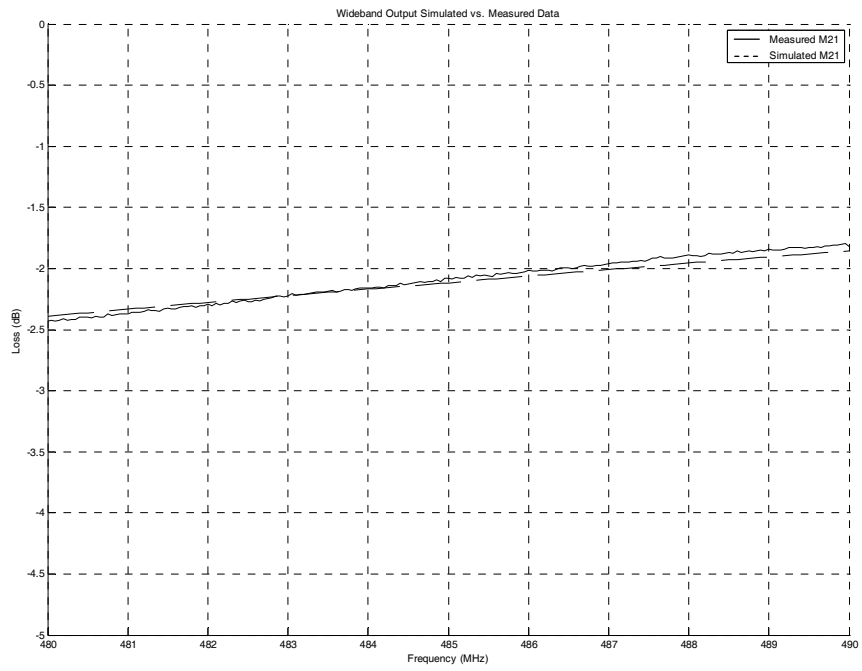


Figure 3.23 M21 Data for the Broadband Output Match for Channel 16

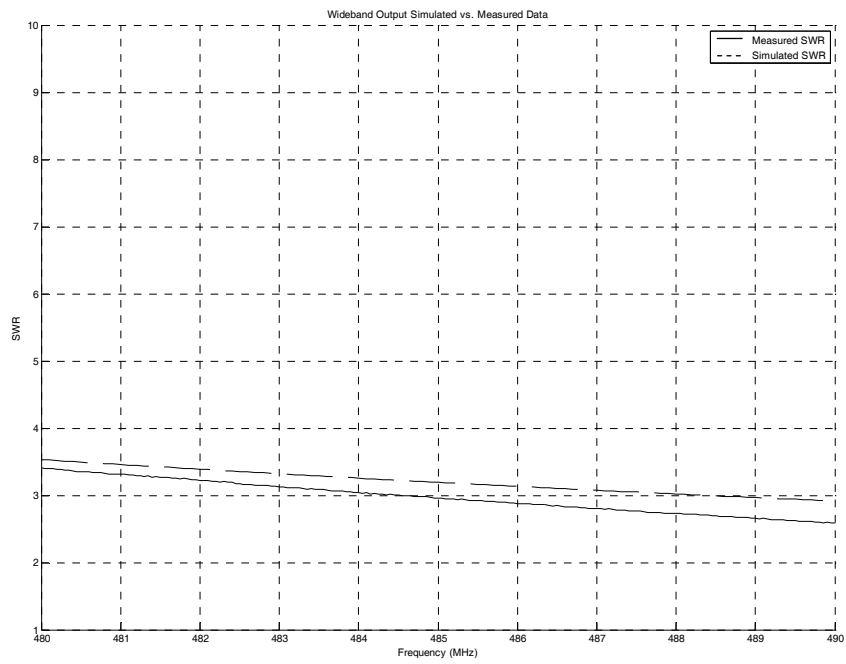


Figure 3.24 SWR Data for the Broadband Output Match for Channel 16

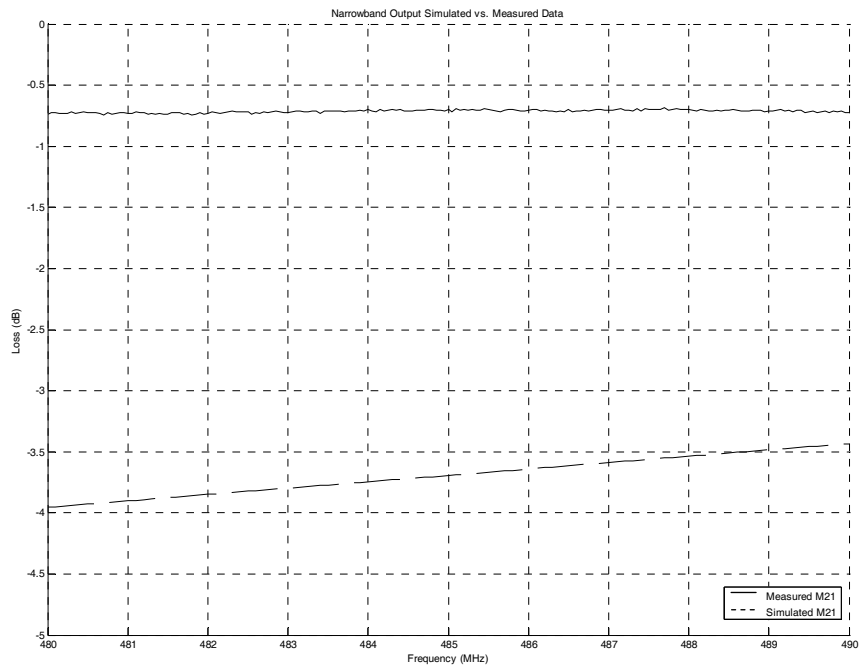


Figure 3.25 Simulated vs. Measured M21 Data for the Narrowband Output Match

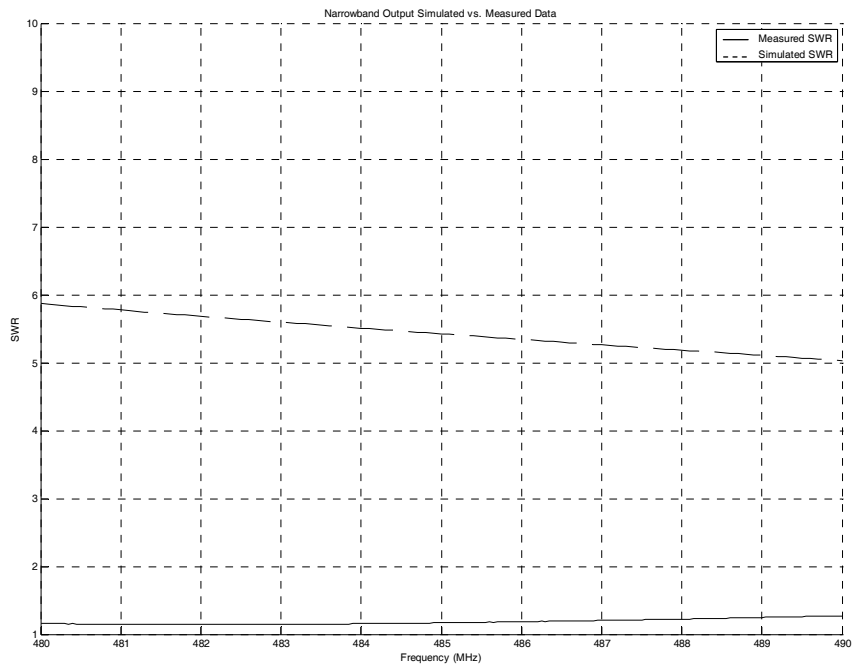


Figure 3.26 Simulated vs. Measured SWR Data for the Narrowband Output Match

As with the input match test results, the measured performance falls off just below the design center of 581MHz but is still within 1 dB of the simulated results. The measured narrowband performance was also significantly better than the simulated results, which is also due to the fact that the actual circuit was tuned for the test configuration while no tuning was changed on the simulation for the test case.

With a simulated loss of 0.3 dB and 0.4 dB in the tuned input and output matching sections, respectively, and a power gain of at least 16.5 dB from the amplifier, each card should realize an overall gain of 15.8 dB. The MRF377 transistor has a rated output [20] of 64 watts. With a loss of 0.4 dB on the output match, the worst case power available at the output of each card is 58.4 watts. In order to drive the transistor to its rated output, an input power of 1.54 watts must be present at the input of the amplifier card. After initial hardware tests, fine tuning was performed on a per-channel basis for each transmitter.

The drain is supplied 32VDC from a switching power supply mounted externally from the amplifier drawer. Each power supply is capable of supplying two PA modules to full power. The 32VDC enters the amplifier card through two standoffs that provide an electrical connection to the power distribution card mounted on top of the amplifier cards. The standoffs on the cards provide both a mechanical mount and an electrical connection between the power distribution card and all nine of the amplifier cards. The power distribution card has a 0.025Ω resistor and a 5μH inductor on each of the nine outputs. The purpose of the resistor is to provide input current monitoring for each amplifier card, and the inductor is to provide additional RF decoupling between the amplifier cards and the power distribution buss. Upon entering the amplifier cards, the

32VDC is filtered with four capacitors before passing through an 8nH inductor that couples the DC to the drain on the transistor and blocks the RF from coupling back through to the DC power supply. The identical circuit appears on both sides of the transistor, one for drain side A and one for side B.

It was desired to have a single DC input per amplifier card, therefore requiring the gate bias circuit be designed on the amplifier card receiving its input voltage from the 32VDC drain voltage. Both the gate bias and drain voltage had to be appropriately coupled and filtered to the circuit as to avoid having the power supply sink the RF, or to have the RF couple into the DC supply. A low-pass dual L-C network was designed and simulated using a pair of inductors in series with the DC and a capacitor to ground. Three additional capacitors are installed on the DC input side of the network to add additional DC filtering for the gate supply. The initial values of the inductors and capacitors were determined using the formula

$$f_c = \frac{1}{2\pi\sqrt{LC}} \quad (3-25)$$

and were fine tuned by performing a computer simulation with MultiSim [21]. The bias circuit filter network can be seen in Figure 3.27.

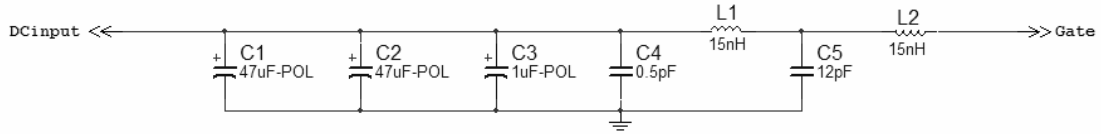


Figure 3.27 Amplifier Bias Filter Network

The bias filter network simulation results are shown in Figure 3.28. From Figure 3.28 it can be seen that the simulated AC response of the bias circuit is 136 dB down at 470 MHz – the low end of the UHF broadcast band. A test circuit was constructed and the response of the circuit at the frequencies of interest was below the measurable values of the test equipment available using an Agilent 8753ET network analyzer which only allowed for 110 dB of dynamic range which is less than the simulated 136 dB. Another test was performed by taking a sample from the DC input to the filter network and running it through a DC block and then to the spectrum analyzer. There was no RF signal indicated above the noise floor on the spectrum analyzer. There are two gate bias filter networks on each amplifier card, one for each transistor in the push-pull transistor package.

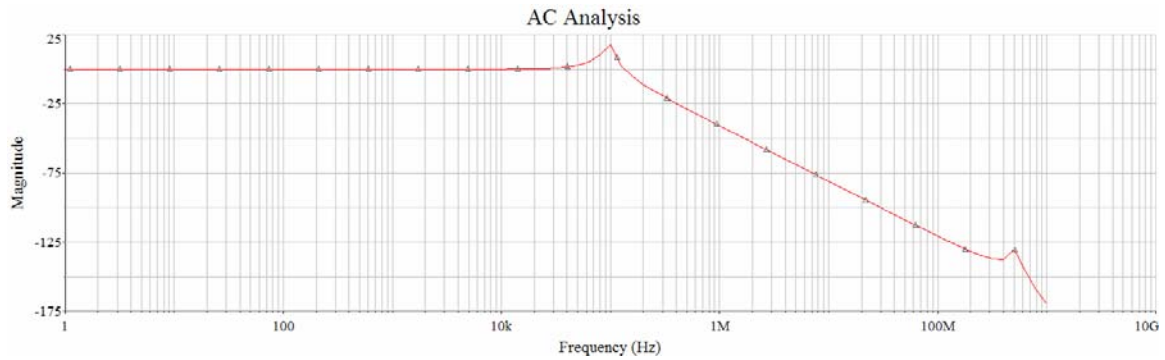


Figure 3.28 Simulation Results for the Input Bias Filter Network

The gate bias filter is fed from the gate bias voltage regulator which is a common regulator for both transistors in each package ensuring a common quiescent operating point for both halves of the package. The 32V DC drain voltage is regulated by a LM78L15 voltage regulator 15V DC. The output of the regulator I.C. is then fed through a voltage divider network with a variable resistor to set the quiescent operating point of the transistor or I_{DQ} . The voltage divider consists of a 10k Ω potentiometer in series with a 8.2k Ω resistor and a 3.3k Ω resistor tied to ground. The output of the divider network is taken at the junction of the 8.2k Ω and the 3.3k Ω resistors. This configuration allows for a bias voltage adjustment range of 2.3-4.3V DC. This can be calculated by taking the two extremes of the potentiometer, 0 Ω and 10k Ω , and working the voltage divider equation:

$$V_{BIAS} = (15) \frac{3300}{3300 + 8200 + 10000} = 2.3V_{dc} \quad (3-26)$$

and

$$V_{BLAS} = (15) \frac{3300}{3300 + 8200 + 0} = 4.3V_{dc} \quad (3-27)$$

This range of 2.3-4.3V DC allows for proper adjustment of the bias voltage from below the gate threshold voltage ($V_{G(th)}$) of 2.7V DC through the gate quiescent voltage $V_{GS(Q)}$ of 3.4V DC. There is also a capacitor on the input of the regulator and a capacitor on the output to filter the DC and minimize the effects of the RF in such close proximity of the circuit. See Figure 3.29 for a complete bias supply schematic and Figure 3.30 for a complete amplifier card block diagram.

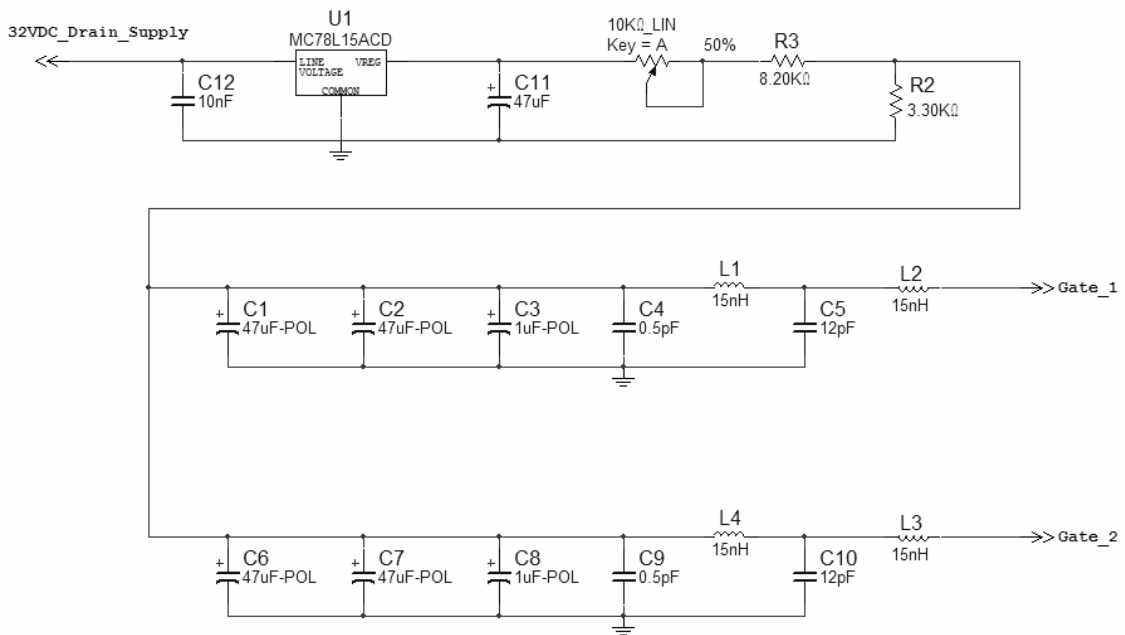


Figure 3.29 Complete Amplifier Gate Bias Supply

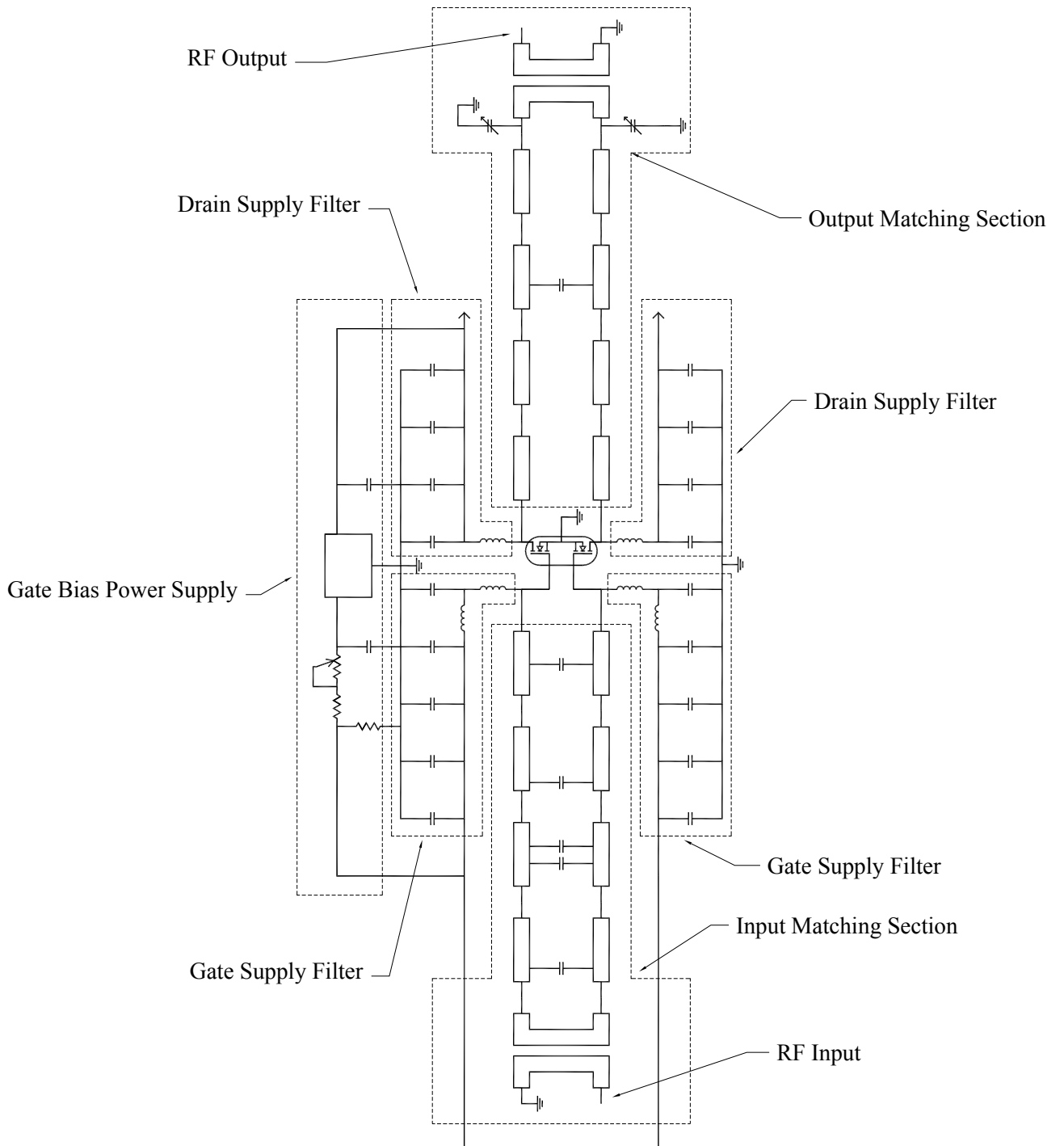


Figure 3.30 Complete Amplifier Card Block Diagram

Wilkinson Combiner and Splitter

The 3-dB Wilkinson splitter and combiner, shown in Figure 3.31 was selected because it is relatively flat over the channel of interest and easy to implement using microstrip technology. It is a three port network that either divides the power input at port 1 equally between ports 2 and 3, or combines the power input from ports 2 and 3 into port 1. When used as a splitter, the power output on ports 2 and 3 are equal in amplitude and phase.[22]

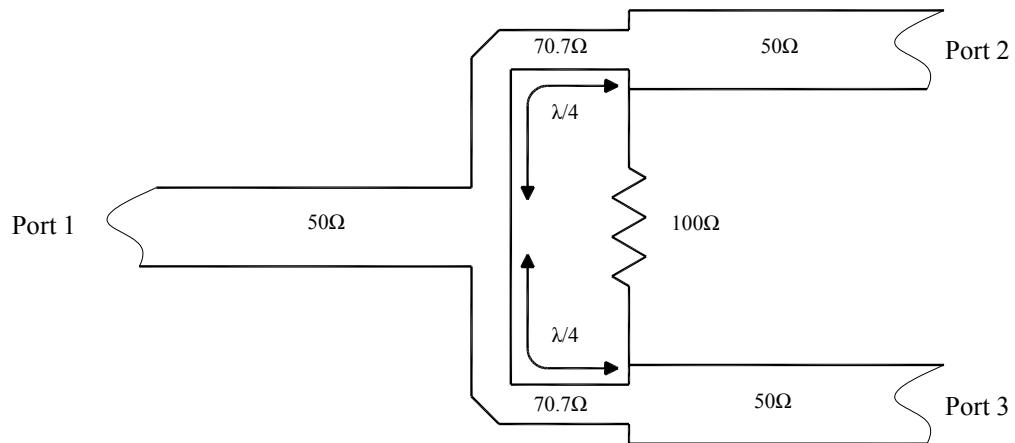


Figure 3.31 Microstrip Implementation of a Wilkinson Splitter / Combiner

When ports 2 and 3 are terminated into 50 ohms, the input port 1 will see 50 ohms. The two 70.7 ohm quarter line sections transform the input impedance from 50 ohms into 100 ohms, but since the ports 2 and 3 are in parallel with the 100 ohm resistor,

all three ports have the desired impedance of 50 ohms. The resistor selected is always twice the impedance to the port 2 and 3 lines, or in this case $R = 2(50) = 100$.

Knowing the impedance of the port 2 and 3 lines, and the balancing resistor, the impedance of the quarter wave matching section can be calculated:

$$Z_0 = 70.7 = \sqrt{100 * 50} \quad (3-28)$$

When operating normally with an equal power flow to or from ports 2 and 3, no power is dissipated by the balancing resistor. This fact proved to be very useful during testing of the amplifier modules by making it very easy to quickly pinpoint an amplifier card failure simply by locating the resistor operating at an elevated temperature.

When a failure occurs at one of the ports, for example port 2, the reflected signal splits between the balancing resistor and the transmission line. These two signals appear at port 3 180 degrees out of phase, therefore cancellation occurs and the extra power is absorbed by the balancing resistor. The complete scattering matrix for a Wilkinson splitter and combiner is:

$$[S] = \begin{bmatrix} 0 & \frac{e^{-j\pi/2}}{\sqrt{2}} & \frac{e^{-j\pi/2}}{\sqrt{2}} \\ \frac{e^{-j\pi/2}}{\sqrt{2}} & 0 & 0 \\ \frac{e^{-j\pi/2}}{\sqrt{2}} & 0 & 0 \end{bmatrix} \quad (3-29)$$

The Wilkinson power splitters and combiners are all constructed in microstrip form using Rogers RT/duroid 6002 substrate 0.060in (1.524mm) thick with 1oz. (35 μ m) rolled copper on both sides of the material, selected because of its excellent power handling capability over the UHF band. This material has a dielectric constant, ϵ_r , of

2.94. Based on a material thickness of 1.524mm, it is estimated that a W/d ratio will be greater than two, see Figure 3.32.

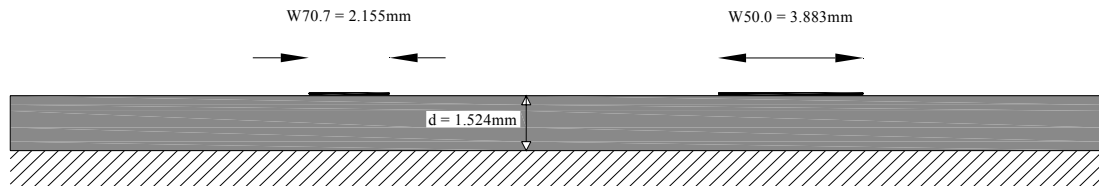


Figure 3.32 70.7 Ω and 50 Ω Line Widths on a 1.524mm Rogers RT/duroid 6002 substrate

With $W/d > 2$ it is possible to calculate the line width required for both 50 Ω and the 70.7 Ω lines and the line length required for the $\lambda/4$ line lengths using the same formulae as for the amplifier card matching sections:

$$\frac{W}{d} = \frac{2}{\pi} \left[B - 1 - \ln(2B - 1) + \frac{\epsilon_r - 1}{2\epsilon_r} \left\{ \ln(B - 1) + 0.39 - \frac{0.61}{\epsilon_r} \right\} \right] \quad (3-30)$$

$$\epsilon_e = \left(\frac{120\pi}{Z_0 [W/d + 1.393 + 0.667 \ln(W/d + 1.444)]} \right)^2 \quad (3-31)$$

$$\ell = \frac{\phi(\pi/180)}{\sqrt{\epsilon_e} k_0} \quad (3-32)$$

$$k_0 = \frac{2\pi f}{c} \quad (3-33)$$

$$B = \frac{377\pi}{2Z_0\sqrt{\epsilon_r}} \quad (3-34)$$

By substituting in for the known values the width of the 50Ω line is found:

$$B_{50} = \frac{377\pi}{2(50)\sqrt{2.94}} = 6.907 \quad (3-35)$$

$$\frac{W_{50}}{d} = \frac{2}{\pi} \left[\frac{6.907 - 1 - \ln(2(6.907) - 1) + \frac{2.94 - 1}{2(2.94)} \left\{ \ln(6.907 - 1) + 0.39 - \frac{0.61}{2.94} \right\}}{2(2.94)} \right] = 2.548 \quad (3-36)$$

$$W_{50} = 2.548(1.524mm) = 3.883mm \quad (3-37)$$

For the 70.7Ω line:

$$B_{70.7} = \frac{377\pi}{2(70.7)\sqrt{2.94}} = 4.885 \quad (3-38)$$

$$\frac{W_{70.7}}{d} = \frac{2}{\pi} \left[\frac{4.885 - 1 - \ln(2(4.885) - 1) + \frac{2.94 - 1}{2(2.94)} \left\{ \ln(4.885 - 1) + 0.39 - \frac{0.61}{2.94} \right\}}{2(2.94)} \right] = 1.414 \quad (3-39)$$

$$W_{70.7} = 1.414(1.524mm) = 2.155mm \quad (3-40)$$

The length of a $\lambda/4$ 70.7Ω at channel center D16 or 485MHz:

$$\epsilon_{e_{70.7}} = \left(\frac{120\pi}{70.7[1.414 + 1.393 + 0.667 \ln(1.414 + 1.444)]} \right)^2 = 2.311 \quad (3-41)$$

$$k_{0_{485}} = \frac{2\pi 485 \times 10^6 \text{ Hz}}{2.998 \times 10^8 \text{ m/s}} = 10.165 \text{ m}^{-1} \quad (3-42)$$

$$\ell_{\lambda/4_{485}} = \frac{90(\pi/180)}{\sqrt{2.311}(10.165)} = 101.65 \text{ mm} \quad (3-43)$$

The splitter and the combiner are constructed so that two sets of four outputs (or inputs) are spaced at three inch intervals so that they can directly couple to the amplifier cards. Between the two sets of four outputs is a six inch gap, with the input (or output) of the splitter or combiner network connected to the driver amplifier card. See Figures 3.33 and 3.34 for the final layout design for the channel 16 divider and combiner networks.

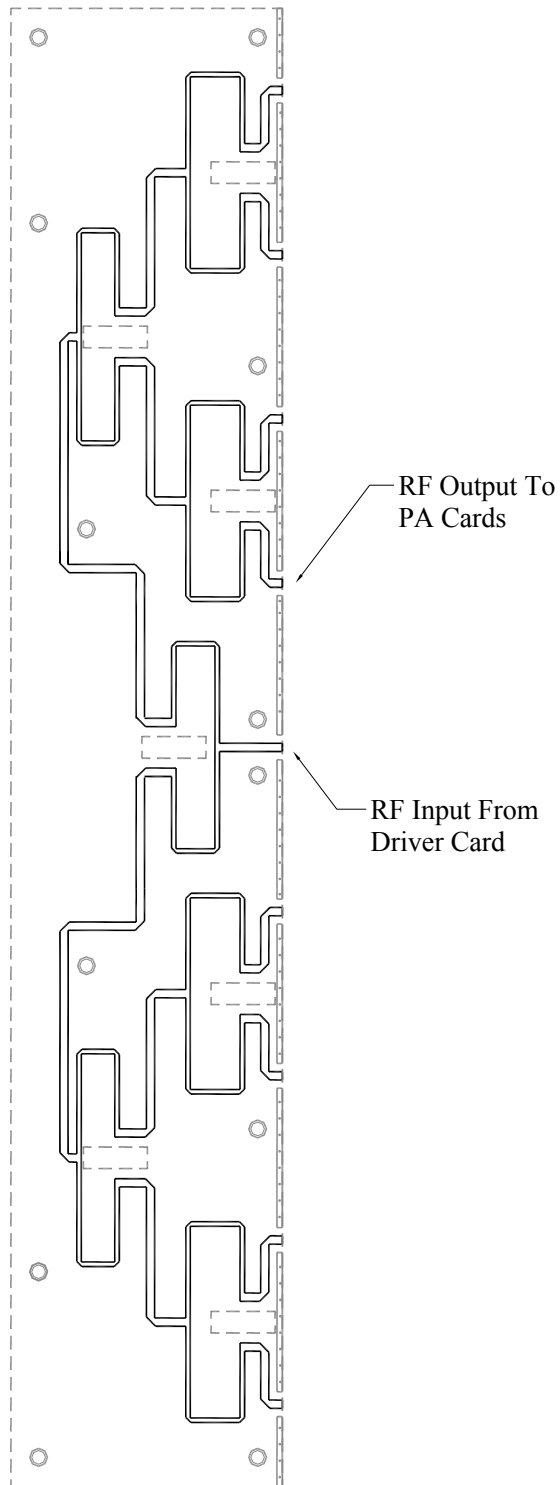


Figure 3.33 Microstrip Layout for the Channel 16 Splitter Card

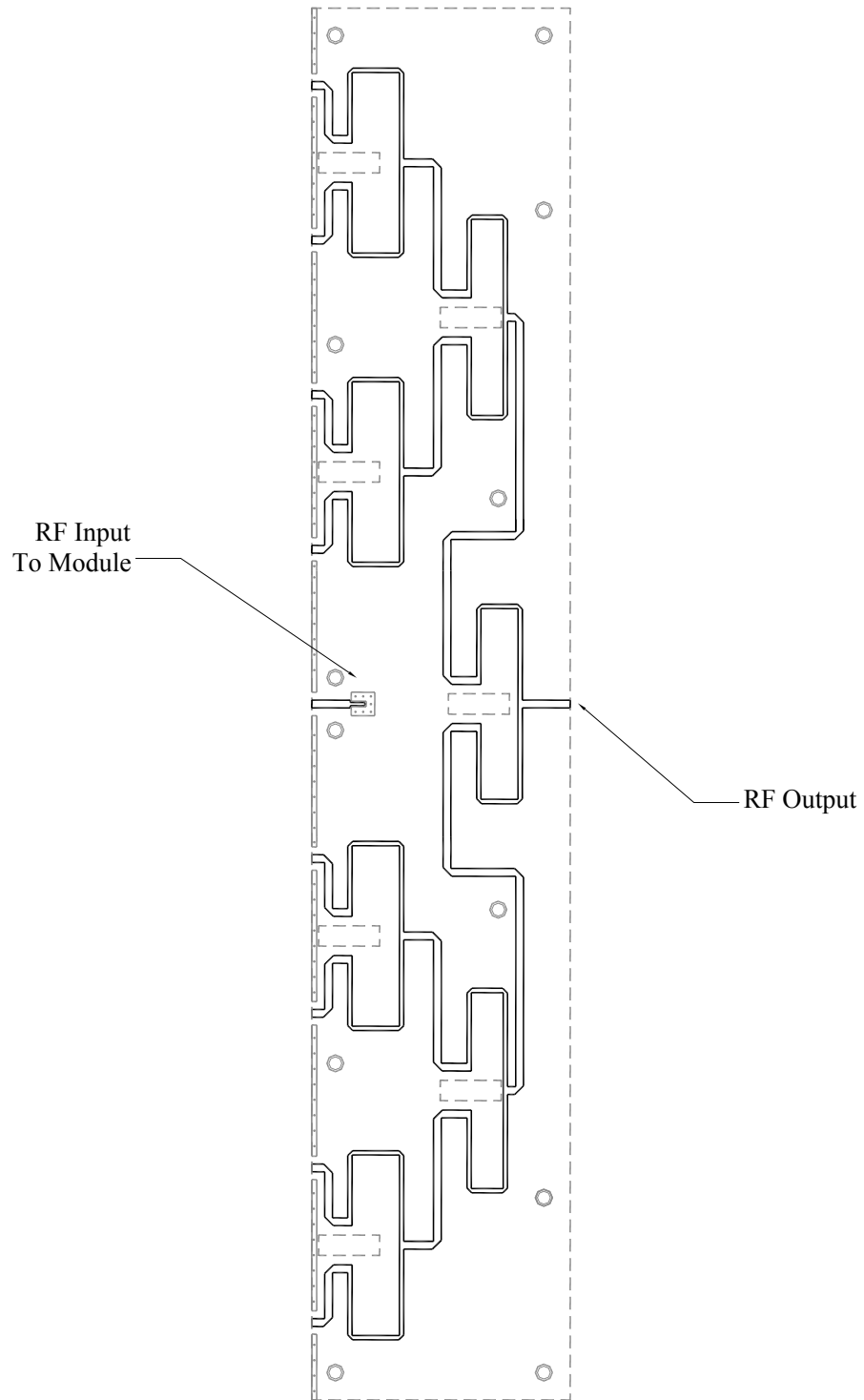


Figure 3.34 Microstrip Layout for the Channel 16 Input / Combiner Card

The splitters and combiners are tested by connecting the eight inputs and outputs together back to back without the amplifier cards in between. This way it is possible to verify the frequency response and the transmission loss over the frequencies of interest. A photograph of the test setup is shown in Figure 3.35.

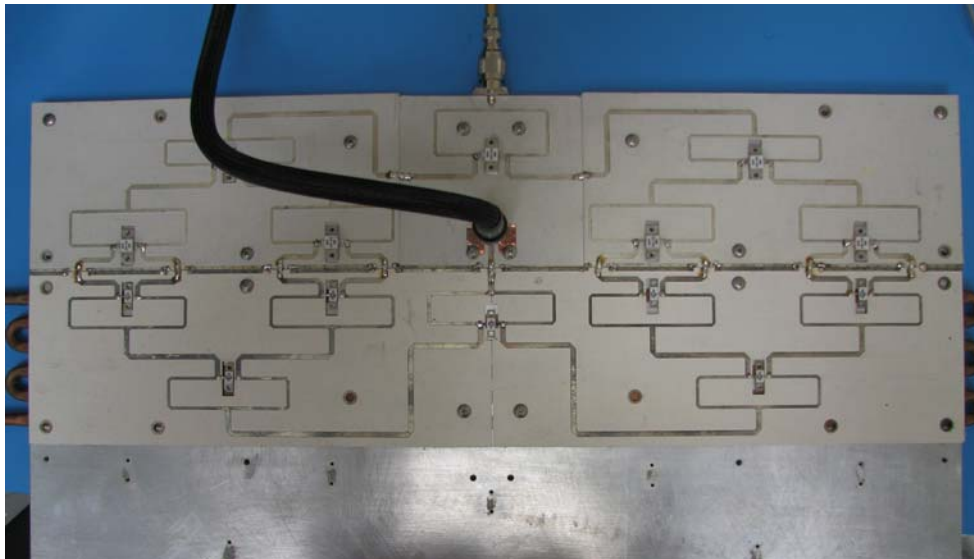


Figure 3.35 Wilkinson Splitter and Combiner Test Setup

The test results for a channel 20 Wilkinson splitter and combiner are shown in Figures 3.36 and 3.37. Figure 3.36 shows the recorded test data over the DVT portion of the UHF band and Figure 3.37 shows the results just over channel 20.

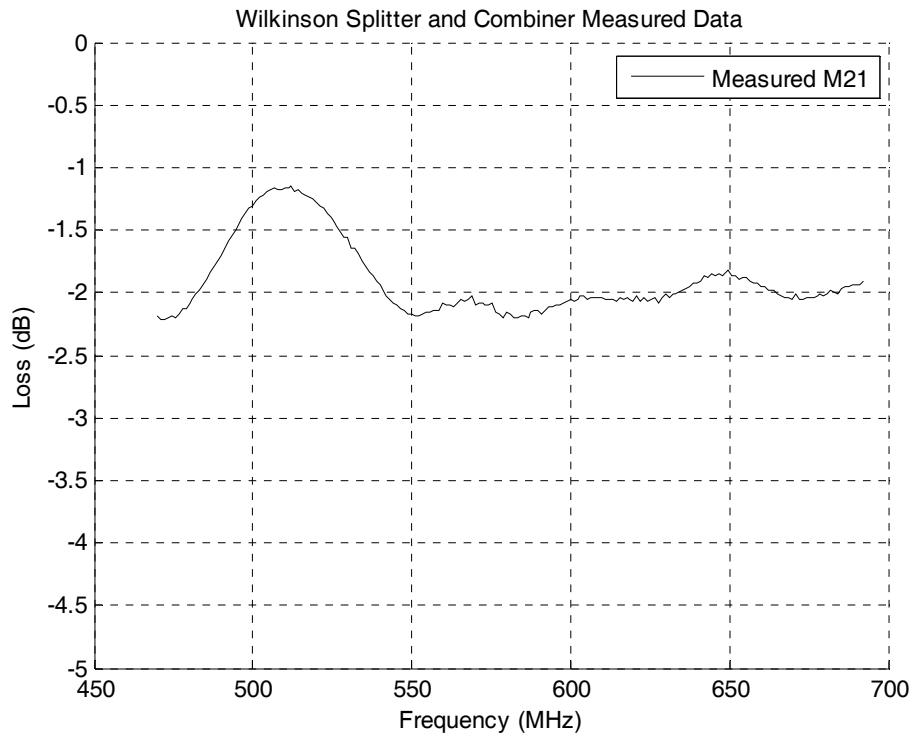


Figure 3.36 Wilkinson Splitter and Combiner Test over the Entire DTV Band

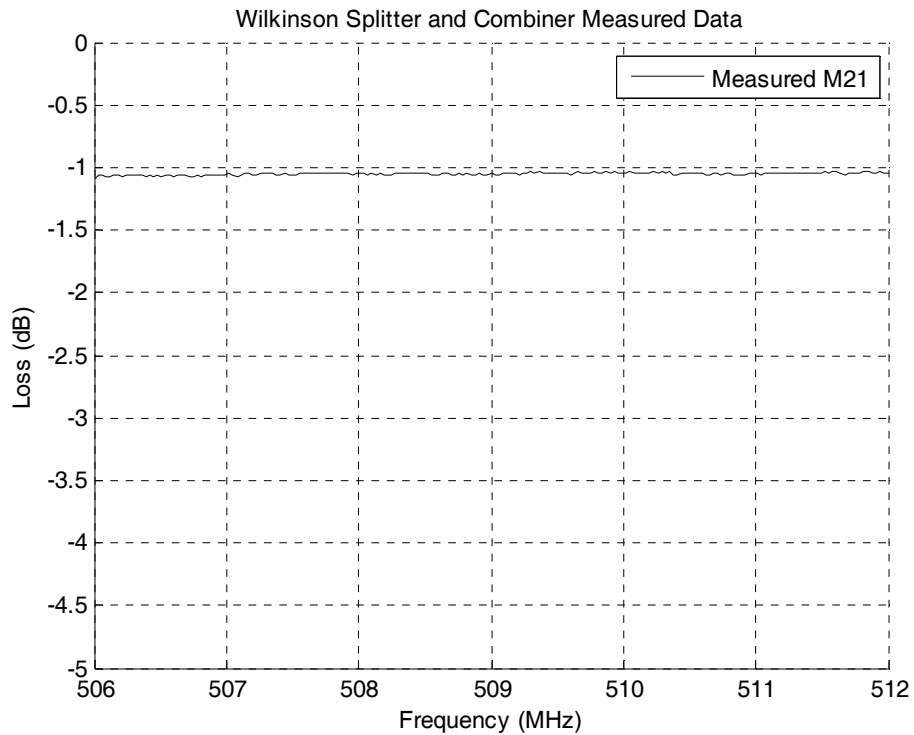


Figure 3.37 Wilkinson Splitter and Combiner Test over Channel 20

Figure 3.36 demonstrates how flat the Wilkinson splitter is over the DTV television band without any optimization, but it is shown in Figure 3.37 that the splitter and combiner combination has a loss of approximately 1 dB over the entire channel, and is very flat over the channel.

The corners of the turns in the microstrip transmission line were mitered to achieve a minimum VSWR at the bend using [23]

$$W = 1.6W_{z_0} \tag{3-44}$$

Where W is the width of the miter and W_{z_0} is the width of the line to be mitered. See Figure 3.38.

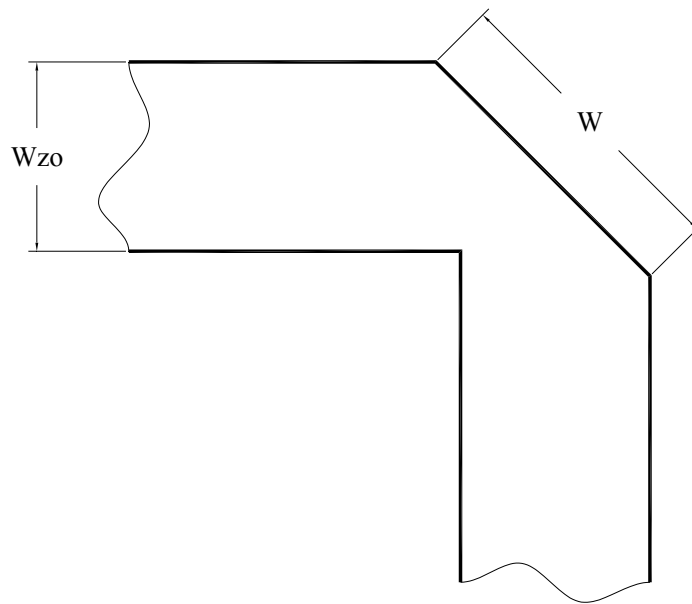


Figure 3.38 Mitered Corner for the Microstrip Splitter and Combiner

Cold Plate

The cold plate or water cooled heat sink was designed to not only cool the nine transistors per amplifier, but also cool the entire amplifier card, the resistors used on the splitters on combiners and act as a mechanical support for the entire amplifier assembly including all the amplifier cards input splitters and output combiners. The same cold plate was used to support both the intermediate power amplifier layout as well as the power amplifier layout to eliminate the added costs in manufacturing and storing two different sets of cold plates that essentially perform the same task. The cold plate measures fifteen inches wide by twenty-seven inches deep and is made from 6063 aluminum with a 3/8 inch copper tube machined into the aluminum plate to be

approximately the same width as the amplifier cards. The copper tube makes six passes on the plate with the inner most two passes measuring slightly wider than the width of the transistor package. This allows the transistor to be mounted directly to the cold plate without risk of penetrating the copper tube. This also allows for the cooling fluid to flow in both directions past each transistor, thereby making all the transistors approximately the same temperature on that module. As is seen in Figure 3.39, by having fluid flow to the left on one side of the transistor and to the right on the other, the temperatures are averaged out along the entire length of all nine transistors, thus keeping all transistors operating at the same point.

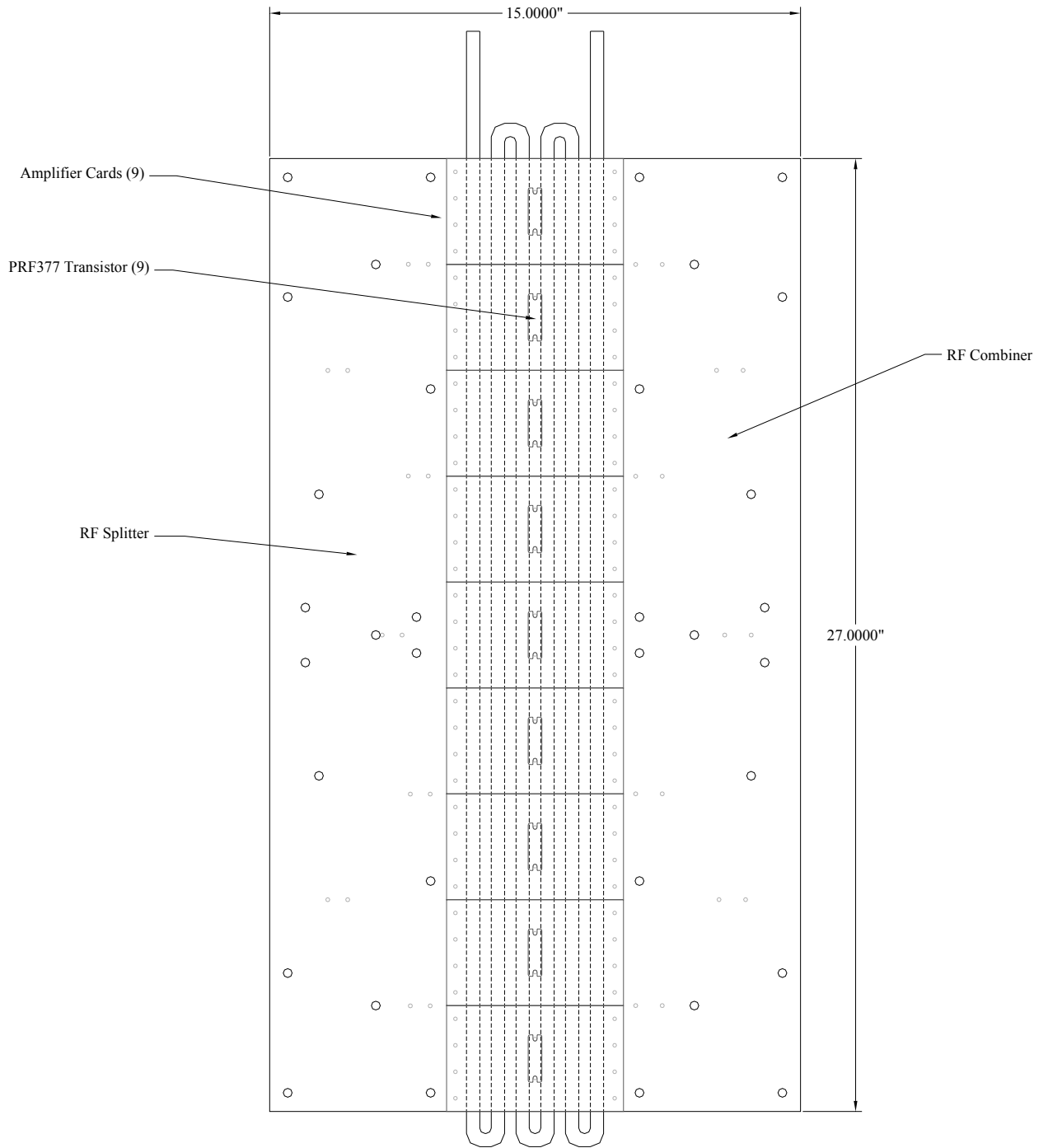


Figure 3.39 Amplifier Cold Plate Mechanical Design

To calculate the cooling requirements for the PA modules, it is known [24] that the transistors are only approximately 25 percent efficient, so with an amplifier module operating at 400 watts average power, the cooling system must be able to dissipate 1230 watts – 150 for each of the final amplifier cards and 30 for the driver card. With a maximum flow of 1.5 gallons per minute per module, the calculated temperature differential can be found using [25]:

$$\Delta t = \frac{Q}{WC_p} \quad (3-45)$$

where Q is the power to be dissipated in Cal/sec, W is the coolant flow rate in g/sec, and C_p is the specific heat of the coolant in cal/g, therefore,

$$\Delta t = \frac{4198}{(747)(0.997)} = 3.13^\circ C \quad (3-46)$$

The transistors have a maximum junction temperature (T_j) of 200°C and a thermal resistance ($R_{\theta JC}$) of 0.37°C/W. The thermal resistance of the heat sink compound is 0.03°C/W and the thermal resistance of the cold plate was measured to be 0.01°C/W.

The maximum theoretical fluid temperature entering the cold plate is calculated using:

$$200^\circ C - (150 \text{ watts} / \text{transistor})(0.37^\circ C/W) - (150 \text{ watts/transistor})(0.03^\circ C/W) - (1230 \text{ watts/module})(0.01^\circ C/W) = 127.7^\circ C \quad (3-47)$$

It was determined that operating the transistors at or near the rated temperature of

127.7°C seriously deteriorated the signal amplified by the transistors by increasing the IP3 noise and reducing the SNR and that temperature is too hot to maintain proper operation of the other components mounted to the cooling plate. Preliminary tests showed that the cooler the transistors were, the better the overall signal performance. During a conference call with the Motorola Engineering Group it was decided that a suitable cooling temperature is 15°C. After initial testing, the coolant input temperature was adjusted to 25°C because the lower temperature caused water to condense on the electronics and interfere with the proper operation of the amplifiers.

Intermediate Power Amplifier

The intermediate power amplifier (IPA) was designed using nine of the amplifier cards discussed earlier in this chapter. One of the cards acts as a driver for the other eight cards, with each providing a 0.4 watt output to drive each of the up to eight power amplifier modules. Prior to the input of the driver card is a MiniCircuits ZHL-3010 amplifier that provides 24 dB of gain (24 dB average, 30 dB peak) to amplify the output of the KTech modulator to an adequate level to excite the driver amplifier. See Figure 3.40 for an RF block diagram of the IPA module.

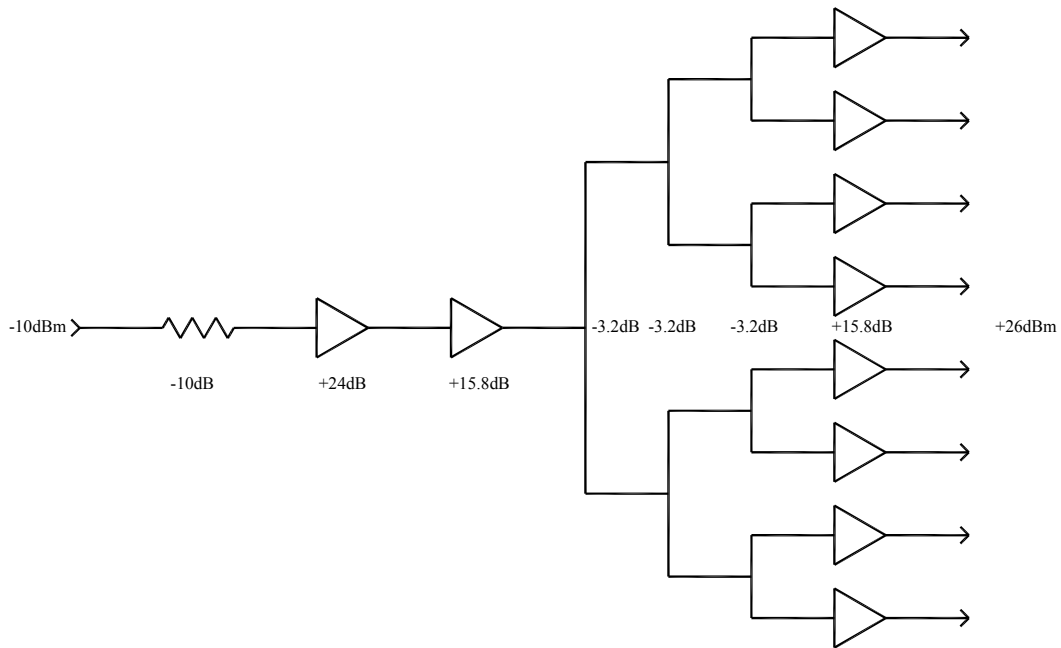


Figure 3.40 Intermediate Power Amplifier RF Block Diagram

The output of the driver card is split eight ways using a 9.6 dB Wilkinson power divider. Originally, broadband dividers were designed that had the bandwidth of approximately one third of the UHF television band, but to improve channel efficiency and linearity, the dividers were re-designed for individual channel use. The output of each of the eight amplifier cards is then fed to an individual SMA connector for distribution to the (up to) eight PA modules.

Power Amplifier

The power amplifier design (PA) is similar to that of the intermediate power amplifier in that it uses the same basic amplifier cards, but the overall module configuration is different (see Figure 3.41). The RF signal enters the module through an SMA connector mounted on the output combiner card. This feeds the input to the driver card with the output of this card feeding the eight-way Wilkinson splitter. The output of the splitter feeds the eight other amplifier cards at a level 9.6 dB below the output of the driver card. The outputs of the eight final amplifier cards are combined using a Wilkinson combiner which then feeds a single output type-N connector. This output can feed into another combiner to be combined with other modules in the transmitter or directly into the mask filter if low power operation is desired. The overall gain of the power amplifier module is 30.4 dB which results in an output of 400 watts average or 1.6 kilowatts peak. Figures 3.42 and 3.43 show pictures of the final assembly of the power amplifier drawer with the DC power distribution card removed and installed, respectively.

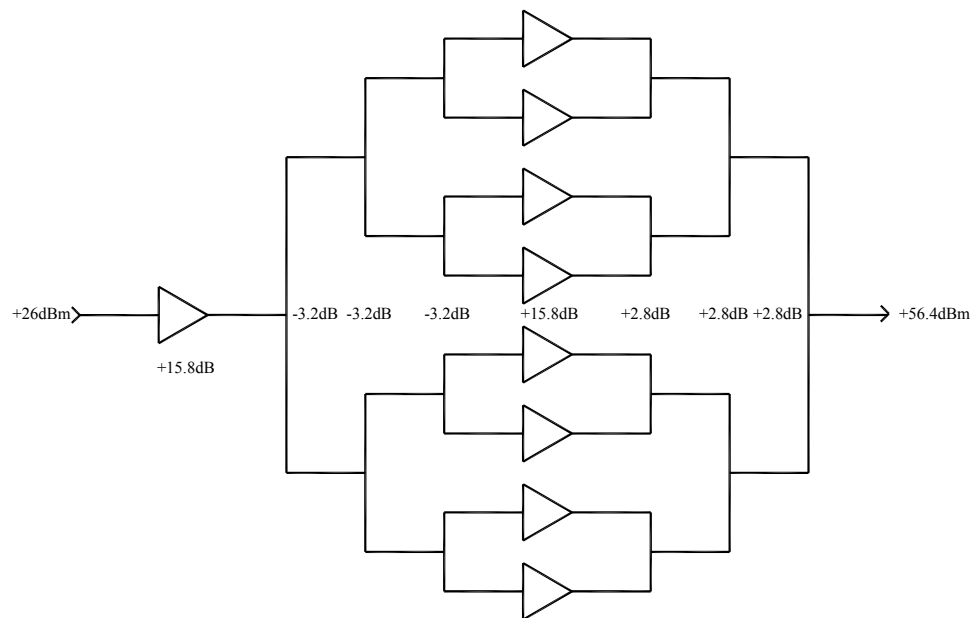


Figure 3.41 Power Amplifier RF Block Diagram

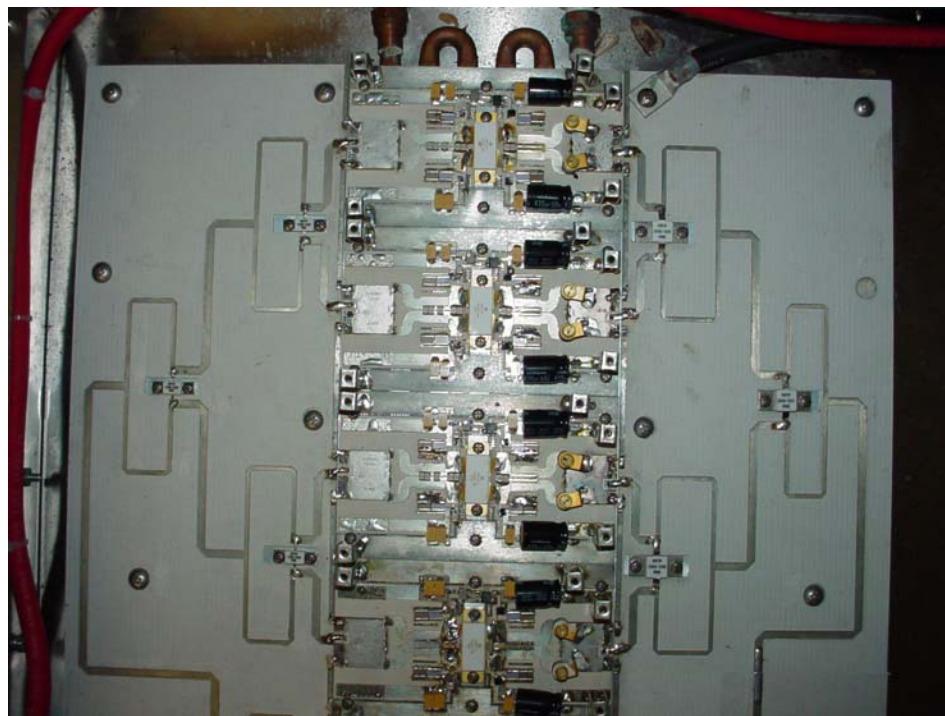


Figure 3.42 Final Amplifier Assembly with Power Distribution Card Removed

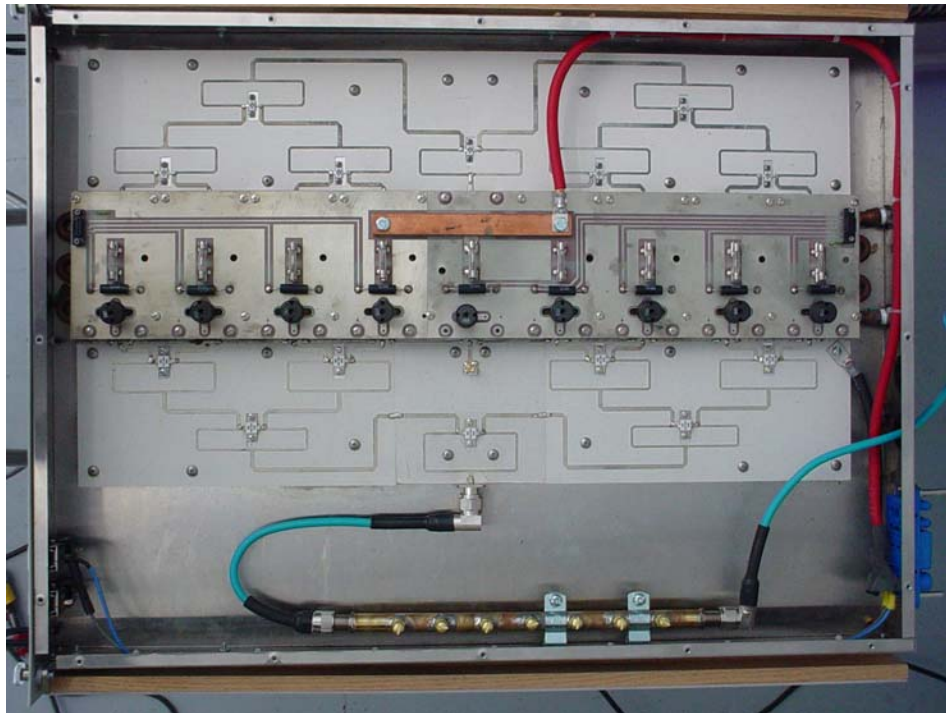


Figure 3.43 Complete Power Amplifier Module

Mask Filter

The last major component before the antenna is the filter. The filter consists of two components, a low pass filter used to trap spurious harmonic emissions generated by non-linear distortion in the amplifier circuits and the mask filter used to shape the output spectrum to keep it within the designated operating channel. The maximum out of band specification by the Federal Communications Commission require that [26]:

- (1) in the first 500KHz from the authorized channel edge, transmitter emissions must be attenuated no less than 47 dB below the average transmitted power;

- (2) more than 6 MHz from the channel edge emissions must be attenuated no less than 110 dB below the average transmitter power; and
- (3) at any frequency between 0.5 MHz and 6 MHz from the channel edge, emissions must be attenuated no less than the value determined by:
attenuation in dB = $11.5(Df+3.6)$ where Df = frequency difference in MHz from the edge of the channel.

See Figure 3.44 for a graphical representation of the DTV Emission Mask specifications.

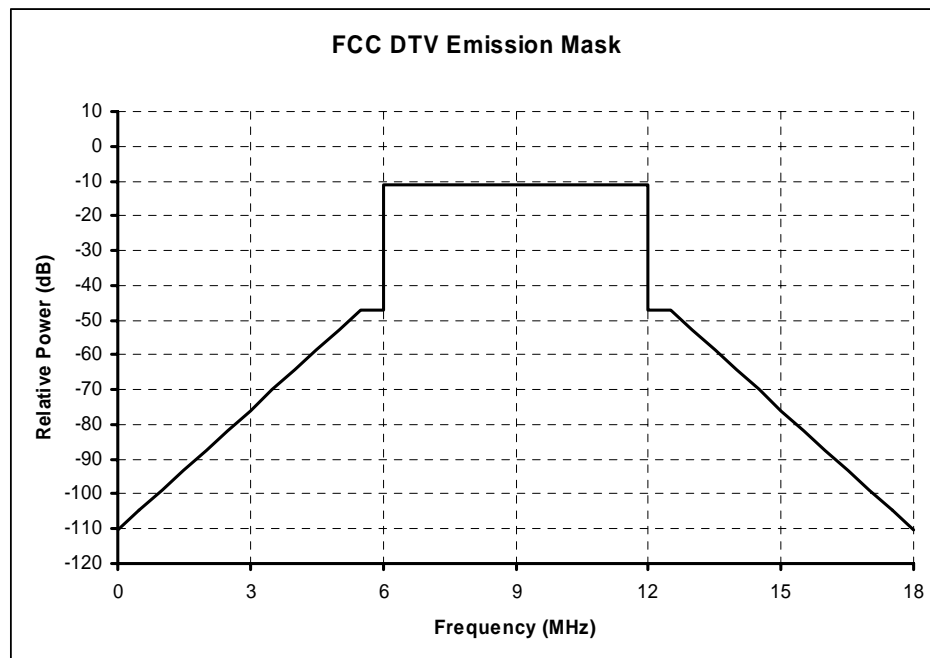


Figure 3.44 FCC DTV Emission Mask

Two types of bandpass filters may be used in a digital transmitter system, reflective or constant impedance. The reflective type filter is much simpler and less expensive than the constant impedance filter and works by simply having a matched

impedance for the inband frequencies and an unmatched impedance, or very large reactance, to the out of band frequencies. The major drawback to the reflective filter is that all the rejected energy is reflected back to the amplifier, which can cause even more non-linear distortion in a high power amplifier. The constant-impedance filter uses two reflective filters in parallel, with a hybrid splitter and hybrid combiner connecting the two filters. Fifty-ohm dummy loads are connected to the unused ports on the hybrids, and any energy reflected from the two filters is absorbed by the loads instead of the amplifier. It is easy to see that the constant-impedance filter is more than twice the cost of the reflective filter just based on the fact that more than twice the hardware is needed for the constant-impedance filter.

Due to cost restrictions, it was determined that a reflective type filter would be used for the 4kW transmitter. To overcome the reflected energy problem, a circulator would be placed at the output of each amplifier module to send any reflected energy to the dummy load and isolate the signal from the amplifier. A Tchebysheff filter design was chosen to accommodate the sharp edge requirements for the bandpass filter. The number of poles for the filter was determined by plotting criteria 2 from the FCC mask filter specification against the 0.01 dB ripple Tchebysheff filter characteristics. It is clear that a nine pole or better filter would suffice for the given specification. See Figure 3.45 for this graphical comparison.

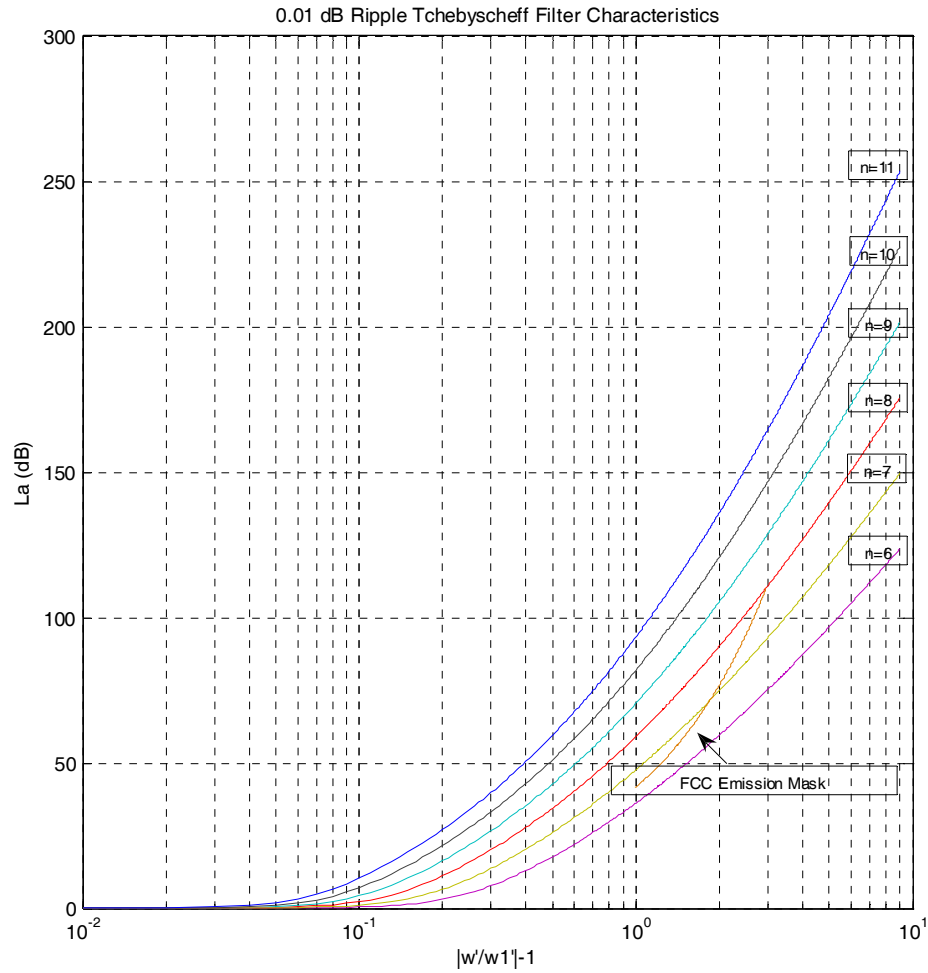


Figure 3.45 Graphical Comparison of 0.01 dB Ripple Tchebyscheff Filter Characteristics

In Figure 3.45, L_a is the maximum attenuation, and w' is the band edge. This figure was generated using the formulae for the Tchebyscheff attenuation characteristic [27]:

$$L_a(\omega') = 10 \log_{10} \left\{ 1 + \varepsilon \cos^2 \left[n \cos^{-1} \left(\frac{\omega'}{\omega_1'} \right) \right] \right\}_{\omega' \leq \omega_1'} \quad (3-48)$$

$$L_a(\omega') = 10 \log_{10} \left\{ 1 + \varepsilon \cosh^2 \left[n \cosh^{-1} \left(\frac{\omega'}{\omega_1'} \right) \right] \right\}_{\omega' \geq \omega_1'} \quad (3-49)$$

where:

$$\varepsilon = \left[10^{\left(\frac{L_{dr}}{10} \right)} \right] - 1 \quad (3-50)$$

$$\frac{\omega'}{\omega_1'} = \frac{2}{w} \left(\frac{f - f_0}{f_0} \right) \quad (3-51)$$

$$w = \frac{\omega_2 - \omega_1}{\omega_0} \quad (3-52)$$

$$\omega_0 = \frac{\omega_2 + \omega_1}{2} \quad (3-53)$$

The first filter constructed is designed for channel 16 with a passband of 482 through 488MHz. A rectangular waveguide filter was selected because of its ease of construction and therefore the specifications for rectangular waveguide WR 1800 is used to accommodate the frequency range for channel 16. A standard $\lambda/2$ nine pole cavity filter with input and output cavities at 485Mhz would be approximately fifteen feet long. A new type of filter was designed to reduce the length of the filter and at the time of construction, a folded waveguide filter was not available from any commercial source. This filter uses a combination of end coupled and side coupled cavities to “fold” the filter in half. This design made it possible to either hang the filter above the transmitter so as

to have a similar footprint as the transmitter, or it can sit on the floor with the folded end down. The irises between the input and output cavities are labeled as $Qe(a)$ and $Qe(b)$, respectively, and the inter-cavity irises are numbered Kij with i and j representing the number of the cavities for which that iris is connecting. See Figure 3.46 for a diagram of the folded waveguide filter and panel numbering scheme.

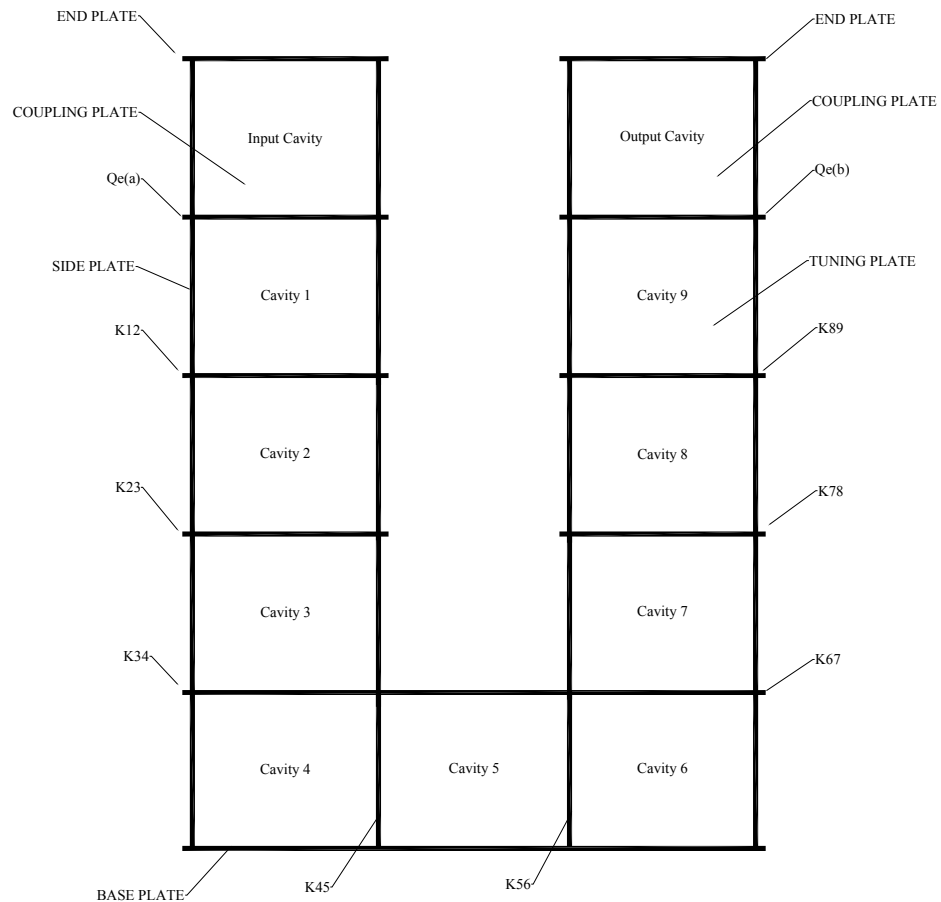


Figure 3.46 Assembly Diagram of the Folded Waveguide Filter

The filter was designed with the following criteria:

Waveguide dimension a	= 18 inches
Waveguide dimension b	= 9 inches
Bandwidth (bw)	= 6 MHz
Center frequency (f_0)	= 485 Mhz
Number of poles (n)	= 9
Number of half guide wavelengths (s)	= 1
Iris thickness	= 0.25''

The free-space wavelength at this frequency is 24.35 inches and the guide wavelength is determined according to:

$$\lambda_g = \frac{\lambda}{\sqrt{1 - \left(\frac{\lambda}{2a}\right)^2}} \quad (3-54)$$

Which gives λ_g of 33.07 inches ($\lambda_g/2 = 16.54$ inches). The cavity dimensions for the TE₁₀₁ waveguide filter are thus 16.54 inches tall, 18.0 inches wide and 9.0 inches deep. Since no data was available to assist in the correction of the iris thickness for cavity size, it is suggested in the literature [28] to measure the cavity height from the centerline of one iris to the centerline of the next.

The iris dimensions are selected from Table 3.4 by moving down the left hand column and selecting the number of poles desired and then reading across that row the low-pass prototype values of the filter [29].

Table 3.4
Element Values for 0.01 dB Ripple Tchebyscheff Filter

Element Values for 0.01 dB Ripple Tchebyscheff Filter											
n	g1	g2	g3	g4	g5	g6	g7	g8	g9	g10	g11
1	0.0960	1.0000									
2	0.4488	0.4077	1.1007								
3	0.6291	0.9702	0.6291	1.0000							
4	0.7128	1.2003	1.3212	0.6476	1.1007						
5	0.7563	1.3049	1.5773	1.3049	0.7563	1.0000					
6	0.7813	1.3600	1.6896	1.5350	1.4970	0.7098	1.1007				
7	0.7969	1.3924	1.7481	1.6331	1.7481	1.3924	0.7969	1.0000			
8	0.8072	1.4130	1.7824	1.6833	1.8529	1.6193	1.5554	0.7333	1.1007		
9	0.8144	1.4270	1.8043	1.7125	1.9057	1.7125	1.8043	1.4270	0.8144	1.0000	
10	0.9106	1.4369	1.8192	1.7311	1.9362	1.7590	1.9055	1.6527	1.5817	0.7446	1.1007

Once the low-pass prototype values are determined, the external Qs, $(Q_e)_A$ and $(Q_e)_B$, are calculated using equation 3-55. The magnetic polarizability, M_I , is found using equation 3-56 followed by the iris dimensions d_1 and d_2 . Because the irises are not small with respect to the free-space wavelength (d_2 considerably less than λ), a magnetic polarizability compensation formula is applied using equation 3-59. The final value for the iris dimensions d_1'' and d_2'' as shown in Figure 3.47 are calculated using equations 3-60 through 3-63 [31]. For a nine-pole filter $g_0, g_{10}=1.000$, $g_1, g_9=0.8144$, $g_2, g_8=1.4270$, $g_3, g_7=1.8043$, $g_4, g_6=1.7125$ and $g_5=1.9057$.

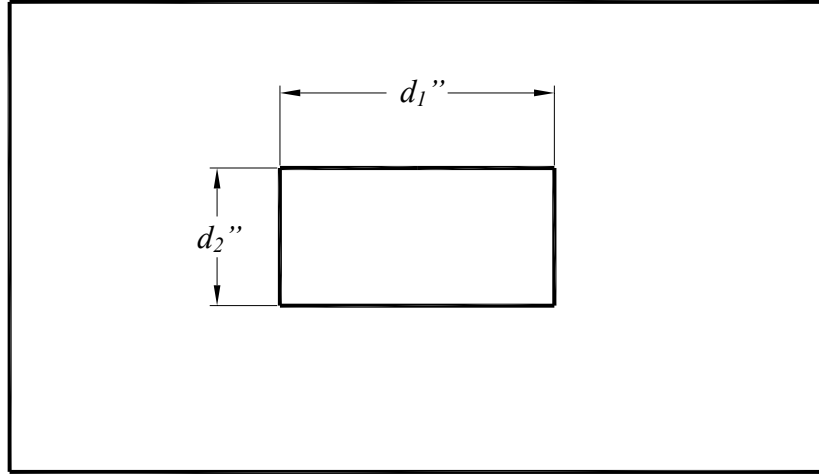


Figure 3.47 Location of d_1 and d_2 on the Coupling Iris

$$(Q_e)_A = (Q_e)_B = \frac{g_0 g_1 \omega l}{w} = \frac{g_9 g_{10} \omega l}{w} = \frac{(1.000)(0.8144)(1)}{0.01237} = 65.8367 \quad (3-55)$$

$$M_1 = \sqrt{\frac{l^3 a^2 b^2 \lambda_g}{4\pi s^2 Q_e \lambda^2}} = \sqrt{\frac{(16.54)^3 (18.0)^2 (9.0)^2 (33.07)}{4\pi (1)^2 (65.8367)(24.35)^2}} = 89.47 \quad (3-56)$$

$$d_1 = \sqrt[3]{\frac{M_1}{0.157}} = \sqrt[3]{\frac{89.47}{0.157}} = 8.29 \quad (3-57)$$

$$d_2 = \frac{d_1}{2} = \frac{8.29}{2} = 4.15 \quad (3-58)$$

$$M_1' = \frac{M_1}{1 - \left(\frac{2d_1}{\lambda}\right)^2} = \frac{89.47}{1 - \left(\frac{2(8.29)}{24.35}\right)^2} = 166.81 \quad (3-59)$$

$$d_1' = \sqrt[3]{\frac{M_1'}{0.157}} = \sqrt[3]{\frac{166.81}{0.157}} = 10.20 \quad (3-60)$$

$$d_2' = \frac{d_1'}{2} = \frac{10.20}{2} = 5.10 \quad (3-61)$$

$$d_1'' = d_1 \left(\frac{d_1}{d_1'} \right) = 8.29 \left(\frac{8.29}{10.20} \right) = 6.74 \text{ inches} \quad (3-62)$$

$$d_2'' = \frac{d_1''}{2} = \frac{6.74}{2} = 3.37 \text{ inches} \quad (3-63)$$

The final iris size for the input and output coupling cavities is 6.74 by 3.37 inches (see Figure 3.48 for the shop drawing).

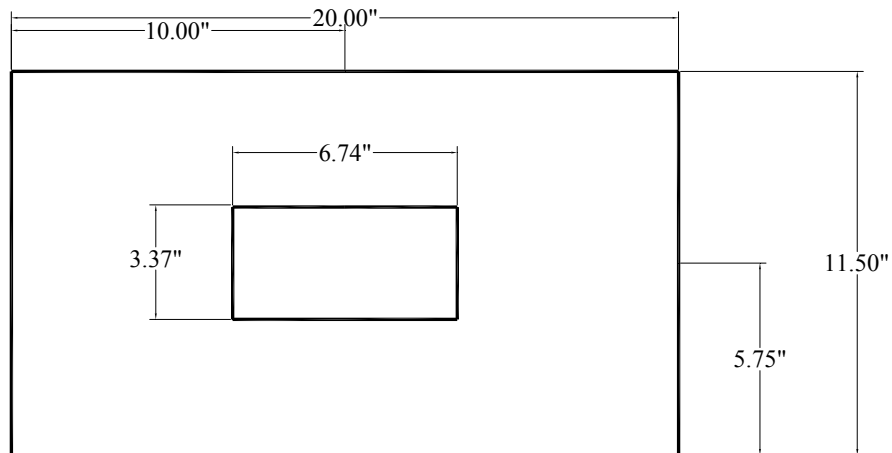


Figure 3.48 Shop Drawing for the Mask Filter Panels Qe(a) and Qe(b)

The inter-cavity panels were oversized to allow for welding, but the final cavity panel size is 9.0 by 18.0 inches once assembled. A partially assembled cavity is shown in Figure 3.49. The square piece welded to the top of the cavity holds a one inch diameter tuning rod for fine tuning of the cavity.



Figure 3.49 Partially Assembled Filter Cavity

The irises in the panels between the end-coupled filter sections were calculated using a similar method as described above for the coupling cavities, only the coupling coefficient k is calculated using the values selected from the Tchebyscheff table and equation 3-64. The magnetic polarizability is calculated using equation 3-65 and the diameter of the coupling irises using 3-66. The magnetic polarizability is once again compensated for using equations 3-67 and 3-68.

$$k_{xy} = \frac{w}{\sqrt{g_x g_y}} \quad (3-64)$$

$$M_{1,xy} = \frac{k_{xy} l^3 ab}{\lambda^2 s^2} \quad (3-65)$$

$$d_{xy} = \sqrt[3]{6M_{1,xy}} \quad (3-66)$$

$$M_{1,xy}' = \frac{M_{1,xy}}{1 - \left(\frac{1.706d_{xy}}{\lambda}\right)^2} 10 \left[\frac{2.73tA}{1.706d_{xy}} \sqrt{1 - \left(\frac{1.706d_{xy}}{\lambda}\right)^2} \right] \quad (3-67)$$

$$d_{xy}' = \sqrt[3]{6M_{1,xy}'} \quad (3-68)$$

The design data for the end-coupled cavities is found in Table 3.5.

Table 3.5

Calculated Values for End-Coupled Cavity Irises

	k _{xy}	M ₁	d	M ₁ '	Diameter (inches)
k12	0.01148	14.171983	4.3973796	12.828642	4.25
k23	0.00771	9.517943	3.8509225	8.1531316	3.66
k34	0.00704	8.6908325	3.7359771	7.3540619	3.53
k67	0.00704	8.6908325	3.7359771	7.3540619	3.53
k78	0.00771	9.517943	3.8509225	8.1531316	3.66
k89	0.01148	14.171983	4.3973796	12.828642	4.25

For the side-coupled cavities we substitute the following formula:

$$M_{l_{xy}} = \frac{k_{xy} l a^3 b}{\lambda^2} \quad (3-69)$$

The design data for the side coupled cavities is found in Table 3.6.

Table 3.6

Calculated Values for Side-Coupled Cavity Irises

	kxy	M1	d	M1'	Diameter (inches)
k45	0.00685	10.023403	3.9179193	8.6465076	3.73
k56	0.00685	10.023403	3.9179193	8.6465076	3.73

where k_{xy} is the coupling coefficient, $M_{l_{xy}}$ is the magnetic polarizability, $M_{l_{xy}}'$ is the magnetic polarizability compensated for small irises with respect to the free-space wavelength, $d_{l_{xy}}$ is the iris diameter and $d_{l_{xy}}'$ is the final iris diameter after having applied the magnetic polarizability compensation formula. Figure 3.50 shows the shop drawing for all the inter-cavity filter panels.

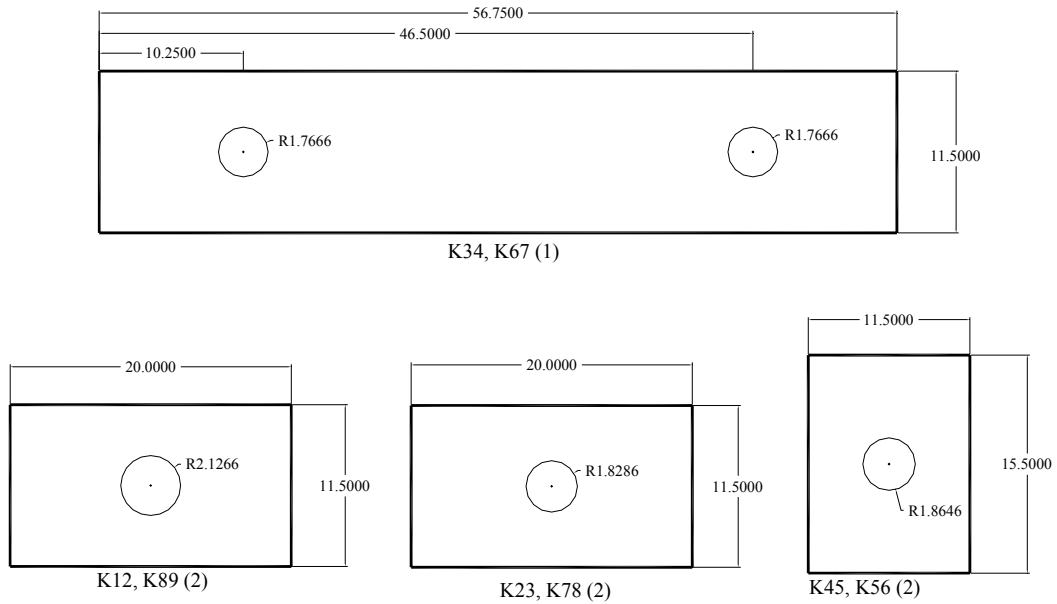


Figure 3.50 Shop Drawing for the Inter-Cavity Filter Panels K12, K23, K34, K45, K56, K78 and K89 (All Units are Inches)

All the metal was precision laser cut from 6061 aluminum 0.25 inch thick at Hawkeye Industries in Tupelo, Mississippi. Once assembled the filter was initially swept and tuned using an Agilent 8753ET network analyzer. Figure 3.51 shows the results of the initial tuning.

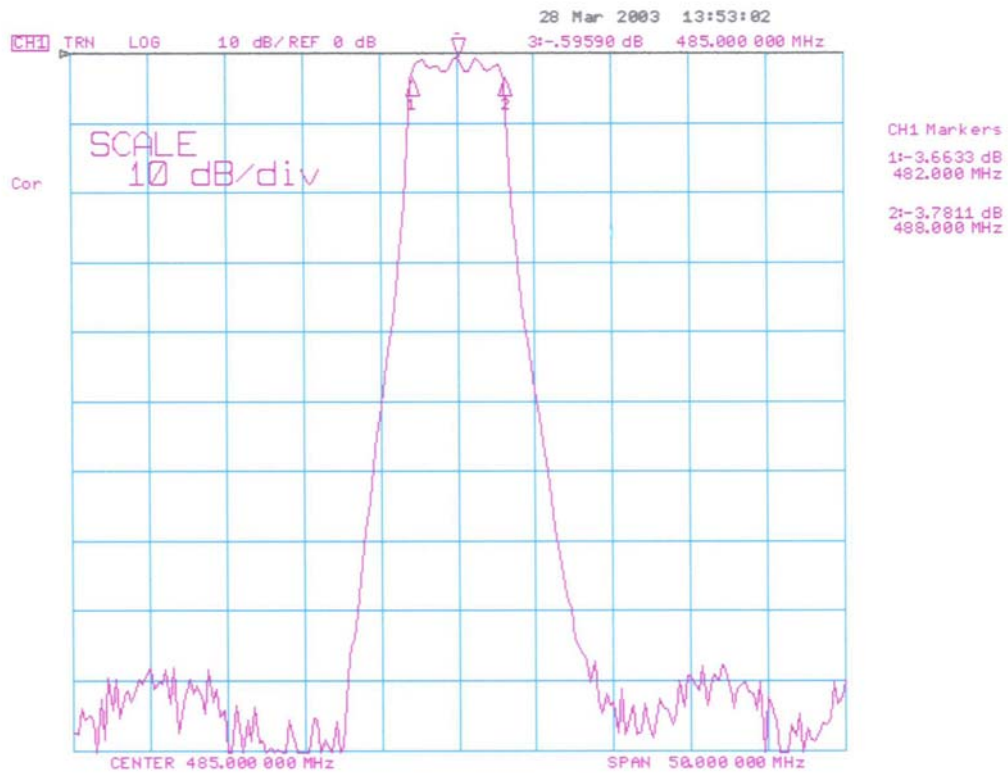


Figure 3.51 Results of the Initial Tuning for the Folded Waveguide Filter

Fine tuning was performed by generating an on-channel digital television signal with the transmitter and viewing the results on a Tektronics RFA300A digital television analyzer. The results of the final tuning are shown in Figure 3.52 and it is evident that the filter meets the FCC mask filter requirements.

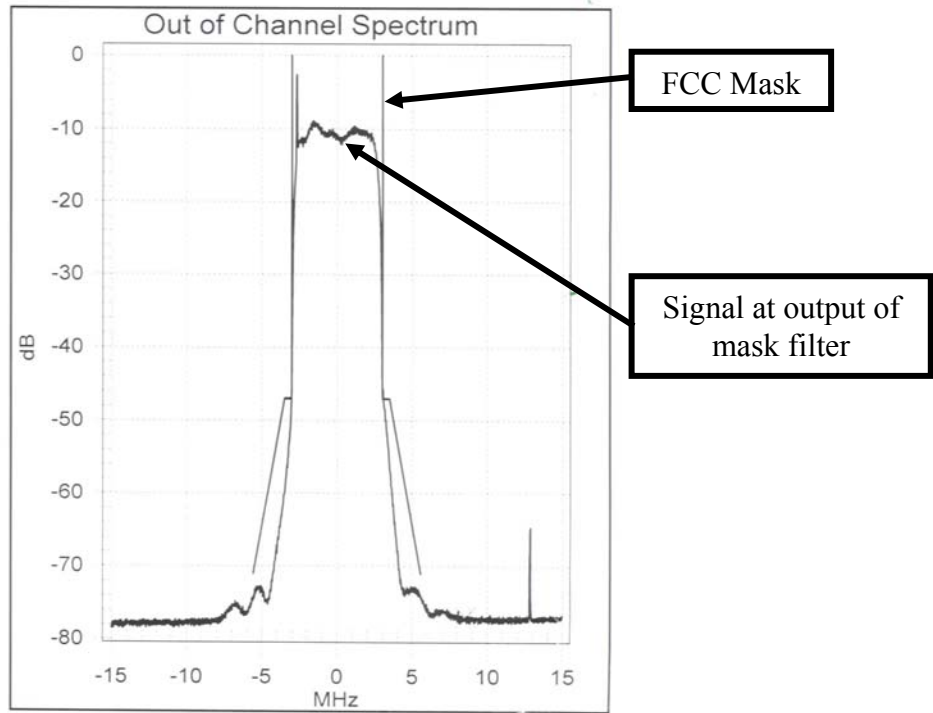


Figure 3.52 Final Tuning Results for the Channel 16 Mask Filter

Figure 3.53 shows the front of the filter during assembly and Figure 3.54 shows the rear. The tuning slugs can be seen in the center of the filter cavities, and the input cavity is cut to accept EIA 3 1/8" transmission line. The completed filter is shown in Figure 3.55.



Figure 3.53 Folded Waveguide Filter Front during Assembly



Figure 3.54 Folded Waveguide Rear during Assembly



Figure 3.55 Complete Folded Waveguide Filter

The input and output waveguide cavities need to transition from and to coaxial transmission lines. This is accomplished by using a reactively tuned simple transition [31] which is the outside diameter of the center conductor of a coaxial line that protrudes into the waveguide cavity at approximately one-quarter wavelength. The depth and

position of the transition post inside the waveguide cavity is adjusted to obtain the optimal match. The input impedance of the waveguide filter [32] is defined by

$$Z_I = R + jX \quad (3-70)$$

where

$$R = \frac{Z_0}{2\pi^2} \frac{\lambda\lambda_g}{ab} \sin^2 \frac{2\pi l}{\lambda_g} \tan^2 \frac{\pi d}{\lambda} \quad (3-71)$$

$$X = \frac{Z_0}{4\pi^2} \frac{\lambda\lambda_g}{ab} \tan^2 \frac{\pi d}{\lambda} \left[2x + \sin \frac{4\pi l}{\lambda_g} \right] \quad (3-72)$$

$$Z_0 = \sqrt{\mu_0 \epsilon_0} = 376.6\Omega \quad (3-73)$$

where λ is the free-space wavelength, λ_g is the guided wavelength, a and b are the waveguide dimensions, d is the probe depth, l is the length of the probe from the closed end of the cavity and x (lowercase) is the reactance of the post normalized with respect to the waveguide impedance, see Figure 3.56. For the channel 16 filter at resonance:

$$X = 0 = (9.5419)(4.9707) \tan^2 \left[\frac{d}{7.7508} \right] \sin \left[\frac{l}{0.3800} \right] \quad (3-74)$$

Where the post reactance is equal to zero when $d=0$ and the filter reactance is zero-valued when the sine term in equation 3-74 is zero which gives [33]

$$d = 0 \quad (3-75)$$

$$\frac{l}{0.3800} = n\pi, \quad n=0,1,2\dots \quad (3-76)$$

The values of l are $\{0'', 8.2675'', 16.5374'', \dots\}$. Choosing $l = 8.2675''$ gives

$$50 = (19.0838)(4.9707)(1.0000) \tan^2 \left[\frac{d}{7.7508} \right] \quad (3-77)$$

Solving equation 3-77 gives $d = 4.8673''$. The probe was constructed of silver plated brass and located at the center of the coupling cavity with a probe depth of $4.875''$, which provided the results shown in Figures 3.51 and 3.52.

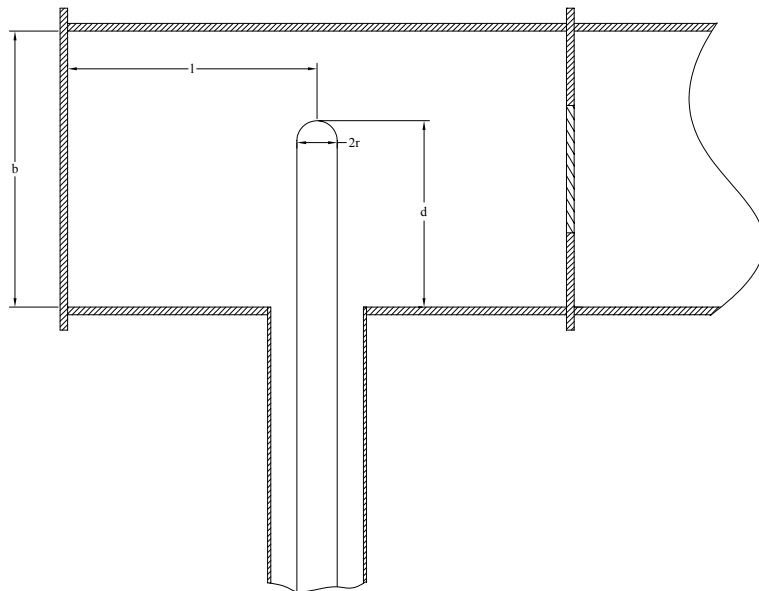


Figure 3.56 Coax-to-Waveguide Transition

Cooling System

The datasheet for the Motorola PRF377 UHF Power Transistor states that the operating junction temperature of the device has a maximum value of 200°C. One of the commonly used and very effective methods of cooling electronic components is by the use of heat sinks which provides an extended surface area to dissipate the heat to the cooling fluid or air [34]. Air cooling of solid-state television transmitters is commonplace, but it is desired to maintain tighter control over the operating characteristics of the transmitter and the transistor operating point. Device reliability is of great concern in the broadcast industry and with stacked and combined RF modules it has been shown [35] that the modules located near the top of the stack have a greater failure rate than those near the bottom due to the increase in temperature at the top of the cabinet. Liquid phase and vapor phase cooling is standard practice for high power klystrons and liquid cold plate technology could easily be adapted to solid-state broadcast transmitters. It has been demonstrated [36] that single device power dissipation has been achieved to 118W/cm² with liquid phase cooling, twice that of standard fin heat sink air cooling.

The transmitter cooling system is driven by an ArtiChill refrigerated liquid chiller which is a weatherproof self contained unit that houses the pump, expansion tank and refrigerated chiller (see Figure 3.57).



Figure 3.57 Refrigerated Chiller Installed at KTFL-TV in Flagstaff, Arizona

The fluid used to cool the transmitter is a 50% mixture of distilled water and DowFrost glycol. The chilled liquid enters the transmitter through the top of the cabinet and immediately enters a combination temperature/pressure/flow gauge custom manufactured by Proteus Industries. After passing through the gauge, the coolant then flows into a nine port manifold and into another identical temperature/pressure/flow gauge. The two gauges monitor the coolant temperature flowing into the transmitter to verify that the chiller is working properly and monitor the temperature of the coolant leaving the transmitter to monitor the proper operation of the transmitter and to help measure the overall efficiency of the system. The pressure sensors are used to measure the differential pressure in the transmitter in order to signal the control system to shut

down the transmitter and pump if the difference between the input and output is too great, possibly indicating a clogged coolant line or a leak. The flow sensors verify that the pump is working correctly and providing enough coolant to the transmitter, and also measure the differential to monitor for coolant leaks. Figure 3.58 details the complete schematic of the cooling system. The manifold consists of two stainless steel tubes each with nine 3/8 inch stainless steel tubes welded on the side. At the end of each of the eighteen 3/8 inch tubes is a quarter-turn ball valve which feed a short length of flexible stainless steel hose that terminates into a quick-disconnect self sealing coupling. Since the modules are built to be removed from the front, a self-sealing type connection is essential to prevent spillage.

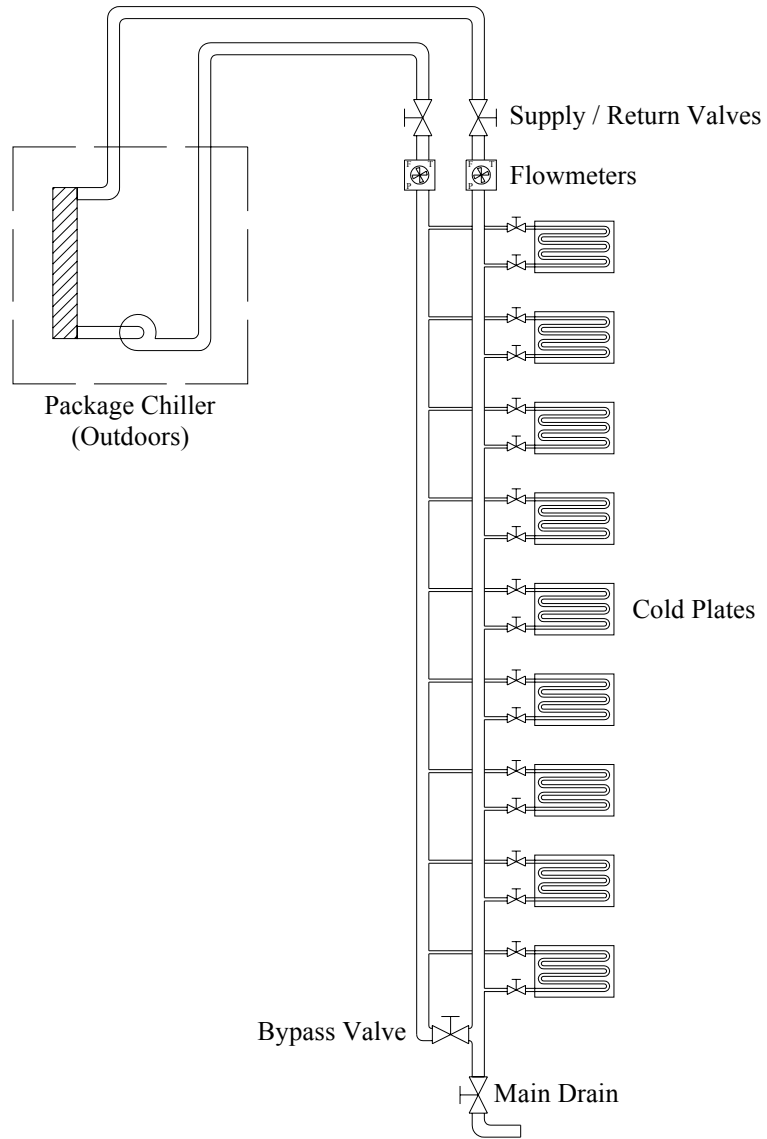


Figure 3.58 Cooling System Schematic

Control System

The control system for the DT-4KU UHF digital television transmitter is built around the GE Fanuc family of products including the GE Fanuc Programmable Logic Controller and a touch-screen graphical user interface running the Cimplicity [37] control software with custom programming for the DT-4KU transmitter. The control system not only provides transmitter system control and a local user interface, but also provides for remote control and monitoring as required by the Federal Communications Commission.

The primary role of the PLC is to interface all the individual hardware control and monitoring components to the software running in the touch-screen graphical user interface. The PLC consists of the power supply and backplane to run the PLC, the CPU module and the input output (I/O) modules. The first module in the rack is the IC693CPU364 central processor unit that is capable of interfacing to 2048 discrete input points, 2048 discrete output points, 2048 analog input points and 512 analog output points. The CPU has up to 9999 internal memory registers and has the ability to talk to a combination of several serial devices, via Ethernet or RS-232 connection.

The second module in the PLC rack is the IC693MDL740 which is a 16 circuit discrete output module with 12 or 24 VDC outputs. This module provides the primary means of system control for the transmitter. The third module in the rack is the IC693MDL645 which has 16 discrete 24VDC inputs for system monitoring. The fourth module in the PLC rack is the IC693ALG222 which is a 16 circuit analog input module capable of monitoring DC voltages from 0 to +10V DC which was optionally installed for remote control and monitoring. The last module in the rack is the IC693ALG223 16

circuit analog input module capable of monitoring a 4-20mA current loop. When possible, the current loop method of analog monitoring was used in the transmitter to avoid RF interference problems commonly found with DC voltage metering in a high level RF environment. Table 3.7 shows a complete list of I/O points for the transmitter system PLC.

Table 3.7

PLC Slot Assignments

PLC Slot	Module	Module Channel	PLC I/O Address	Module Terminal Number	Wire Color	Description
1	IC693CPU364				RD	Main PA 480V Contactor
2	IC693MDL940	1	Q1	2	RD	
2	IC693MDL940	2	Q2	3	RD	Power Lower
2	IC693MDL940	3	Q3	4	RD	Power Raise
2	IC693MDL940	4	Q4	5	user	Chiller Start
2	IC693MDL940	5	Q5	7		
2	IC693MDL940	6	Q6	8		
2	IC693MDL940	7	Q7	9		
2	IC693MDL940	8	Q8	10		
2	IC693MDL940	9	Q9	12		
2	IC693MDL940	10	Q10	13		
2	IC693MDL940	11	Q11	14	GN	IPA Power Supply A Inhibit
2	IC693MDL940	12	Q12	15	GN	IPA Power Supply B Inhibit
2	IC693MDL940	13	Q13	17	GN	PA Power Supply 1 Inhibit
2	IC693MDL940	14	Q14	18	GN	PA Power Supply 2 Inhibit
2	IC693MDL940	15	Q15	19	GN	PA Power Supply 3 Inhibit
2	IC693MDL940	16	Q16	20	GN	PA Power Supply 4 Inhibit
3	IC693MDL645	1	Q17	2	BL	IPA Power Supply A Present
3	IC693MDL645	2	Q18	3	RD	IPA Power Supply A Fault
3	IC693MDL645	3	Q19	4	BL	IPA Power Supply B Present
3	IC693MDL645	4	Q20	5	RD	IPA Power Supply B Fault
3	IC693MDL645	5	Q21	6	BL	PA Power Supply 1 Present
3	IC693MDL645	6	Q22	7	RD	PA Power Supply 1 Fault
3	IC693MDL645	7	Q23	8	BL	PA Power Supply 2 Present
3	IC693MDL645	8	Q24	9	RD	PA Power Supply 2 Fault
3	IC693MDL645	9	Q25	10	BL	PA Power Supply 3 Present
3	IC693MDL645	10	Q26	11	RD	PA Power Supply 3 Fault
3	IC693MDL645	11	Q27	12	BL	PA Power Supply 4 Present
3	IC693MDL645	12	Q28	13	RD	PA Power Supply 4 Fault
3	IC693MDL645	13	Q29	14		
3	IC693MDL645	14	Q30	15		
3	IC693MDL645	15	Q31	16		
3	IC693MDL645	16	Q32	17	RD/BK	Three Phase Detector Input
4	LEFT EMPTY FOR EXPANSION					
5	IC693ALG223	1	AI17	3	GN	Water Flow In
5	IC693ALG223	2	AI18	4	BL	Water Temperature In
5	IC693ALG223	3	AI19	5	WH	Water Pressure In
5	IC693ALG223	4	AI20	6	GN	Water Flow Out
5	IC693ALG223	5	AI21	7	BL	Water Temperature Out
5	IC693ALG223	6	AI22	8	WH	Water Pressure Out
5	IC693ALG223	7	AI23	9	WH	IPA Power Supply A Current
5	IC693ALG223	8	AI24	10	WH	IPA Power Supply B Current
5	IC693ALG223	9	AI25	11	WH	PA Power Supply 1 Current
5	IC693ALG223	10	AI26	12	WH	PA Power Supply 2 Current
5	IC693ALG223	11	AI27	13	WH	PA Power Supply 3 Current
5	IC693ALG223	12	AI28	14	WH	PA Power Supply 4 Current
5	IC693ALG223	13	AI29	15		
5	IC693ALG223	14	AI30	16		
5	IC693ALG223	15	AI31	17	RD	RF Forward Power
5	IC693ALG223	16	AI32	18	OR	RF Reflected Power

Provisions are made for hardware input and output for remote control and remote monitoring, but to date have never been implemented. All systems built to date were remote controlled using either an ethernet or RS-232 link directly from the touch screen controller.

All the I/O connections to the PLC were made using foil shielded with drain low-voltage wiring. All the shield wires were connected to a single common point ground located in close proximity to the PLC to minimize the RF interference from this transmitter and other transmitter systems that may be operating in close proximity to this unit. The block diagram of the DT-4KU control system can be seen in Figure 3.59.

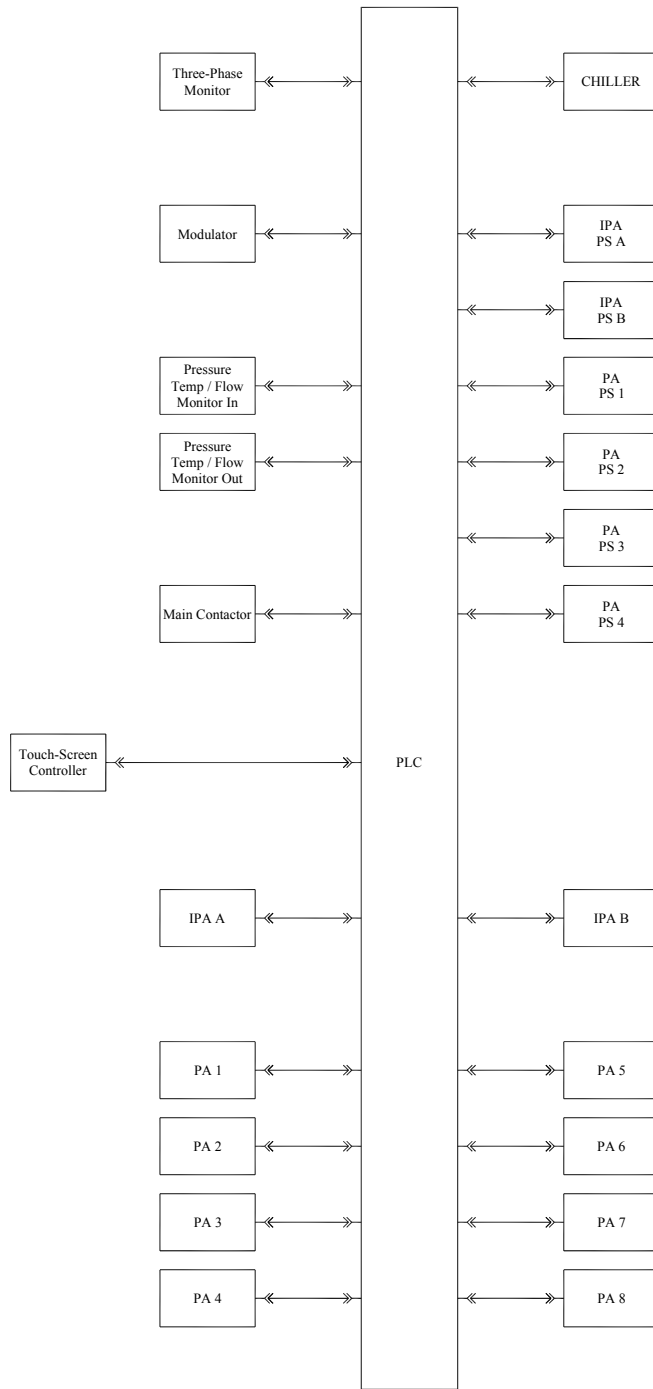


Figure 3.59 Control System Block Diagram

The system software was written using GE Fanuc's Cimplicity PLC programming language. The software was written to not only control the transmitter, but to protect it and its users from damage due to component failure or potential misuse. The software constantly monitors the water flow, temperature and pressure, the RF out of the transmitter, the reflected power back into the transmitter, the AC line voltage, the status of the modulator and the status of the power supplies. Should any one of these monitored points produce an out of tolerance condition, the control system will tag it as either a warning or a failure, record the event, try to correct the event and shut the transmitter down if the failure cannot be corrected. The control system and modulator are backed up by an uninterruptible power supply that protects these critical components from a power anomaly and maintains operation of the control system during a power interruption. Should an interruption occur, the three phase monitor sends a signal to the PLC indicating a failure. The PLC then puts the transmitter in a shutdown condition and waits for power to be restored. Depending on the length of the interruption, the controller will either immediately turn the transmitter back on when power is restored, or re-cycle the transmitter from a cold-start condition if the power is off for an extended period.

Upon first powering up the transmitter, the user is presented with the Operator Menu, see Figure 3.60. From this menu, the operator has the ability to perform the basic transmitter functions – transmitter on and off, transmitter power raise and lower. Also from this menu, the operator also has the ability to monitor the forward and reflected power, the water temperature, pressure and flow and the current active alarms. The user can also select the advanced menu from the main menu. From the advanced menu, he

can navigate to other screens that include a full alarm screen, with alarm reset capability, the alarm history screen that shows a complete list of transmitter alarms for the past thirty days, the power amplifier screen that displays some diagnostic information about the PA modules and can also select the cooling screen that displays additional information about the cooling system and offers some options to the user.

The advanced menu also has four additional softkeys that are for system calibration and configuration. The system limits screen allows the operator to set the warning and alarm trip points for all the analog monitor points. The operator also has the ability to bypass specific alarms if he feels the alarm is in error and needs to get back on the air.

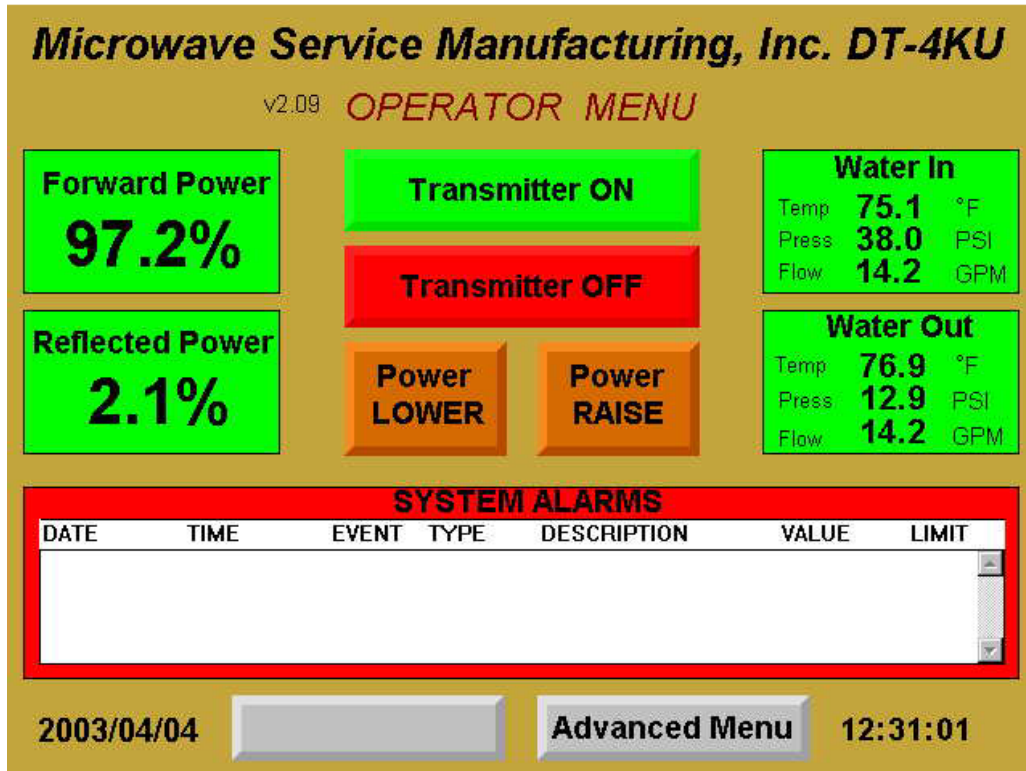


Figure 3.60 Transmitter Control System Operator Menu

The system faults screen is used to set the trip condition of a discrete input and the use can also bypass an input on this screen, in case of a false trip. There is also a configuration softkey that allows the user to calibrate the analog input signals. All the analog inputs are calibrated at the time of system installation, but if the operator feels the need to re-calibrate, he has the ability to do so. The last button in this group of four is the system shutdown button. This key is password interlocked and shuts only the software down in case the user needs to perform maintenance on the touch-screen computer. The transmitter will remain in the state it was last in when the software is shutdown with limited fault checking from the program running inside the PLC. It is therefore not

recommended that the operator have access to this button without thorough knowledge of the transmitter system.

Running in the PLC CPU module is a small routine that checks to make sure the water is flowing properly in the transmitter, and is within the proper temperature range. This is a failsafe routine that will inhibit the closure of the 480V AC contactor that supplies power to the amplifier modules, but will not generate any alarms. Primary control resides with the touch-screen controller, and the failsafe resides within the PLC.

AC and DC Power Distribution

The transmitter is normally powered by a 480 volt, 100 amp, three phase service that supplies power to the entire transmitter including the chiller and the 120 volt electronics. The service enters the transmitter through the CB1, a 100A three phase circuit breaker marked MAIN on the front of the PA rack. From there the power is split into three directions, first to CB107, a 20A three phase breaker that feeds the chiller. Second to CB2, a 15A three phase breaker that feeds T1, the 9.6 kVA step down transformer that steps the 480 volt three phase input down to 120/208 three phase power for the modulator and control system. The third path is through K1 which is the main contactor that provides power to all the 32V DC power supplies that power the IPA and PA amplifier modules.

On the low voltage side of T1, there is CB3, a 30A three phase breaker that acts as the main for all the 120/208 volt equipment that feeds eight other breakers. CB10 is a single pole 20A breaker that feeds the convenience outlet in the driver and control rack.

CB11 is a single pole 20A breaker that feeds the convenience outlet in the amplifier rack. CB12 is a 30A single pole breaker that feeds the 3kW uninterruptible power supply that supplies power for all the modulator and control electronics. CB13 is a dual phase 1A breaker that feeds T2, which ultimately drives K1, the main contactor for the amplifier power supplies. CB14 is a 5A single pole breaker that feeds a 24V DC power supply that is used for general purpose control. CB15 is a single pole 5A breaker that feeds the cabinet cooling fans in both the control and amplifier cabinets. CB16 and CB17 are both 5A single pole breakers that feed the lights in the control and amplifier cabinets respectively.

One leg of the 24V AC output of T2 feeds directly to K1, with the other leg passing through K2 and F1. K2 is a solid-state relay that receives control voltage directly from the system controller and when closed supplies 24VAC through F1 to K1 causing K1 to close. The purpose of F2 is twofold, first it is to protect the solid-state relay K2 and control transformer T2 in case of a coil failure on K1, but to also act as an anti-pump safety in the event of a brown-out, single phase or low voltage condition. F1 is a 0.5A fast blow cartridge fuse that will blow after approximately one tenth of a second of pumping action of K1, thus protecting the 32V DC power supplies and amplifier modules.

The output of K1 feeds circuit breakers CB100 and CB101 which are three phase 10A breakers that feed IPA power supply "A" and IPA power supply "B" respectively. The DC outputs of these two supplies are combined with steering diodes to supply the intermediate power amplifier. Since there is only a single IPA tray, two redundant power

supplies are used to supply power to this module as a failsafe backup. Should either supply fail, the other supply can handle the full load of the IPA. This also allows hot swapping of the IPA power supplies without having to shut down the transmitter and go off the air.

Circuit Breakers CB102 through CB105 are all 10A three phase breakers that supply 480V AC to the PA module power supplies. Each power supply is capable of driving two PA modules, therefore only four PA power supplies are needed to drive the full compliment of eight modules. CB106 is a 10A three phase breaker that is a spare with no load side connection. Figure 3.61 outlines the entire AC and DC power distribution for the transmitter.

The startup sequence occurs by K2 receiving a command from the system controller, causing K2 to close and supply 24VAC to K1. K1 then closes and supplies 480VAC to the IPA and PA power supplies. A half second after receiving an “AC SUPPLY GOOD” signal from all the installed supplies, the controller then issues a command back to the supplies to turn on the DC output. The transmitter shutdown sequence occurs in the reverse order as the startup sequence.

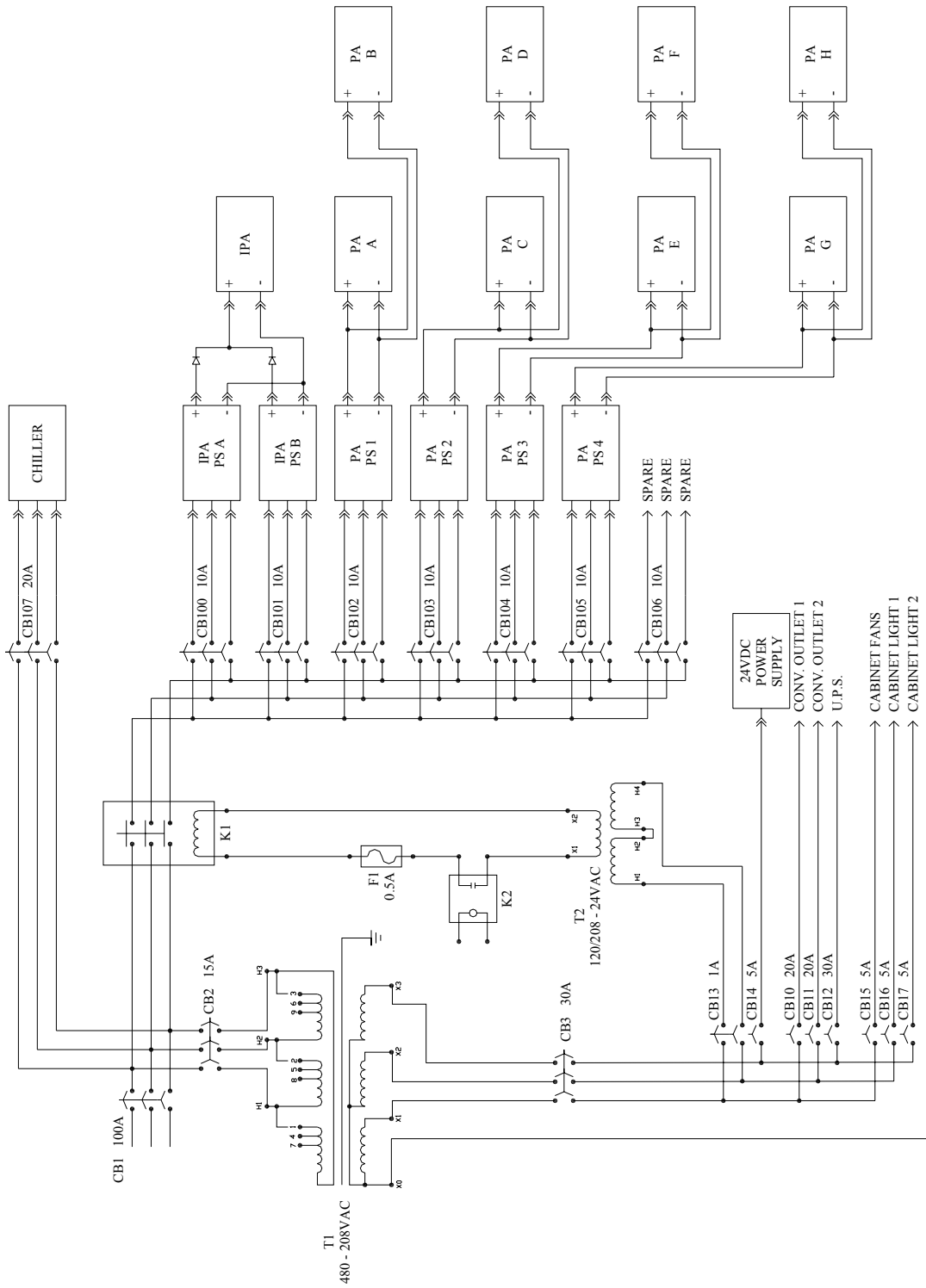


Figure 3.61 AC and DC Power Distribution

CHAPTER IV

TRANSMITTER PERFORMANCE EVALUATION

This chapter will discuss the test results of the completed transmitter and the operational history of the units installed for WLOV television in West Point, Mississippi and KTFB television in Flagstaff, Arizona – the first two units installed in a working television facility. In order to better understand the performance measurements, the first part of this chapter will discuss the measurement techniques used to evaluate the operation of the completed transmitters.

Although there are a number of measurements and a number of measurement techniques that can be used to characterize a radiofrequency transmitter system, there are a handful that are best suited for a digital 8VSB transmitter – average power, the pilot amplitude error, the constellation diagram, signal to noise ratio (SNR), complex modulus error ratio (MER) and the error vector magnitude (EVM) because they are able to easily characterize the operation of the modulator and amplifier(s), and unlike analog television, can all be performed while the station is operating on the air during normal programming. Analog television measurements generally must be performed after hours or during an interruption of programming in order to inject the appropriate test signal into the transmitter. Other than average power, none of the aforementioned tests would apply to analog transmitter operation.

Power Measurement

Average power is important to measure for any transmitter since it gives a generic picture of the overall operation of the power amplifier. If the average power is too low, it could indicate trouble with the amplifier. If the average power is too high, it could indicate a situation by which unnecessary stress is being placed on the filters, transmission line, or antenna which could promote premature system failure. Average power is also defined by the station license as issued by the FCC, and any deviation from the operating point could result in severe fines.

Average power is best measured using water calorimetry. This is accomplished by flowing water over a load at a fixed rate and by measuring the difference in the water temperature flowing into the load versus the water temperature leaving the load, the average power can be calculated from [38]

$$P = Kt(T1 - T2)QF \quad (4-1)$$

Where P is the power fed into the load in kilowatts, Kt is the coolant multiplying factor, $T1$ is the outlet water temperature in degrees Celsius, $T2$ is the water inlet temperature in degrees Celsius, Q is the water flow in gallons per minute and F is the flow meter correction factor. Figure 4.1 can be used to determine the Kt for ethylene-glycol and water mixtures based on temperature. Figure 4.2 is a nomograph to be used to calculate the flowmeter correction factor for fluid temperature and density. Peak power can statistically be calculated from the average power, but for 8VSB uncompressed

transmission can be estimated by adding 6 dB to the average power. All measurements were taken with a measured average power of 400 watts into the load before the filter unless otherwise noted.

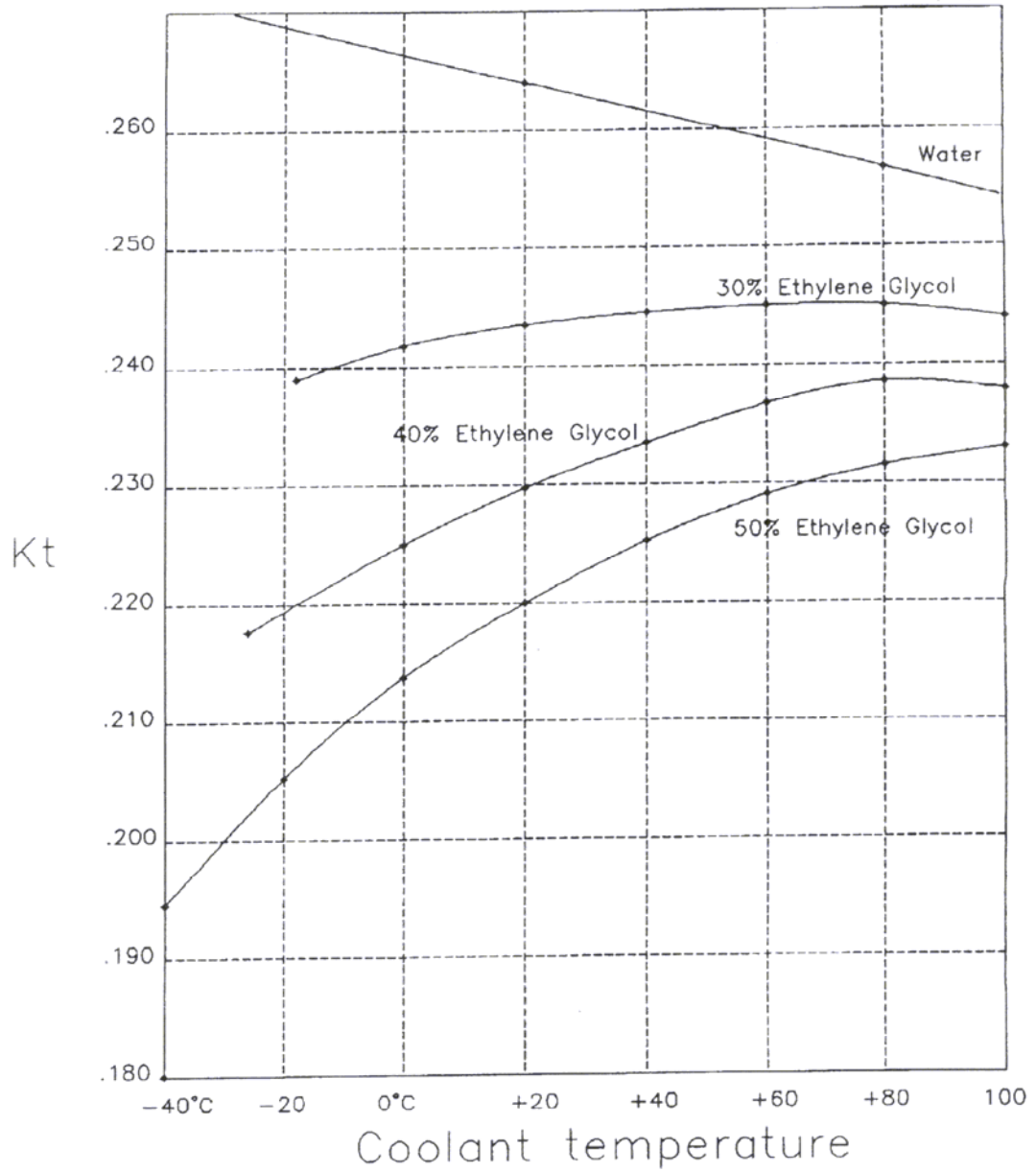


Figure 4.1 Kt for Ethylene-Glycol/Water Mixtures vs. Temperature [39]

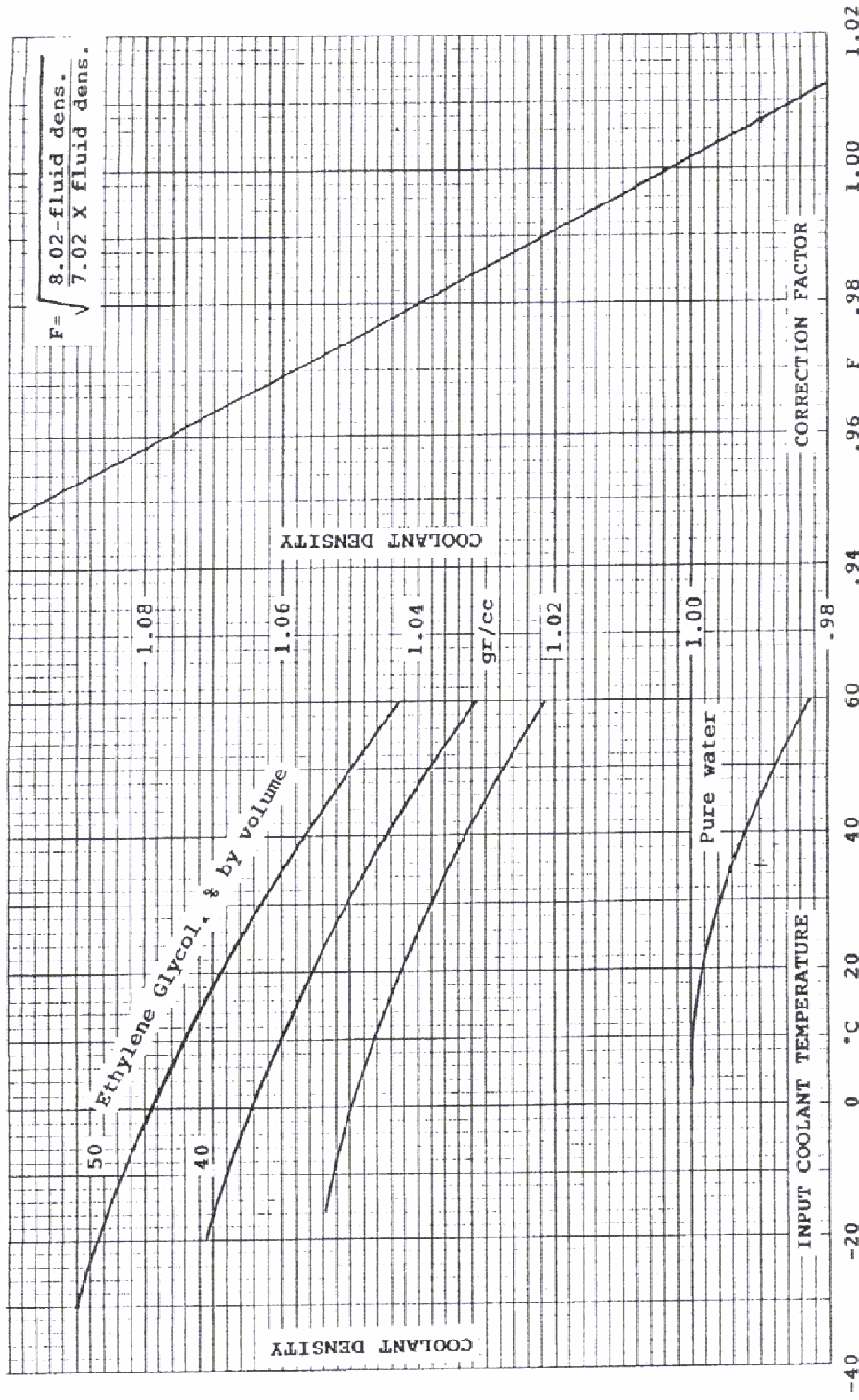


Fig.-11 Density of Ethylene Glycol and Water Mixtures at Various Temperatures

Fig.-12 Flow-Meter Correction Factor

(The above graphs may be used together as a nomograph)

Figure 4.2 Flowmeter Correction Factor for Fluid Temperature and Density [40]

Peak-to-Average Ratio

The Peak-to-Average Power is the ratio of the peak transient power to the average envelope power. The peak power is occasionally (randomly) at the peak envelope power and can be plotted statistically as a distribution function verses time. Figure 4.3 illustrates the Peak-to-Average power measurement curve along with the ideal curve. A properly functioning transmitter will track the ideal curve, and any deviation from the ideal would indicate amplifier non-linearities.

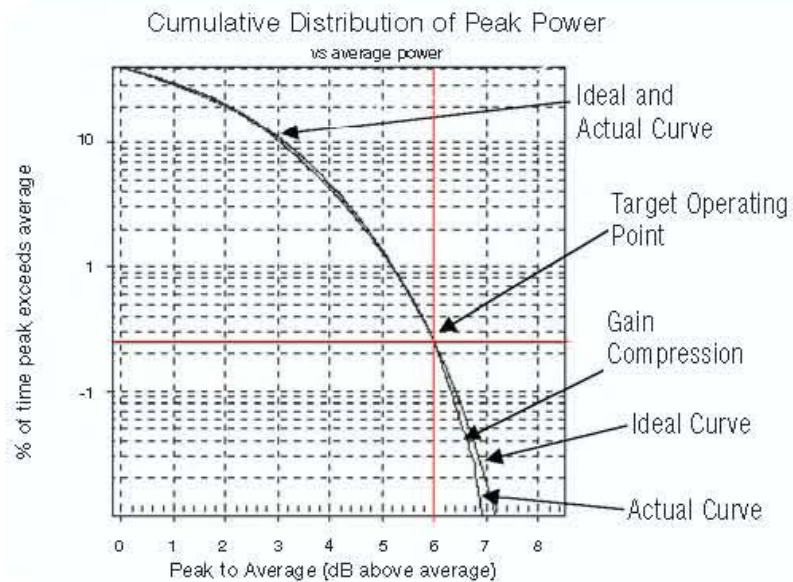


Figure 4.3 Typical Distribution of Peak Power for 8VSB Transmission [41]

8VSB Constellation

The constellation diagram is perhaps the single most useful tool used to analyze the quality of the 8VSB signal by giving a real-time snapshot of the transmitter operation. Figure 4.4 illustrates that the x-axis displays the in-phase (I) channel information and the y-axis represents the quadrature (Q) channel [42]. The eight vertical lines correspond to the eight transmitted amplitude levels, -7, -5, -3, -1, 1, 3, 5 and 7. Table 4.1 shows the how the transmit levels correspond to the 8 bit data values [43, 44].

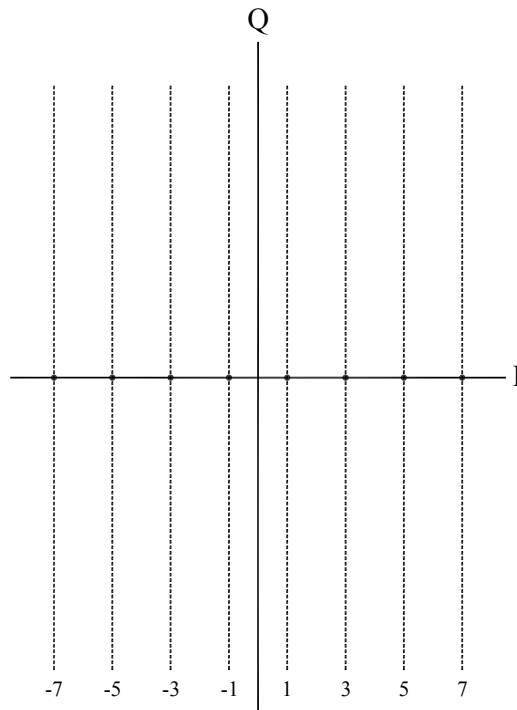


Figure 4.4 I-Q Diagram for an 8VSB Signal

Table 4.1

Map of 8VSB Constellation Points [45].

R	Z2	Z1	Z0
-7	0	0	0
-5	0	0	1
-3	0	1	0
-1	0	1	1
1	1	0	0
3	1	0	1
5	1	1	0
7	1	1	1

Figure 4.5 illustrates an ideal constellation display with all the data points aligned to the eight transmit levels. Figure 4.6 shows a constellation diagram with noise effects induced into the transmitted signal. Figure 4.7 illustrates a transmitter operating in the non-linear region of the amplifier with clipping or compression effects evident as parentheses shaped lines. This is an amplitude error or AM-AM conversion error which can be measured directly as pilot amplitude error (see Figure 4.3). Figure 4.8 has S shaped data which indicates phase errors in the transmission and is call AM-PM conversion error which occurs when the signal amplitude is modulation the carrier's phase.

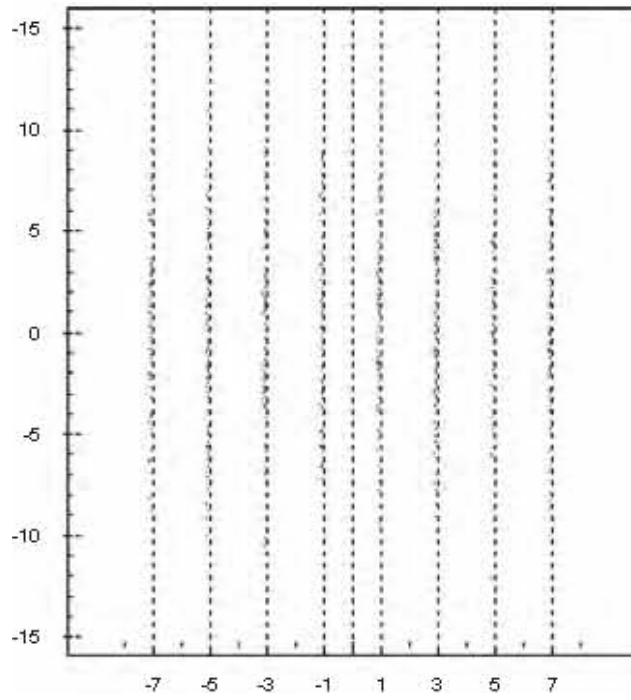


Figure 4.5 Ideal 8VSB Constellation Diagram[46]

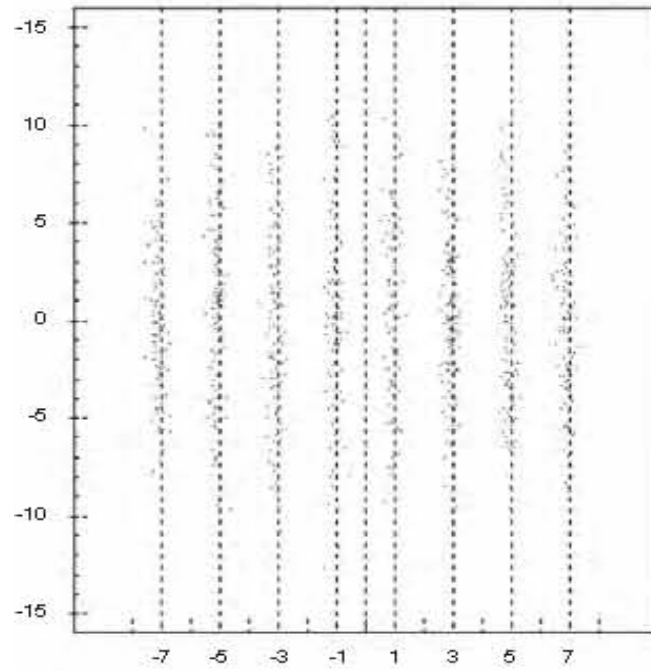


Figure 4.6 8VSB Constellation Diagram with Noise Effects[47]

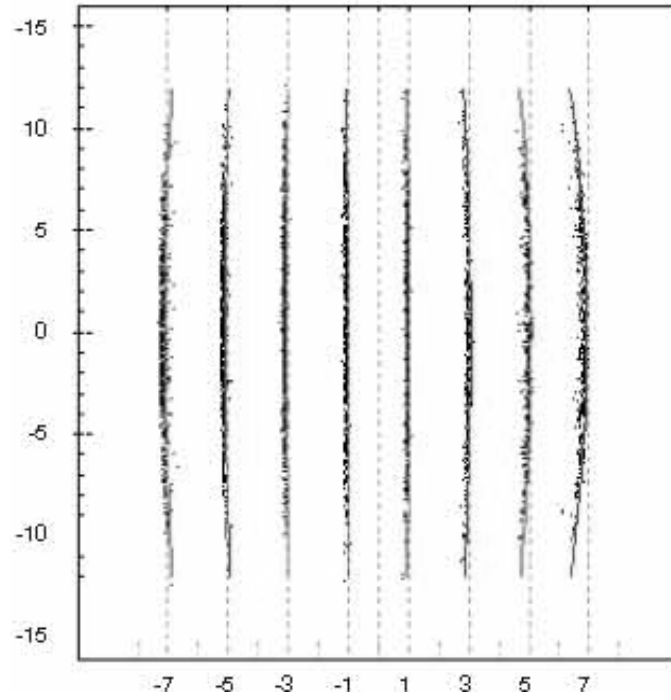


Figure 4.7 8VSB Constellation Diagram with Clipping Effects or AM/AM Conversion Error[48]

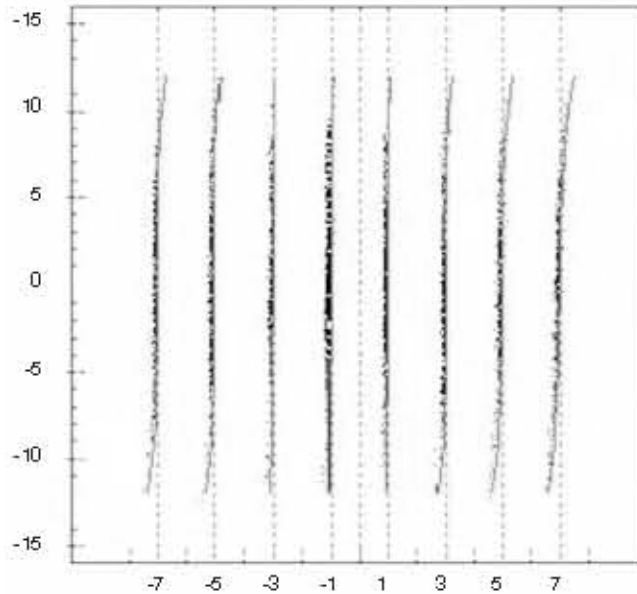


Figure 4.8 8VSB Constellation Diagram with Phase Effects or AM/PM Conversion Error[49]

Signal to Noise Ratio and Modulus Error Ratio

The signal to noise ratio (SNR or S/N) is defined as the average power of ideal symbol values divided by the noise power [50] and should be above 27 dB for reliable signal delivery to the consumer. SNR is calculated by:

$$S/N = \frac{Power(Ideal I)}{Power(Ideal I - Actual I)} \quad (4-2)$$

The Modulus Error Ratio (MER) is the complex form of the SNR measurement that is calculated from both the I-channel information and the Q-channel information. In a properly functioning transmitter, the SNR and MER should be approximately the same.

Error Vector Magnitude

The Error Vector Magnitude (EVM) is the RMS value of the magnitude of the symbol errors along the I-channel axis divided by the magnitude of the I-channel portion of the outermost constellation state [51] or,

$$EVM = \frac{RMS(Ideal I - Actual I) \times 100\%}{+ 7.0} \quad (4-3)$$

As with the MER, EVM also includes both the I and Q channels and will indicate transmitter clipping slightly before it would be seen in the SNR. The transmitters EVM performance should not exceed 4.6%, but should be as small as possible.

Transmitter Measurements

Figures 4.10 through 4.14 are measurements at various points along the amplifier chain made using the Channel 16 transmitter installed for WLOV in West Point, Mississippi operating with a single PA drawer at 400 watts. Figure 4.15 and 4.16 are from measurements made with the transmitter operating at 450 watts in an overdriven condition. Although the amplifier was designed for operation at 500 watts, final testing showed that operation much in excess of 400 watts quickly resulted in a signal that was less than optimal for 8VSB transmission. All power measurements were made using an Altronic 9750 liquid-cooled load resistor and a Bird BPM-3M-UM power monitor with a

Bird 3129 display interface. All signal quality measurements were made using a Tektronix RFA 300A 8VSB Measurement Set. The test setup is shown in Figure 4.9.

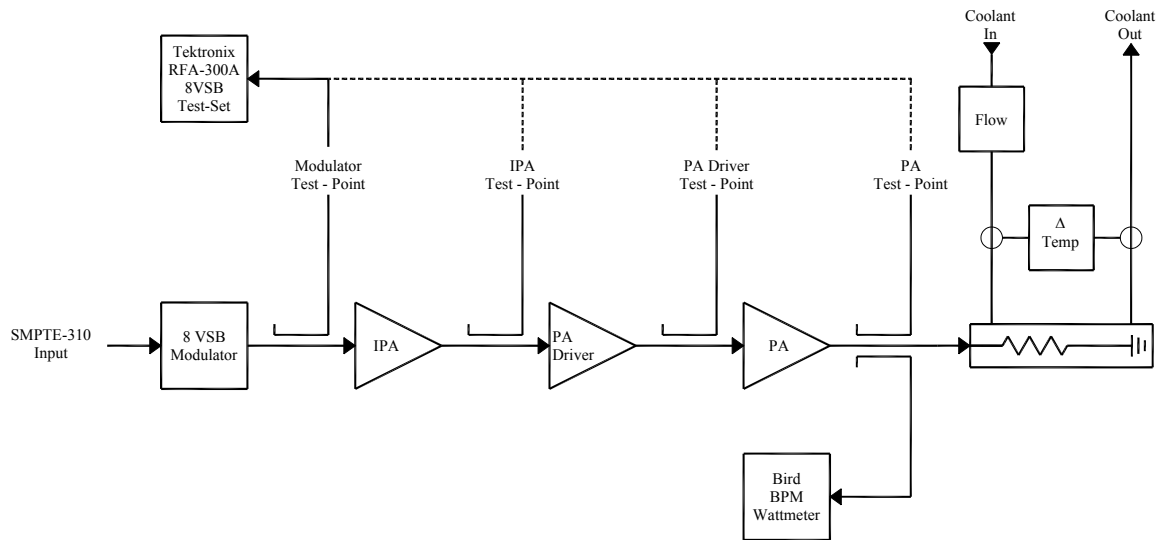


Figure 4.9 Transmitter System Test Setup

Modulator

Figure 4.10 illustrates measurements taken immediately following the K-Tech modulator output. The modulator for this and all subsequent measurements was operating using the internal pseudo-random test signal generator (PNGEN) and all automatic pre-correction switched on with pre-correction table 3 selected. The

measurement at the output of the modulator is critical in that it sets the benchmark for all measurements further down the amplifier chain. Based on the information in Figure 4.10, it is not possible for any amplifier to operate with an SNR of better than 44.4 dB, an EVM of less than 0.6%, and a Pilot Amplitude Error of less than 0.77 dB.

Measured: Friday, August 01, 2003 2:36:29PM
Printed: Friday, August 01, 2003 2:36:30PM
Measurement: Signal/Noise & EVM
Smoothing: High
Frequency: 482.31 MHz

Signal/Noise	44.4 dB
EVM	0.6 %
Complex MER	44.0 dB
Pilot Amplitude Error	0.77 dB

Use Equalizer	On
Subtract Pilot Offset from Symbol axis	On

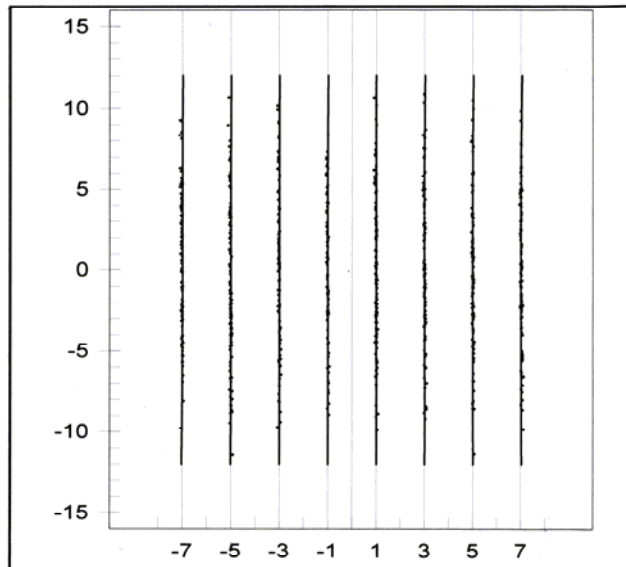


Figure 4.10 8VSB Constellation Diagram of the Transmitter Measured at the Output of the Modulator with the Transmitter Operating at 400 Watts with One Amplifier Module and I_{DQ} set to 1.8A

Intermediate Power Amplifier

Figure 4.11 shows results taken from one of the outputs of the IPA drawer. As would be expected, the signal quality is slightly less than that of the modulator. Since the amplifiers are not ideal, a slight degradation of the signal quality is expected at each amplifier stage. The data shown is still well within acceptable range for excellent 8VSB broadcast transmitter operation and the constellation diagram shows eight straight lines as is desired for excellent transmitter performance.

Measurement: Signal/Noise & EVM
Smoothing: High
Frequency: 482.31 MHz

Signal/Noise 39.4 dB
EVM 1.0 %
Complex MER 38.9 dB
Pilot Amplitude Error 0.25 dB

Use Equalizer On
Subtract Pilot Offset from Symbol axis On

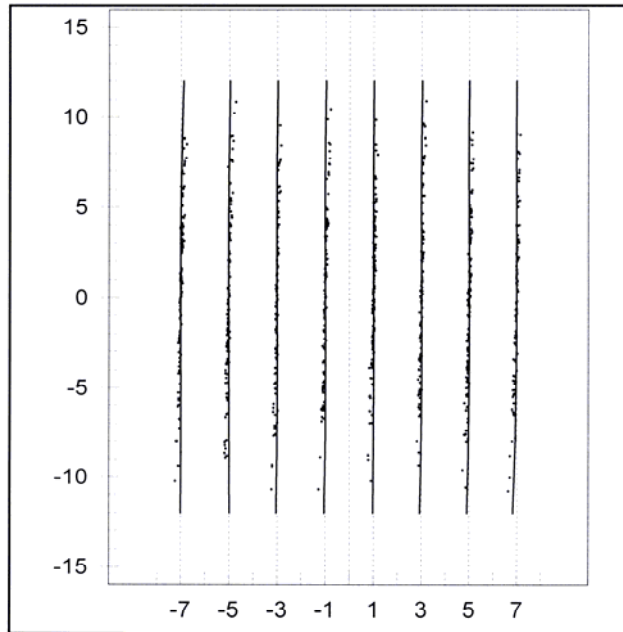


Figure 4.11 8VSB Constellation Diagram of the Transmitter Measured at the Output of the Intermediate Power Amplifier with the Transmitter Operating at 400 Watts with One Amplifier Module and I_{DQ} set to 1.8A

Power Amplifier

The output of the PA driver driver amplifier is shown in Figure 4.12. Once again a slight reduction in the signal quality is noted by the SNR, EVM, MER and Pilot Amplitude Error. The constellation diagram is starting to show a slight indication of AM-PM error, or system phase distortion. The overall quality of the signal is still more than acceptable at this point in the amplifier chain.

Measurement: Signal/Noise & EVM
Smoothing: High
Frequency: 482.31 MHz

Signal/Noise	38.2 dB
EVM	1.2 %
Complex MER	37.7 dB
Pilot Amplitude Error	0.98 dB

Use Equalizer	On
Subtract Pilot Offset from Symbol axis	On

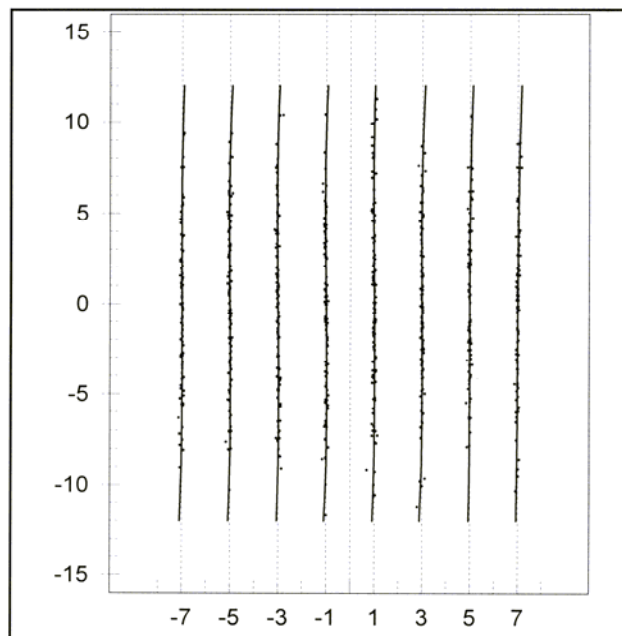


Figure 4.12 8VSB Constellation Diagram of the Transmitter Measured at the Output of the Driver Card on the Power Amplifier with the Transmitter Operating at 400 Watts with One Amplifier Module and I_{DQ} set to 1.8A

The final output of the transmitter before the filter is shown in Figure 4.13. There is a slight reduction of signal quality from the output of the driver card, and the AM-PM error show a slight increase in the constellation diagram, but overall shows excellent operation at 400 watts average power. The SNR is 36.6 dB and is well above the required 27 dB with the MER at 36.3 dB indicating very linear system operation. The measured EVM is only 1.4%, well below the theoretical limit of 4.7%.

Measurement: Signal/Noise & EVM
 Smoothing: High
 Frequency: 482.31 MHz

Signal/Noise	36.6 dB
EVM	1.4 %
Complex MER	36.3 dB
Pilot Amplitude Error	1.38 dB

Use Equalizer	On
Subtract Pilot Offset from Symbol axis	On

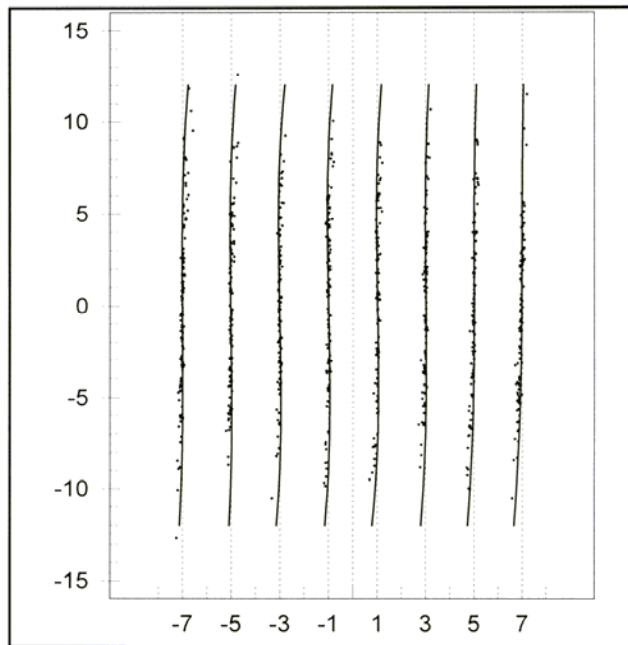


Figure 4.13 8VSB Constellation Diagram of the Transmitter Measured at the Output of the Power Amplifier with the Transmitter Operating at 400 Watts with One Amplifier Module and I_{DQ} set to 1.8A

Figure 4.14 is shows the Peak-to-Average power ratio at the output of the transmitter. Ideally this number would be 6.0 dB and the actual curve would overlay the ideal curve almost exactly. With a Peak-to-Average ratio of 5.9 dB and a slight tendency for the ideal curve to lean towards the right indicates slight compression is present in the system. Although 6.0 dB would be perfect, with a SNR of 36.6 dB and an EVM of only 1.4%, the transmitter system is operating very well, and a Peak-to-Average ratio of 0.1 dB less than ideal should be considered negligible.

Measurement: Peak/Average & Channel Spectrum
 Smoothing: High
 Frequency: 482.31 MHz

Peak to Average 5.9 dB
 Actual-to-Ideal Difference -0.1 dB

Planning Factor (dB): 6
 % of Time: 0.25

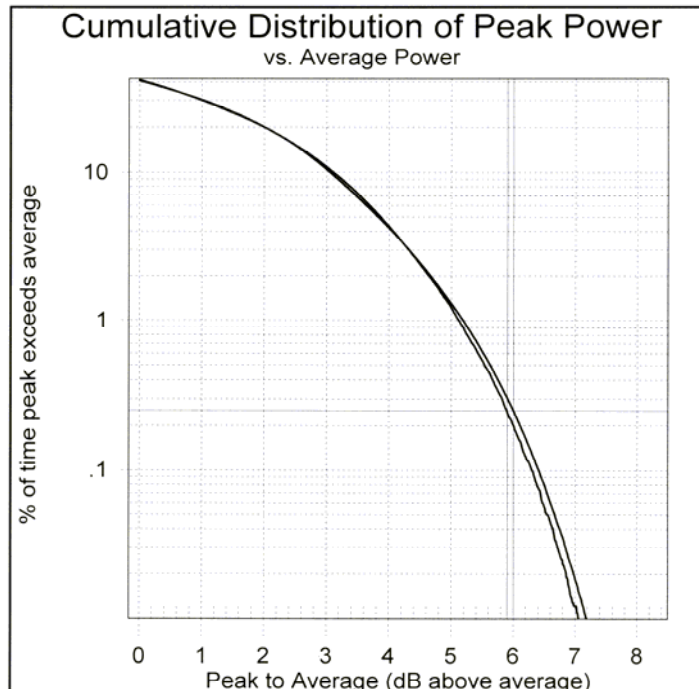


Figure 4.14 Cumulative Distribution of Peak Power Measured at the Output of the Power Amplifier with the Transmitter Operating at 400 Watts with One Amplifier Module and I_{DQ} set to 1.8 Amps

Overdriven Power Amplifier

Figure 4.15 is data taken with the transmitter operating at 450 watts. It is evident that the SNR is greatly reduced and the EVM is greatly increased over the 400 watt case. The constellation diagram shows greater phase modulation error. Although all these parameters are still technically acceptable, and operation at 450 watts still passed video data, the transmitter was operating on the edge of acceptability. Therefore, the PA amplifier module was rated for operation at 400 watts average power for this and subsequent transmitters.

Measurement: Signal/Noise & EVM
Smoothing: High
Frequency: 482.31 MHz

Signal/Noise	28.0 dB
EVM	3.7 %
Complex MER	27.9 dB
Pilot Amplitude Error	1.29 dB

Use Equalizer	On
Subtract Pilot Offset from Symbol axis	On

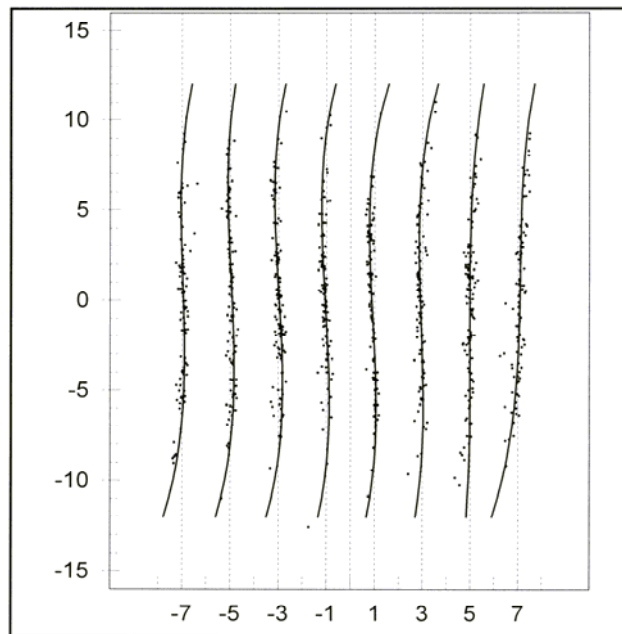


Figure 4.15 8VSB Constellation Diagram of the Transmitter Measured at the Output of the Power Amplifier with the Transmitter Operating at 450 Watts with One Amplifier Module and I_{DQ} set to 1.8A

The cumulative distribution of peak power for the system operating at 450 watts is shown in Figure 4.16. It is noted that the Peak-to-Average ration is beginning to rapidly decrease as the power is increased, forcing operation of the amplifier into the non-linear regime.

Measurement: Peak/Average & Channel Spectrum
 Smoothing: High
 Frequency: 482.31 MHz

Peak to Average 5.8 dB
 Actual-to-Ideal Difference -0.2 dB

Planning Factor (dB): 6
 % of Time: 0.25

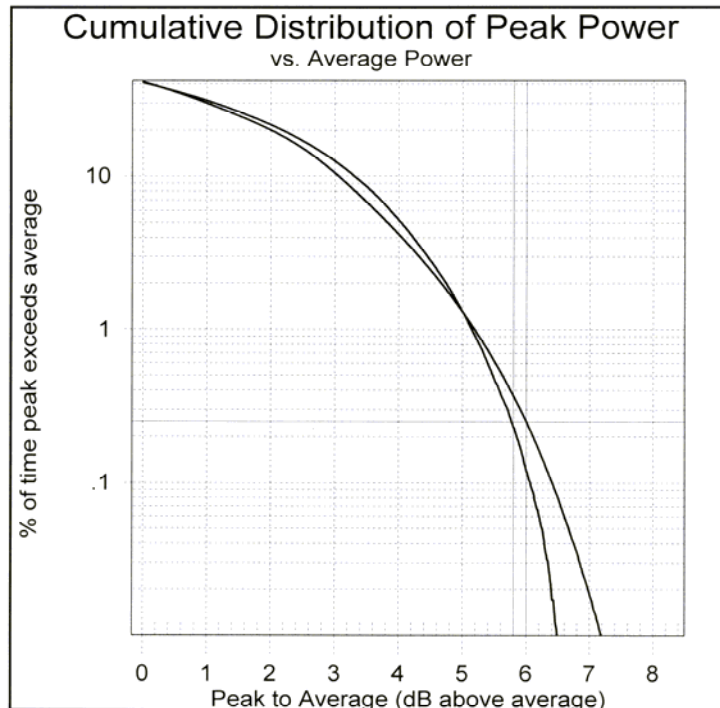


Figure 4.16 Cumulative Distribution of Peak Power Measured at the Output of the Power Amplifier with the Transmitter Operating at 450 Watts with One Amplifier Module and I_{DQ} set to 1.8 Amps

System Performance of WLOV and KTFL

The transmitters for WLOV DT-16 in West Point, Mississippi, and KTFL DT-18 in Flagstaff, Arizona, were both installed in early fall 2003. Both systems had the identical failure at startup related to the water and temperature and flow sensors installed in the transmitter. All four (input and output for both stations) tested fine at the factory but indicated erroneous readings when installed in the field. It was determined that RF from other transmitters operating within the same proximity as the DT-4KUs were radiating enough RF interference to force an external bias on the sensors. To correct this problem, all four sensors were disassembled and the internal wiring from the sensors to the control boards were replaced with twisted pair wire, and 0.01 μ F capacitors were added to the signal inputs on the control boards. This simple modification corrected the problem and the transmitters operated normally.

The KTFL transmitter was decommissioned in August 2006, and the WLOV transmitter was turned off in February 2007. During their lifetime, only a few failures were reported. Figure 4.17 shows the completed installation at WLOV and Figure 4-18 shows the installation for KTFL.



Figure 4.17 UHF-4DTV Transmitter Installed for WLOV Television in West Point, Mississippi



Figure 4.18 UHF-4DTV Transmitter Installed for KTFL Television in Flagstaff, Arizona.

In the summer of 2005, the WLOV transmitter shutdown due to a chiller failure, and it was found that a pinhole leak had formed in a solder joint in the Freon line within the chiller itself. The leak was repaired, the Freon recharged and the system was returned to operation within less than 48 hours. Also in summer 2005, the KTFL transmitter experienced a massive failure that destroyed the control system, all power supplies, fans, chiller, and started a fire inside the UPS. Unfortunately, seven other broadcast transmitters were damaged or destroyed at exactly the same time at the Mormon Mountain transmitter farm. This failure was a result of Arizona Power Company accidentally swapping feeds during a repair after a forest fire, causing a several thousand volt spike on the primary power that feeds the Mormon Mountain site. Arizona Power paid for all damages to the equipment for all the stations involved.

The only other failures reported were due to a failure within the modulator. First at KTFL and then at WLOV, the upconverter cards inside the modulator failed causing the Bit Error Rate in the data stream to increase, which caused the receivers at the consumers sites to become muted. K-Tech was aware of the problem with the upconverters and replaced all of the units that were installed prior to January 2006 for free.

As of this writing, there are still several DT-4KU transmitters in operation, and as of this writing, none of the owners have reported a failure with the hardware that was designed or built that is encompassed by this thesis.

CHAPTER V

CONCLUSIONS AND RECOMMENDATIONS

Techniques to improve the performance of individual components in the transmitter system are discussed in this chapter.

Currently, the transmitter control system controls and monitors the complete transmitter operation with little emphasis on the monitoring of the individual components. Ideally, the user would be able to monitor and control each individual amplifier module so that in the event of a failure, an initial diagnosis could be made without the aid of any external test equipment. Once the diagnosis is made, the user should have the option to disable a specific amplifier module and return the transmitter to service while awaiting parts to repair the defective component. It would also be beneficial for the user to have the ability to monitor the voltage and current at each individual transistor on a regular basis with trend logging so that preventative maintenance can be performed before a failure actually occurs.

The splitters and combiners on each module were designed for a specific channel. Ideally these should be designed to operate over several channels or even the entire UHF-DTV band. This would minimize the number of stock components required and allow for easier module design, construction and maintenance.

The current mask filter design works very well, but the limitations of the filter have not been tested or documented. This filter was tested at ten kilowatts for several hours without arcing or failure but the upper power limit is unknown. If the filter were tested at higher power levels, it could be a viable stand-alone product that could be marketed independent of the actual transmitter. This filter is a reflective type filter which requires the use of circulators on the output of the amplifier modules. It would be advantageous to design and implement a constant impedance filter that would use two of the existing filters connected together with 90 degree hybrids and dummy loads to eliminate the need for additional circulators and loads at the amplifier.

The transmitter was designed to have hot pluggable modules so that the modules could be removed or inserted while the system was on the air, allowing the remaining modules to continue to operate with the one module removed. Although all the components to do this are in place – blind mating RF input and output connectors, blind mating water connections and blind mating power and control connections, this was never able to be used because all the transmitters sold were configured for low-power, single-module operation. Since these systems were configured with one module, the hot plugability of the module was never needed. The hot plug design was tested during the design phase with two modules and worked seamlessly when removing or inserting either module, but unfortunately was never needed in the field.

All the units sold as of this writing were configured for low power operation. Therefore, the eight-way Gysel[52] combiner that was designed for the system was never implemented. Although the initial design is complete, it was never prototyped or tested.

If any high power transmitters are to be manufactured, the combiner will have to be built and tested before any more work can proceed. Figure 5-1 shows the initial design of the channel 16 eight-way Gysel combiner.

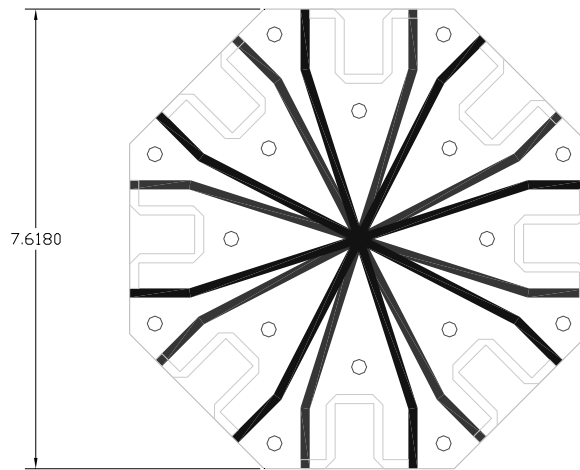


Figure 5.1 Eight-Way Gysel Combiner Layout for High-Power Combiner

REFERENCES

- [1] G.W. Collins, *Fundamentals of Digital Television Transmission*. New York, New York: J. Wiley & Sons, 2001, pp. 3-4.
- [2] *Transmission Measurement and Compliance for Digital Television – ATSC Standard, Revision A*, Advanced Television Standards Committee ATSC A/64, 17 Nov., 1997.
- [3] G. Breed, “IMD Characteristics and Performance Issues in Wide Bandwidth Systems,” *High Frequency Electronics*, Vol. 4, no. 3, pp. 50-53, Mar. 2005.
- [4] H. Fries and B. Jenkins, “Measuring the DTV Signal,” *IEEE Trans. Broadcasting*, Vol. 46, no.2, pp. 114-120, June 2000.
- [5] *Transmission Measurement and Compliance for Digital Television – ATSC Standard, Revision A*, Advanced Television Standards Committee ATSC A/64, 17 Nov., 1997.
- [6] C. Davis and J. Hawkins, “Solid-state DTV Transmitters,” *IEEE Trans. Broadcasting*, Vol. 43, no.3, pp. 252-260, Sept. 1997.
- [7] B. Jasper, “IP3 (3rd Order Intercept),” Test Edge Inc., San Diego, CA.
- [8] H. Ku, W. Woo and J.S. Kenney, “Carrier-to-Interference Ratio Estimation of Arbitrary Signals Distorted by Nonlinear Devices.”
- [9] H. Ku, W. Woo and J.S. Kenney, “Carrier-to-Interference Ratio Estimation of Arbitrary Signals Distorted by Nonlinear Devices.”
- [10] C. Davis and J. Hawkins, “Solid-state DTV Transmitters,” *IEEE Trans. Broadcasting*, Vol. 43, no.3, pp. 252-260, Sept. 1997.
- [11] F. De Castro et al, “8-VSB Channel Coding Analysis for DTV Broadcast,” *IEEE Trans. On Consumer Electronics*, Vol. 46, No. 3, pp. 539-547, Aug. 2000.
- [12] “8VSB Measurements Using the RFA300A,” Tektronix [PDF Online]. <http://www.tektronix.com/video>.

- [13] B. Jenkins, "Understanding SNR in a Digital World," *National Association of Broadcasters 1999 Broadcast Engineering Conference Proceedings*, pp. 261-265.
- [14] H. Fries and B. Jenkins, "Measuring the DTV Signal," *IEEE Trans. Broadcasting*, Vol. 46, no.2, pp. 114-120, June 2000.
- [15] B. Jenkins, "Understanding SNR in a Digital World," *National Association of Broadcasters 1999 Broadcast Engineering Conference Proceedings*, pp. 261-265.
- [16] D. Henkes, "LINC," [Software], Applied Computational Sciences, Escondido, CA., 1995.
- [17] D. M. Pozar, *Microwave Engineering, Second Ed.* New York, New York: J. Wiley & Sons, 1998.
- [18] "WinSmith 2.0," [Software], Noble Publishing Corp., Tucker, GA., 1998.
- [19] D. Henkes, "LINC," [Software], Applied Computational Sciences, Escondido, CA., 1995.
- [20] "RF Power Field-Effect Transistor MRF-377 (PRF-377)," Motorola, [PDF Email], received from Christine Chinchilla, Richardson Electronics, Inc., 18 Sept., 2002.
- [21] "MultiSim," [Software], National Instruments, Austin TX.
- [22] G. Gonzalez, *Microwave Transistor Amplifiers Analysis and Design.* New Jersey: Prentice Hall, 1984.
- [23] H. Howe, *Stripline Circuit Design.* Dedham, Massachusetts: Artech House, 1974, pp. 47-52.
- [24] "RF Power Field-Effect Transistor MRF-377 (PRF-377)," Motorola, [PDF Email], received from Christine Chinchilla, Richardson Electronics, Inc., 18 Sept., 2002.
- [25] D.S. Steinberg, *Cooling Techniques for Electronic Equipment, Second Edition.* New York: J. Wiley & Sons, 1991.
- [26] *Transmission Measurement and Compliance for Digital Television – ATSC Standard, Revision A*, Advanced Television Standards Committee ATSC A/64, 17 Nov., 1997.

- [27] G. Mattaei, L. Young and E. Jones, *Microwave Filters, Impedance-Matching Networks and Coupling Structures*. New York, New York: McGraw-Hill, 1964.
- [28] G. Mattaei, L. Young and E. Jones, *Microwave Filters, Impedance-Matching Networks and Coupling Structures*. New York, New York: McGraw-Hill, 1964.
- [29] G. Mattaei, L. Young and E. Jones, *Microwave Filters, Impedance-Matching Networks and Coupling Structures*. New York, New York: McGraw-Hill, 1964.
- [30] G. Mattaei, L. Young and E. Jones, *Microwave Filters, Impedance-Matching Networks and Coupling Structures*. New York, New York: McGraw-Hill, 1964.
- [31] W.B.W. Allison, *A Handbook for the Mechanical Tolerancing of Waveguide Components*. Norwood, Massachusetts: Artech House, 1987.
- [32] W.B.W. Allison, *A Handbook for the Mechanical Tolerancing of Waveguide Components*. Norwood, Massachusetts: Artech House, 1987.
- [33] R.E. Collin, *Field Theory of Guided Waves, Second Edition*. New York, New York: IEEE and Wiley, 1990.
- [34] H. Shaukatullah, "Bibliography of Liquid-cooled Heat Sinks for Thermal Enhancement of Electronic Packages," presented at the IEEE Fifteenth Semiconductor Thermal Measurement and Management Symposium, San Diego, California, 1994.
- [35] M. Behnia, "Cooling Problems and Thermal Issues in High Power Electronics – A Multi Faceted Design Approach," presented at the Fifth International Conference on Thermal and Mechanical Simulation and Experiments in Micro-electronics and Micro-Systems, Novotel Tour Noire, Brussels, Belgium, 2004.
- [36] H.D. Zhang, D. Pinjala and P.-S. Teo, "Thermal Management of High Power Dissipation Electronic Packages: from Air Cooling to Liquid Cooling," presented at the IEEE 2003 Electronics Packaging Technology Conference, Singapore, 2003.
- [37] "Cimplicity," [Software], GE Fanuc, Charlottesville, VA., 2002.
- [38] "Liquid-Cooled Coaxial Load Resistor Model 9750," [Instruction Manual], Altronic Reseach, Inc., Yellville, Arkansas, 9750M rev. Apr. 2003.
- [39] "Liquid-Cooled Coaxial Load Resistor Model 9750," [Instruction Manual], Altronic Reseach, Inc., Yellville, Arkansas, 9750M rev. Apr. 2003.

- [40] “Liquid-Cooled Coaxial Load Resistor Model 9750,” [Instruction Manual], Altronic Reseach, Inc., Yellville, Arkansas, 9750M rev. Apr. 2003.
- [41] “8VSB Measurements Using the RFA300A,” Tektronix [PDF Online]. <http://www.tektronix.com/video>, p. 3.
- [42] G.W. Collins, *Fundamentals of Digital Television Transmission*. New York, New York: J. Wiley & Sons, 2001, p. 9.
- [43] “8VSB Measurements Using the RFA300A,” Tektronix [PDF Online]. <http://www.tektronix.com/video>, p. 7.
- [44] G.W. Collins, *Fundamentals of Digital Television Transmission*. New York, New York: J. Wiley & Sons, 2001, p. 51.
- [45] G.W. Collins, *Fundamentals of Digital Television Transmission*. New York, New York: J. Wiley & Sons, 2001, p. 51.
- [46] “8VSB Measurements Using the RFA300A,” Tektronix [PDF Online]. <http://www.tektronix.com/video>, p.7.
- [47] “8VSB Measurements Using the RFA300A,” Tektronix [PDF Online]. <http://www.tektronix.com/video>, p. 7.
- [48] “8VSB Measurements Using the RFA300A,” Tektronix [PDF Online]. <http://www.tektronix.com/video>, p. 8.
- [49] “8VSB Measurements Using the RFA300A,” Tektronix [PDF Online]. <http://www.tektronix.com/video>, p. 8.
- [50] “8VSB Measurements Using the RFA300A,” Tektronix [PDF Online]. <http://www.tektronix.com/video>, p. 9.
- [51] “8VSB Measurements Using the RFA300A,” Tektronix [PDF Online]. <http://www.tektronix.com/video>, p. 9.
- [52] U. H. Gysel, “A New N-Way Power Divider/Combiner Suitable for High-Power Applications,” in *Microwave Theory and Technology Symposium Digest*, 1975.

APPENDIX A
MSMRF, INC. UHF-4DTV TRANSMITTER
BILL OF MATERIALS

DT-4KU Digital Transmitter
Bill of Materials

Prefix	Part Number	Description	Manufacturer	Manufacturer Part Number	Sub-Assembly	Supplier	Supplier Item Number
AA	P27RT7036F	Rack	APW			Crouse Kimzey	P27RT7036F
AA	P27RT7036F	Rack	APW			Crouse Kimzey	P27RT7036F
AA	T4FP1931F	Rack Fan Top	APW			Crouse Kimzey	T4FP1931F
AA	T4FP1931F	Rack Fan Top	APW			Crouse Kimzey	T4FP1931F
AA	PDV2770RF	Rack Door	APW			Crouse Kimzey	PDV2770RF
AA	PDV2770RF	Rack Door	APW			Crouse Kimzey	PDV2770RF
AA	PHL100	Rack Lock	APW			Crouse Kimzey	PHL100
AA	PHL100	Rack Lock	APW			Crouse Kimzey	PHL100
AA	4291002	Rack Rail 19 Inch (Pair)	APW			Crouse Kimzey	
AA	4291002	Rack Rail 19 Inch (Pair)	APW			Crouse Kimzey	
AA	PRMT70F	Rack Rail 24 Inch (Pair)	APW			Crouse Kimzey	PRMT70F
AA	PRMT70F	Rack Rail 24 Inch (Pair)	APW			Crouse Kimzey	PRMT70F
AA	4291003	Rack Rail 23.5 Inch (Pair)	APW			Crouse Kimzey	
AA	4291003	Rack Rail 23.5 Inch (Pair)	APW			Crouse Kimzey	
AA	PSS7036F	Rack Side Panel	APW			Crouse Kimzey	PSS7036F
AA	PSS7036F	Rack Side Panel	APW			Crouse Kimzey	PSS7036F
AA	TMHT750C	Monitor Rack Mount Kit	JVC			Mission Service Supply	TMHT750C
AA	TKHS17	Reference Receiver	PEC			Ktech	TKHS17
AA	DVM100	ATV Encoder	Ktech			Ktech	DVM100
AA	SRG100	Static PSIP Generator	Harmonics			Ktech	SRG100
AA	SRG100	Static PSIP Generator	Ktech			Ktech	SRG100
AA	VS8-ENC-200	Modular	Ktech			Ktech	VS8-ENC-200
AA	VS8-ENC-200	Modular	Ktech			Ktech	VS8-ENC-200
AA	S31400R	Uninterruptible Power Supply	Solar / Hevi-Duty			Allied Electronics	S31400R
AA	9422TF1	Main Disconnect Switch	Square D			Granger	9422TF1
AA	9422A1	Disconnect Lever	Square D			Granger	9422A1
AA	HTLF9AS	480v - 208V DvY Transformer	Hevi-Duty			Allied Electronics	HTLF9AS
AA	PTD500PG	120/208v - 24V Transformer	Hammond			Allied Electronics	PTD500PG
AA	KTK-5	Fuse	Acme Electric			Allied Electronics	KTK-5
AA	DR1202410	24vdc Power Supply	Computer Dynamics			Allied Electronics	DR1202410
AA	ACCESS-C104	Touch Screen Control Panel	Computer Dynamics			Bluff City Electronics	ACCESS-C104-850
AA	CB1	Circuit Breaker	Alltech			Allied Electronics	501-2474
AA	CB2	Circuit Breaker	Alltech			Allied Electronics	501-2466
AA	CB3	Circuit Breaker	Alltech			Allied Electronics	501-2471
AA	CB4	Circuit Breaker	Alltech			Allied Electronics	501-2050
AA	CB5	Circuit Breaker	Alltech			Allied Electronics	501-2050
AA	CB6	Circuit Breaker	Alltech			Allied Electronics	501-2050
AA	CB7	Circuit Breaker	Alltech			Allied Electronics	501-2050
AA	CB8	Circuit Breaker	Alltech			Allied Electronics	501-2058
AA	CB9	Circuit Breaker	Alltech			Allied Electronics	501-2058
AA	CB10	Circuit Breaker	Alltech			Allied Electronics	501-2058
AA	CB11	Circuit Breaker	Alltech			Allied Electronics	501-2058
AA	CB12	Circuit Breaker	Alltech			Allied Electronics	501-2058
AA	CB101	Circuit Breaker	Alltech			Allied Electronics	501-2470
AA	CB102	Circuit Breaker	Alltech			Allied Electronics	501-2470
AA	CB103	Circuit Breaker	Alltech			Allied Electronics	501-2470

DT-4KU Digital Transmitter
Bill of Materials

Prefix	Part Number	Description	Manufacturer	Manufacturer Part Number	Sub-Assembly	Supplier	Supplier Item Number
AA	CB104	Circuit Breaker	Altech	3DU20		Allied Electronics	501-2470
AA	CB105	Circuit Breaker	Altech	3DU20		Allied Electronics	501-2470
AA	CB106	Circuit Breaker	Altech	3DU20		Allied Electronics	501-2470
AA	CB107	Circuit Breaker	Altech	IDU5		Allied Electronics	501-2058
AA	CB108	Circuit Breaker	Altech	IDU5		Allied Electronics	501-2058
AA	CB109	Circuit Breaker	Altech	IDU5		Allied Electronics	501-2058
AA	CB110	Circuit Breaker	Altech	3DU30		Allied Electronics	501-2474
AA		Buss Bar	Altech			Allied Electronics	
AA		Buss Bar	Altech			Allied Electronics	
AA	IC693CHS391M	PLC Backplane	GE Fannie	IC693CHS391M		Allied Electronics	IC693CHS391M
AA	IC693PWR330	PLC Power Supply	GE Fannie	IC693PWR330		Bluff City Electronics	IC693PWR330
AA	IC693CPU364	PLC CPU	GE Fannie	IC693CPU364		Bluff City Electronics	IC693CPU364
AA	IC693MDL940	PLC Relay Module	GE Fannie	IC693MDL940		Bluff City Electronics	IC693MDL940
AA	IC693MDL645	PLC Describe Input Module	GE Fannie	IC693MDL645		Bluff City Electronics	IC693MDL645
AA	IC693ALG223	PLC Analog Current Input	GE Fannie	IC693ALG223		Bluff City Electronics	IC693ALG223
AA	BC646MRN150	PLC Machine Edition	GE Fannie	BC646MRN150		Bluff City Electronics	BC646MRN150
AA	PMPU	Three Phase Detector	Macromatic	PMPU		Allied Electronics	819-0004
AA	70169-D	Three Phase Detector Socket	Macromatic	70169-D		Allied Electronics	819-7061
AA	GRD84130101	Solid State Relay	Cruzet	GRD84130101		Allied Electronics	793-6006
AA	16370-2	Terminal Block Neutral and Ground	Buss	16370-2		Granger	3XH64
AA	CPDB-2	Terminal Block Cover	Buss	CPDB-2		Granger	3XH81
AA	FXP6000-32V	Power Supply 32vdc x 7	Power One	FXP6000-32V		G2 Sales	
AA	FRH6000S110	Power Supply Rack	Power One	FRH6000S110		G2 Sales	
AA	FRH6000S110	Power Supply Rack	Power One	FRH6000S110		G2 Sales	
AA	FRH6000S110	Power Supply Rack	Power One	FRH6000S110		G2 Sales	
AA	4297070	Filter Door	MSM			Hawkeye	
AA	44755K23	Valve 1" SS Water In				McMaster-Carr	44755K23
AA	44755K23	Valve 1" SS Water Out				McMaster-Carr	44755K23
AA	4509K23	1" Buna-N Sanitary Caskel				McMaster-Carr	4509K23
AA	5048SK511	1" Male Pipe Adapter				McMaster-Carr	5048SK511
AA	4322K711	1" Sanitary Clamp				McMaster-Carr	4322K711
AA	5793K15	1" SS Union Hose				McMaster-Carr	5793K15
AA	IPADU8	1" SS Union Hose	MSM			McMaster-Carr	5793K15
AA	PADU400	PA Drawer	MSM		HH		
AA	PADU400	PA Drawer 1	MSM		GG		
AA	PADU400	PA Drawer 2	MSM		GG		
AA	PADU400	PA Drawer 3	MSM		GG		
AA	PADU400	PA Drawer 4	MSM		GG		
AA	PADU400	PA Drawer 5	MSM		GG		
AA	PADU400	PA Drawer 6	MSM		GG		
AA	PADU400	PA Drawer 7	MSM		GG		
AA	PADU400	PA Drawer 8	MSM		GG		
AA	4297011	Panel - Exciter and Control Power	MSM			Hawkeye	
AA	20030429.03	Panel - PA Power	MSM	20030429.03		Hawkeye	
AA	1102A55	Drawer Slide (Pair)				McMaster-Carr	1102A55
AA	1102A55	Drawer Slide (Pair)				McMaster-Carr	1102A55

DT-4KU Digital Transmitter
Bill of Materials

Prefix	Part Number	Description	Manufacturer	Manufacturer Part Number	Sub-Assembly	Supplier	Supplier Item Number
AA	1102A55	Drawer Slide (Pair)				McMaster-Carr	1102A55
AA	1102A55	Drawer Slide (Pair)				McMaster-Carr	1102A55
AA	1102A55	Drawer Slide (Pair)				McMaster-Carr	1102A55
AA	1102A55	Drawer Slide (Pair)				McMaster-Carr	1102A55
AA	1102A55	Drawer Slide (Pair)				McMaster-Carr	1102A55
AA	1102A55	Drawer Slide (Pair)				McMaster-Carr	1102A55
AA	9507K61	Grommet 1"				McMaster-Carr	1102A55
AA	9507K61	Grommet 1"				McMaster-Carr	1102A55
AA	M0918	Mainfold	MSM		BB	McMaster-Carr	
AA	ZL18x25x1	Filter - Air	Glasfloss	ZL18x25x1		Fab Shop	ZL18x25x1
AA	1568A46	Handle - Filter Door				McMaster-Carr	
AA	11955A67	Hinge - Filter Door				McMaster-Carr	
AA	11955A67	Hinge - Filter Door				McMaster-Carr	
AA	DR52621	Convenience Outlet	Acme Electric	DR52621		Allied Electronics	
AA	DR52621	Convenience Outlet	Acme Electric	DR52621		Allied Electronics	
AA	DR52621	Convenience Outlet	Acme Electric	DR52621		Allied Electronics	
AA	RASB19BK1	Rear Rack Support Bar 19"	Hammond	RASB19BK1		Allied Electronics	806-3924
AA	RASB19BK1	Rear Rack Support Bar 19"	Hammond	RASB19BK1		Allied Electronics	806-3924
AA	20030429.01	Control Panel Rack Mount	MSM	20030429.01		Allied Electronics	
AA	20030429.02	PLC Rack Mount	MSM	20030429.02		Allied Electronics	
AA	BP1902	Blank Panel 2x19	MSM				
AA	BP1905	Blank Panel 5x19	MSM				
AA	BP2406	Blank Panel 6x24	MSM				
AA	BP2402	Blank Panel 2x24	MSM				
AA	BP2404	Blank Panel 4x24	MSM				
AA	BP2404	Blank Panel 4x24	MSM				
AA	BP2404	Blank Panel 4x24	MSM				
AA	RA241909	Rack Adapter 9x24x19	MSM				
AA	RA241909	Rack Adapter 9x24x19	MSM				
AA	SBLHRPS	PS Rear Support Bracket LH	MSM				
AA	SBLHRPS	PS Rear Support Bracket RH	MSM				
AA	1585T8A1	Power Strip 8 Outlet 36"	Hammond	1585T8A1		Allied Electronics	806-1148
AA	1585T8A1	Power Strip 8 Outlet 36"	Hammond	1585T8A1		Allied Electronics	806-1148
AA	4296996	Power Distribution Chassis	MSM				
AA	4296995	PA Power Distribution Chassis	MSM				
AA	4292001	Light Fixture	MSM				
AA	4292001	Light Fixture	MSM				
AA	4292002	Lamp	Sylvania				
AA	4292002	Lamp	Sylvania				
AA	0770P24TPI	Flow / Pressure / Temp Sensor	Proteus Industries	0770P24TPI		Proteus Industries	0770P24TPI
AA	0770P24TPI	Flow / Pressure / Temp Sensor	Proteus Industries	0770P24TPI		Proteus Industries	0770P24TPI
AA	0770P24TPI	Flow / Pressure / Temp Sensor	Proteus Industries	0770P24TPI		Proteus Industries	0770P24TPI
AA		Terminal Block +24vdc x 10					
AA		Terminal Block degn'd x 10					
AA		Terminal Block Audio Interface x 6					
AA		Terminal Block Earth x 3					
AA		Modem - USB	Zoom Telephonics			Staples	

DT-4KU Digital Transmitter
Bill of Materials

Prefix	Part Number	Description	Manufacturer	Manufacturer Part Number	Sub-Assembly	Supplier	Supplier Item Number
BB	9157K12	Nipple 3/8" x 1"				McMaster-Carr	9157K12
BB	9157K12	Nipple 3/8" x 1"				McMaster-Carr	9157K12
BB	9157K55	Nipple 3/8" x 4"				McMaster-Carr	9157K55
BB	9157K55	Nipple 3/8" x 4"				McMaster-Carr	9157K55
BB	9157K55	Nipple 3/8" x 4"				McMaster-Carr	9157K55
BB	9157K55	Nipple 3/8" x 4"				McMaster-Carr	9157K55
BB	9157K55	Nipple 3/8" x 4"				McMaster-Carr	9157K55
BB	9157K55	Nipple 3/8" x 4"				McMaster-Carr	9157K55
BB	9157K55	Nipple 3/8" x 4"				McMaster-Carr	9157K55
CC	CHILLER	Water Chiller 5.0 Ton	ArctiChill	Chiller Sub-Assembly - Prefix CC PACVVPV050584		ArctiChill	
DD		Total Aluminum Parts	MSM	Mask Filter Sub-Assembly - Prefix DD		Hawkeye	
DD		Tuning Pin 1"x8"	MSM			45 Machine and Tool	
DD		Tuning Block 2"x2"	MSM			45 Machine and Tool	
DD		Bolt x 9					
DD		Washer Flat x 9					
DD		Washer Flat x 9					
DD		Washer Lock x 9					
DD		Washer Lock x 9					
DD		Nut x 9					
EE	C01	47 uF, 16V Tantalum Chip Cap	AVX	UHF Amplifier Card Sub-Assembly - Prefix EE TPSD476K016R0150		Allied Electronics	213-1304
EE	C02	47 uF, 16V Tantalum Chip Cap	AVX	TPSD476K016R0150		Allied Electronics	213-1304
EE	C03	1 uF, 50V Ceramic Chip Cap	Kemet	C1825C109K5RAC7U		Allied Electronics	
EE	C04	0.5 uF Chip Capacitor	ATC	100B0R5CW500XT		ATC	
EE	C05	12 uF Chip Capacitor, 0603	ATC	100B120R8500XT		ATC	
EE	C06	47 uF, 16V Tantalum Chip Cap	AVX	TPSD476K016R0150		Allied Electronics	213-1304
EE	C07	47 uF, 16V Tantalum Chip Cap	AVX	TPSD476K016R0150		Allied Electronics	213-1304
EE	C08	1 uF, 50V Ceramic Chip Cap	Kemet	C1825C109K5RAC7U		Allied Electronics	
EE	C09	0.5 uF Chip Capacitor	ATC	100B0R5CW500XT		ATC	
EE	C10	12 uF Chip Capacitor, 0805	ATC	100B120R8500XT		ATC	
EE	C11	47 uF, 16V Tantalum Chip Cap	AVX	TPSD476K016R0150		Allied Electronics	213-1304
EE	C12	0.01 uF, 100V Ceramic Chip Cap	Kemet	C1825C103J1GACTU		Allied Electronics	
EE	C13	0.01 uF, 100V Ceramic Chip Cap	Kemet	C1825C103J1GACTU		Allied Electronics	
EE	C14	0.01 uF, 100V Ceramic Chip Cap	Kemet	C1825C103J1GACTU		Allied Electronics	
EE	C15	0.56 uF, 50V Ceramic Chip Cap	Kemet	KEMC1825C564K5RAC7U		Allied Electronics	
EE	C16	0.56 uF, 50V Ceramic Chip Cap	Kemet	KEMC1825C564K5RAC7U		Allied Electronics	
EE	C17	10 uF, 50V Chip Capacitor	AVX	TPSD10M4035R0300		Allied Electronics	

DT-4KU Digital Transmitter
Bill of Materials

Prefix	Part Number	Description	Manufacturer	Manufacturer Part Number	Sub-Assembly	Supplier	Supplier Item Number
EE	C18	10 uF, .50V Chip Capacitor	AVX	TPSD106M04035R0300		Allied Electronics	
EE	C19	470 uF, .50V Electrolytic Cap	Nichicon	UVR1H471MHA		Allied Electronics	859-2222
EE	C20	470 uF, .50V Electrolytic Cap	Nichicon	UVR1H471MHA		Allied Electronics	859-2222
EE	C21+	FREQUENCY DEPENDANT AS NEEDED PER CHANNEL					
EE	L1	15 nH Inductor, .0603	Coilcraft	0603HC-15NXJBW		Coilcraft	
EE	L2	15 nH Inductor, .0603	Coilcraft	0603HC-15NXJBW		Coilcraft	
EE	L3	15 nH Inductor, .0603	Coilcraft	0603HC-15NXJBW		Coilcraft	
EE	L4	15 nH Inductor, .0603	Coilcraft	0603HC-15NXJBW		Coilcraft	
EE	L5	8 nH Coil Inductor	Coilcraft	A03TJ		Coilcraft	
EE	L6	8 nH Coil Inductor	Coilcraft	A03TJ		Coilcraft	
EE	R3	82 Kohm, 1%	NTE	SR1-1206-382		Allied Electronics	
EE	R2	3.3 Kohm, 1%	NTE	SR1-1206-333		Allied Electronics	
EE	BAL1	UHF Balun Transformer	Anaren	3A325		Allied Electronics	
EE	BAL2	UHF Balun Transformer	Anaren	3A325		Allied Electronics	
EE	VRI	10 Kohm pot	Bourns	3224W-1-103E		Allied Electronics	
EE	IC1	Voltage Regulator, 15V	National Semi	LM78L15ACMX		Allied Electronics	
EE	PCB1	Printed Circuit Board, UHF Amp	Motorola	MRF377		Richardson Electronics	MRF377
EE	HW1	Screw Terminal	Keystone		7699	Allied Electronics	
EE	HW2	Screw Terminal	Keystone		7699	Allied Electronics	
EE	HW3	Screw Terminal	Keystone		7699	Allied Electronics	
EE	HW4	Screw Terminal	Keystone		7699	Allied Electronics	
EE	HW5	Screw Terminal	Keystone		7699	Allied Electronics	
EE	UHFCARD	UHF Amplifier Card	MSM			Allied Electronics	
UHF Power Distribution Card Sub-Assembly - Prefix FF							
FF		Power Dist PC Board 1	MSM				
FF	R1	Resistor, 0.025 Ohm, 1% 5W	Ohmite	15FR025		Allied	296-5108
FF	R2	Resistor, 0.025 Ohm, 1% 5W	Ohmite	15FR025		Allied	296-5108
FF	R3	Resistor, 0.025 Ohm, 1% 5W	Ohmite	15FR025		Allied	296-5108
FF	R4	Resistor, 0.025 Ohm, 1% 5W	Ohmite	15FR025		Allied	296-5108
FF	R5	Resistor, 0.025 Ohm, 1% 5W	Ohmite	15FR025		Allied	296-5108
FF	R6	Resistor, 0.025 Ohm, 1% 5W	Ohmite	15FR025		Allied	296-5108
FF	R7	Resistor, 0.025 Ohm, 1% 5W	Ohmite	15FR025		Allied	296-5108
FF	R8	Resistor, 0.025 Ohm, 1% 5W	Ohmite	15FR025		Allied	296-5108
FF	R9	Resistor, 0.025 Ohm, 1% 5W	Ohmite	15FR025		Allied	296-5108
FF	L1	Inductor 5uH, 15A, 0.007Ohm	J.W. Miller	5601		Allied	
FF	L2	Inductor 5uH, 15A, 0.007Ohm	J.W. Miller	5601		Allied	
FF	L3	Inductor 5uH, 15A, 0.007Ohm	J.W. Miller	5601		Allied	
FF	L4	Inductor 5uH, 15A, 0.007Ohm	J.W. Miller	5601		Allied	
FF	L5	Inductor 5uH, 15A, 0.007Ohm	J.W. Miller	5601		Allied	
FF	L6	Inductor 5uH, 15A, 0.007Ohm	J.W. Miller	5601		Allied	
FF	L7	Inductor 5uH, 15A, 0.007Ohm	J.W. Miller	5601		Allied	
FF	L8	Inductor 5uH, 15A, 0.007Ohm	J.W. Miller	5601		Allied	
FF	L9	Inductor 5uH, 15A, 0.007Ohm	J.W. Miller	5601		Allied	

DT-4KU Digital Transmitter
Bill of Materials

Prefix	Part Number	Description	Manufacturer	Manufacturer Part Number	Sub-Assembly	Supplier	Supplier Item Number
FF	CNI	DB9 Female PC Mount					
FF	F1	Fuse, PC Mount, Solder 1/16A	LittleFuse	251.062.1/16		Allied	846-2000
FF	F2	Fuse, PC Mount, Solder 1/16A	LittleFuse	251.062.1/16		Allied	846-2000
FF	BB1	Copper Buss Bar	MSM				
UHF PA Mobile Sub-Assembly - Prefix: GG							
GG	4297001	PA Drawer Bottom	MSM			Hawkeye	
GG	4297000	PA Drawer Top	MSM			Hawkeye	
GG	UPD48V9	Power Dist Card	MSM		FF		
GG	4298103	Heatsink	Aavid Thermalloy				
GG	USLB148	UHF Splitter Card	MSM			MSM	
GG	UCLB881	UHF Combiner Card	MSM			MSM	
GG	U600A320	Amplifier Card 1	MSM			MSM	
GG	U600A320	Amplifier Card 2	MSM		EE	MSM	
GG	U600A320	Amplifier Card 3	MSM		EE	MSM	
GG	U600A320	Amplifier Card 4	MSM		EE	MSM	
GG	U600A320	Amplifier Card 5	MSM		EE	MSM	
GG	U600A320	Amplifier Card 6	MSM		EE	MSM	
GG	U600A320	Amplifier Card 7	MSM		EE	MSM	
GG	U600A320	Amplifier Card 8	MSM		EE	MSM	
GG	D06D100	Driver Card	Crydom	D06D100		Allied Electronics	
GG	CA85	Solid State Relay 100A	Setco	CA85		Allied Electronics	
GG	LB03KW01	Power Indicator Body	NKK	LB03KW01		Allied Electronics	870-8804
GG	A14177JF	Power Indicator Bezel	NKK	A14177JF		Allied Electronics	870-0031
GG	A1635F	Power Indicator Lamp	NKK	A1635F		Allied Electronics	870-0022
GG	LB03KW01	Interlock Indicator Body	NKK	LB03KW01		Allied Electronics	870-8804
GG	A14177JF	Interlock Indicator Bezel	NKK	A14177JF		Allied Electronics	870-0031
GG	A1635F	Interlock Indicator Lamp	NKK	A1635F		Allied Electronics	870-0022
GG	LB03KW01	Overtemp Indicator Body	NKK	LB03KW01		Allied Electronics	870-8804
GG	A14177JC	Overtemp Indicator Bezel	NKK	A14177JC		Allied Electronics	870-0029
GG	A1635C	Overtemp Indicator Lamp	NKK	A1635C		Allied Electronics	870-0020
GG	LB03KW01	VSWR Indicator Body	NKK	LB03KW01		Allied Electronics	870-8804
GG	A14177JC	VSWR Indicator Bezel	NKK	A14177JC		Allied Electronics	870-0029
GG	A1635C	VSWR Indicator Lamp	NKK	A1635C		Allied Electronics	870-0020
GG	SPT832-0.25	Screw 8-32 x 1/4 Phillips Truss				McMaster-Carr	
GG	SPT832-0.25	Screw 8-32 x 1/4 Phillips Truss				McMaster-Carr	
GG	SPT832-0.25	Screw 8-32 x 1/4 Phillips Truss				McMaster-Carr	
GG	SPT832-0.25	Screw 8-32 x 1/4 Phillips Truss				McMaster-Carr	
GG	SPT832-0.25	Screw 8-32 x 1/4 Phillips Truss				McMaster-Carr	
GG	SPT832-0.25	Screw 8-32 x 1/4 Phillips Truss				McMaster-Carr	
GG	98432865685	Handle 2" C-C Black Alum 1/4" Round	Unicorp	98432865685		McMaster-Carr	
GG	98432865685	Handle 2" C-C Black Alum 1/4" Round	Unicorp	98432865685		McMaster-Carr	
GG	SALL-832-0.5	Screw 8-32 x 1/2 Allen				McMaster-Carr	
GG	SALL-832-0.5	Screw 8-32 x 1/2 Allen				McMaster-Carr	

DT-4KU Digital Transmitter
Bill of Materials

Prefix	Part Number	Description	Manufacturer	Manufacturer Part Number	Sub-Assembly	Supplier	Supplier Item Number
GG	SALL832-0.5	Screw 8-32 x 1/2 Allen				McMaster-Carr	
GG	SALL832-0.5	Screw 8-32 x 1/2 Allen				McMaster-Carr	
GG	SALL832-0.5	Screw 8-32 x 1/2 Allen				McMaster-Carr	
GG	SALL832-0.5	Screw 8-32 x 1/2 Allen				McMaster-Carr	
UHF IPA Module Sub-Assembly - Prefix HH							
HH	4297001	IPA Drawer Bottom	MSM			Hawkeye	
HH	4297000	IPA Drawer Top	MSM			Hawkeye	
HH	UPD48V9	Power Dist Card	MSM		FF		
HH	4298103	Heatsink	MSM				
HH	USI B158	UHF Splitter Card	MSM				
HH	UPA888	UHF IPA RF Distribution Card	MSM				
HH	U600A320	Amplifier Card 1	MSM		EE		
HH	U600A320	Amplifier Card 2	MSM		EE		
HH	U600A320	Amplifier Card 3	MSM		EE		
HH	U600A320	Amplifier Card 4	MSM		EE		
HH	U600A320	Amplifier Card 5	MSM		EE		
HH	U600A320	Amplifier Card 6	MSM		EE		
HH	U600A320	Amplifier Card 7	MSM		EE		
HH	U600A320	Amplifier Card 8	MSM		EE		
HH	U600A320	Driver Card	MSM		EE		
HH	D06D100	Solid State Relay 100A	Crydom	D06D100		Allied Electronics	
HH	CA85	Thermal Switch	Selco	CA85		Allied Electronics	
HH	LB03KW01	Power Indicator Body	NKK	LB03KW01		Allied Electronics	870-8804
HH	A14177JF	Power Indicator Bezel	NKK	A14177JF		Allied Electronics	870-0031
HH	A1635F	Power Indicator Lamp	NKK	A1635F		Allied Electronics	870-0022
HH	LB03KW01	Interlock Indicator Body	NKK	LB03KW01		Allied Electronics	870-8804
HH	A14177JF	Interlock Indicator Bezel	NKK	A14177JF		Allied Electronics	870-0031
HH	A1635F	Interlock Indicator Lamp	NKK	A1635F		Allied Electronics	870-0022
HH	LB03KW01	Overtemp Indicator Body	NKK	LB03KW01		Allied Electronics	870-8804
HH	A14177JC	Overtemp Indicator Bezel	NKK	A14177JC		Allied Electronics	870-0029
HH	A1635C	Overtemp Indicator Lamp	NKK	A1635C		Allied Electronics	870-0020
HH	LB03KW01	VSWR Indicator Body	NKK	LB03KW01		Allied Electronics	870-8804
HH	A14177JC	VSWR Indicator Bezel	NKK	A14177JC		Allied Electronics	870-0029
HH	A1635C	VSWR Indicator Lamp	NKK	A1635C		Allied Electronics	870-0020
HH	SPTR832-0.25	Screw 8-32 x 1/4 Phillips Truss				McMaster-Carr	
HH	SPTR832-0.25	Screw 8-32 x 1/4 Phillips Truss				McMaster-Carr	
HH	SPTR832-0.25	Screw 8-32 x 1/4 Phillips Truss				McMaster-Carr	
HH	SPTR832-0.25	Screw 8-32 x 1/4 Phillips Truss				McMaster-Carr	
HH	SPTR832-0.25	Screw 8-32 x 1/4 Phillips Truss				McMaster-Carr	
HH	SPTR832-0.25	Screw 8-32 x 1/4 Phillips Truss				McMaster-Carr	
HH	98432865685	Handle 2" C-C Black Alum 1/4" Round	Unicorp	98432865685		McMaster-Carr	
HH	98432865685	Handle 2" C-C Black Alum 1/4" Round	Unicorp	98432865685		McMaster-Carr	
HH	SALL832-0.5	Screw 8-32 x 1/2 Allen				McMaster-Carr	
HH	SALL832-0.5	Screw 8-32 x 1/2 Allen				McMaster-Carr	
HH	SALL832-0.5	Screw 8-32 x 1/2 Allen				McMaster-Carr	

DT-4KU Digital Transmitter
Bill of Materials

Prefix	Part Number	Description	Manufacturer	Manufacturer Part Number	Sub-Assembly	Supplier	Supplier Item Number
HH	SALL832-0.5	Screw 8-32 x 1/2 Allen				McMaster-Carr	
HH	SALL832-0.5	Screw 8-32 x 1/2 Allen				McMaster-Carr	
HH	SALL832-0.5	Screw 8-32 x 1/2 Allen				McMaster-Carr	
END OF BILL OF MATERIALS							

APPENDIX B
MOTOROLA PRF-377 (MRF-377)
DATA SHEET

The RF MOSFET Line
RF Power Field-Effect Transistor
N-Channel Enhancement-Mode Lateral MOSFET

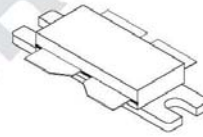
Designed for broadband commercial and industrial applications with frequencies from 470 to 860 MHz. The high gain and broadband performance of this device make it ideal for large-signal, common source amplifier applications in 32 volt transmitter equipment.

- Typical OFDM Performance @ 860 MHz, 32 Volts, $I_{DQ} = 1.8$ A
Output Power – 64 Watts AVG
Power Gain – 16.3 dB
Efficiency – 25%
ACPR – -59 dBc
- Typical Broadband Two-Tone Performance @ $f_1 = 857$ MHz,
 $f_2 = 863$ MHz, 32 Volts, $I_{DQ} = 1.6$ A
Output Power – 250 Watts PEP
Power Gain – 15 dB
Efficiency – 40%
IMD – -31 dBc
- Internally Matched: Input and Output
- Integrated ESD Protection
- Excellent Thermal Stability
- Characterized with Series Equivalent Large-Signal Impedance Parameters

MRF377

Order sample parts by PRF377
ENGINEERING PROTOTYPE

470 – 860 MHz, 250 W, 32 V
LATERAL N-CHANNEL
BROADBAND
RF POWER MOSFET



CASE 375G-04, STYLE 1
(NI-860C3)

MAXIMUM RATINGS (1)

Rating	Symbol	Value	Unit
Drain-Source Voltage	V_{DSS}	65	Vdc
Gate-Source Voltage	V_{GS}	+15, -0.5	Vdc
Drain Current – Continuous	I_D	17	Adc
Total Device Dissipation @ $T_C = 25^\circ\text{C}$ Derate above 25°C	P_D	473 2.70	W W/ $^\circ\text{C}$
Storage Temperature Range	T_{stg}	-65 to +150	$^\circ\text{C}$
Operating Junction Temperature	T_J	200	$^\circ\text{C}$

ESD PROTECTION CHARACTERISTICS

Test Conditions	Class
Human Body Model	? (Minimum)
Machine Model	M? (Minimum)
Charge Device Model	? (Minimum)

THERMAL CHARACTERISTICS

Characteristic	Symbol	Max	Unit
Thermal Resistance, Junction to Case	$R_{\theta JC}$	0.37	$^\circ\text{C/W}$

(1) Each side of device measured separately.

NOTE – **CAUTION** – MOS devices are susceptible to damage from electrostatic charge. Reasonable precautions in handling and packaging MOS devices should be observed.

“ENGINEERING PROTOTYPE” devices are products in development and may not be produced or released. This information is provided as information only to assist Motorola in product development and market assessment.

REV 2

© Motorola, Inc. 2002



ELECTRICAL CHARACTERISTICS ($T_C = 25^\circ\text{C}$ unless otherwise noted)

Characteristic	Symbol	Min	Typ	Max	Unit
----------------	--------	-----	-----	-----	------

OFF CHARACTERISTICS (1)

Drain-Source Breakdown Voltage ($V_{GS} = 0\text{ Vdc}$, $I_D = 10\ \mu\text{A}$)	$V_{(BR)DSS}$	65	—	—	Vdc
Zero Gate Voltage Drain Current ($V_{DS} = 32\text{ Vdc}$, $V_{GS} = 0\text{ Vdc}$)	I_{DSS}	—	—	1	μAdc
Gate-Source Leakage Current ($V_{GS} = 5\text{ Vdc}$, $V_{DS} = 0\text{ Vdc}$)	I_{GSS}	—	—	1	μAdc

ON CHARACTERISTICS (1)

Gate Threshold Voltage ($V_{DS} = 10\text{ Vdc}$, $I_D = 200\ \mu\text{A}$)	$V_{GS(th)}$	—	2.7	—	Vdc
Gate Quiescent Voltage ($V_{DS} = 32\text{ Vdc}$, $I_D = 225\text{ mA}$)	$V_{GS(Q)}$	—	3.4	—	Vdc
Drain-Source On-Voltage ($V_{GS} = 10\text{ Vdc}$, $I_D = 3\text{ A}$)	$V_{DS(on)}$	—	0.27	—	Vdc

DYNAMIC CHARACTERISTICS (1)

Reverse Transfer Capacitance ($V_{DS} = 28\text{ Vdc}$, $V_{GS} = 0$, $f = 1\text{ MHz}$)	C_{rss}	—	2.5	—	pF
--	-----------	---	-----	---	----

FUNCTIONAL CHARACTERISTICS, Two-Tone Testing, Narrowband Fixture (2). 50 ohm system, unless otherwise noted

Common Source Power Gain ($V_{DD} = 32\text{ Vdc}$, $P_{out} = 250\text{ W PEP}$, $I_{DQ} = 2 \times 800\text{ mA}$, $f_1 = 857\text{ MHz}$, $f_2 = 863\text{ MHz}$)	G_{ps}	—	16.5	—	dB
Drain Efficiency ($V_{DD} = 32\text{ Vdc}$, $P_{out} = 250\text{ W PEP}$, $I_{DQ} = 2 \times 800\text{ mA}$, $f_1 = 857\text{ MHz}$, $f_2 = 863\text{ MHz}$)	η	—	37	—	%
Intermodulation Distortion ($V_{DD} = 32\text{ Vdc}$, $P_{out} = 250\text{ W PEP}$, $I_{DQ} = 2 \times 800\text{ mA}$, $f_1 = 857\text{ MHz}$, $f_2 = 863\text{ MHz}$)	IMD	—	-31.5	—	dBc
Output Mismatch Stress ($V_{DD} = 32\text{ Vdc}$, $P_{out} = 250\text{ W CW}$, $I_{DQ} = 2 \times 800\text{ mA}$, $f_1 = 857\text{ MHz}$, $f_2 = 863\text{ MHz}$, $V_{SWR} = 5:1$ at all phase angles of test)	ψ	No Degradation in Output Power			

TYPICAL CHARACTERISTICS, Two-Tone Operation, Broadband Fixture (2). 50 ohm system, unless otherwise noted

Common Source Power Gain ($V_{DD} = 32\text{ Vdc}$, $P_{out} = 250\text{ W PEP}$, $I_{DQ} = 2 \times 800\text{ mA}$, $f_1 = 857\text{ MHz}$, $f_2 = 863\text{ MHz}$)	G_{ps}	—	15	—	dB
Drain Efficiency ($V_{DD} = 32\text{ Vdc}$, $P_{out} = 250\text{ W PEP}$, $I_{DQ} = 2 \times 800\text{ mA}$, $f_1 = 857\text{ MHz}$, $f_2 = 863\text{ MHz}$)	η	—	40	—	%
Intermodulation Distortion ($V_{DD} = 32\text{ Vdc}$, $P_{out} = 250\text{ W PEP}$, $I_{DQ} = 2 \times 800\text{ mA}$, $f_1 = 857\text{ MHz}$, $f_2 = 863\text{ MHz}$)	IMD	—	-31	—	dBc

(1) Each side of device measured separately.

(2) Measured in push-pull configuration.

SCHEMATIC TO COME

Figure 1. 470—860 MHz Broadband Test Circuit Schematic

Table 1. 470—860 MHz Broadband Test Circuit Component Designations and Values

Part	Description	Value, P/N or DWG	Manufacturer
B1, B2	0603 Chipbead, Ferrite, Surface Mount	2506033007Y0	Fair-Rite
C1	18 pF 0603 Chip Capacitor	06033J180GBT	AVX ACCU
C2A, C2B	8.2 pF 0603 Chip Capacitors	06035J8R2BBT	AVX ACCU
C3	15 pF Chip Capacitor, A Case	100A150JP150X	ATC
C4	5.1 pF Chip Capacitor, A Case	100A5R1CW150X	ATC
C5	12 pF Chip Capacitor, A Case	100A120JW150X	ATC
C6	10 pF Chip Capacitor, A Case	100A100JW150X	ATC
C7A, C7B	2.2 μ F, 50 V Ceramic Capacitors	C1825C225J5RAC3810	Kemet
C8A, C8B, C8C, C8D	0.01 μ F, 100 V Ceramic Capacitors	C1825C103J1GAC	Kemet
C9A, C9B, C9C, C9D	47 μ F, 16 V Tantalum Capacitors	593D476X9016D2T	Vishay
C10	0.8–8.0 pF Variable Capacitor	27291SL	Gigatronics
C11, C18	0.6–4.5 pF Variable Capacitors	27271SL	Gigatronics
C12	13 pF Chip Capacitor	180R130JW 500X	ATC
C13	12 pF Chip Capacitor	180R120JW 500X	ATC
C14	10 pF Chip Capacitor	180R100JW 500X	ATC
C15	16 pF Chip Capacitor	180R160JW 500X	ATC
C16A, C16B	10 μ F, 50 V Tantalum Capacitors	522Z-050/100MTRE	Tecate
C17A, C17B	0.56 μ F, 50 V Ceramic Capacitors	C1825C564J5GAC	Kemet
C19	0.4–2.5 pF Variable Capacitor	27283PC	Gigatronics
C20A, C20B	470 μ F, 63 V Electrolytic Capacitors	NACZF471M63V (18x22)	Nippon
L1	10 nH Inductor	0603HC-10NHJBU	Coilcraft
L2A, L2B	8 nH Inductors	A03T-5	Coilcraft
R1A, R1B	22.1 Ω Chip Resistors (0603)		
PCB	MRF377 Printed Circuit Board Assembly with Integrated Balun	RO3003/RO3006	DS Electronics

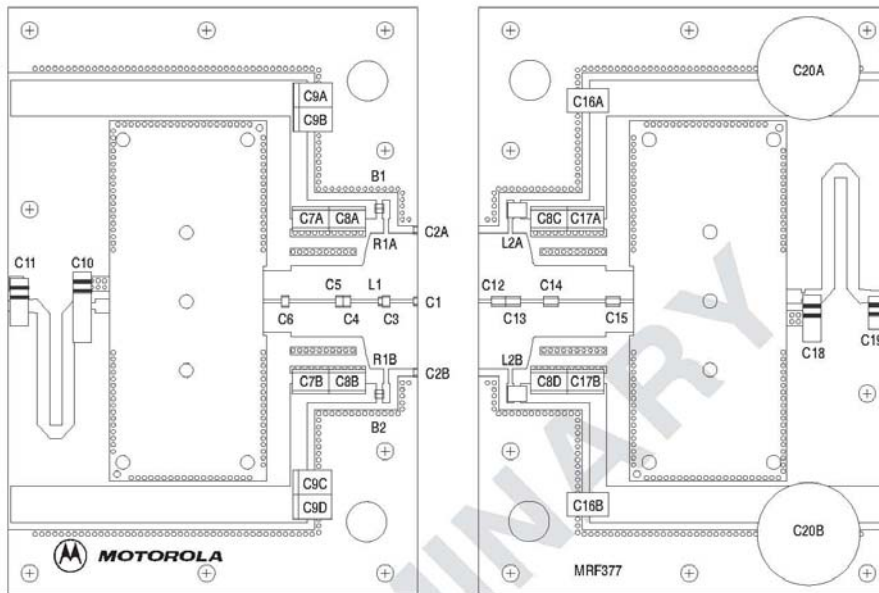


Figure 2. 470-860 MHz Broadband Test Circuit Component Layout

TYPICAL TWO-TONE BROADBAND CHARACTERISTICS

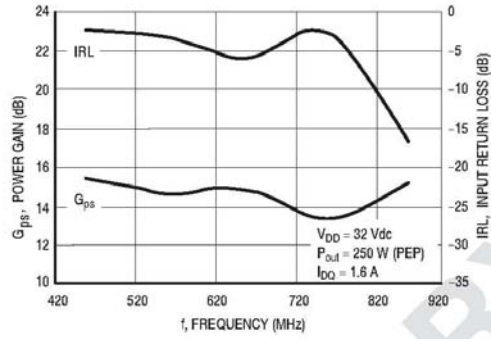


Figure 3. Two-Tone Broadband Gain and IRL versus Frequency

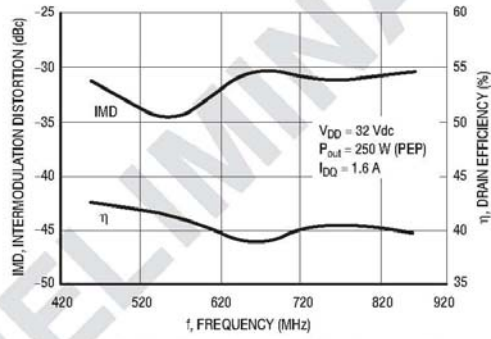
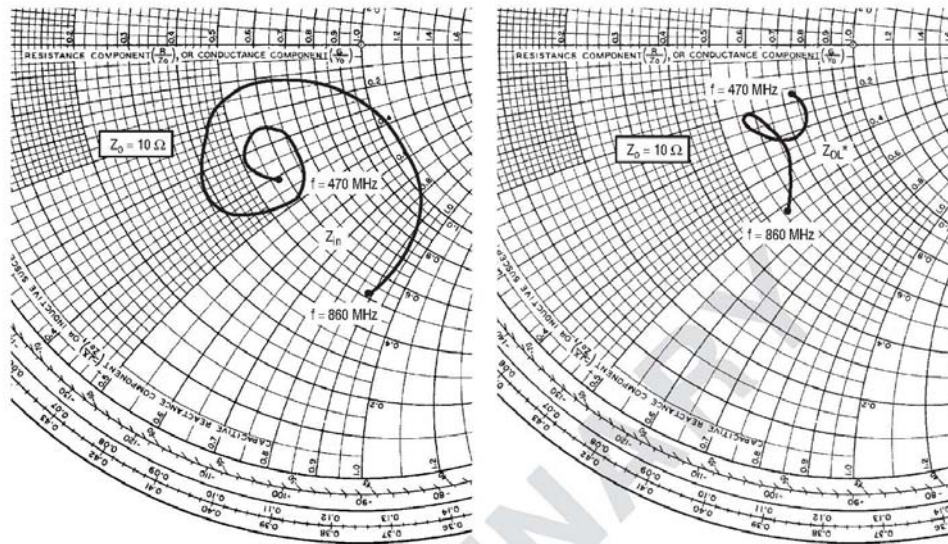


Figure 4. Two-Tone Broadband Efficiency and IMD versus Frequency



$V_{D0} = 32 \text{ V}$, $I_{D0} = 1.6 \text{ A}$, $P_{out} = 250 \text{ W}$

f MHz	Z_{in} Ω	Z_{OL}^* Ω
470	$5.7 - j4.01$	$7.38 - j1.72$
560	$5.91 - j2.5$	$6.18 - j2.63$
660	$5 - j4.77$	$5.81 - j2.12$
760	$4.78 - j1.78$	$6.06 - j2.69$
860	$5.09 - j8.84$	$5.6 - j5.19$

Z_{in} = Complex conjugate of source impedance.

Z_{OL}^* = Complex conjugate of the optimum load impedance at a given output power, voltage, IMD, bias current and frequency.

Note: Z_{in} and Z_{OL}^* were chosen based on tradeoffs between gain, output power, drain efficiency and intermodulation distortion.

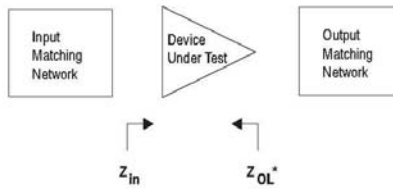
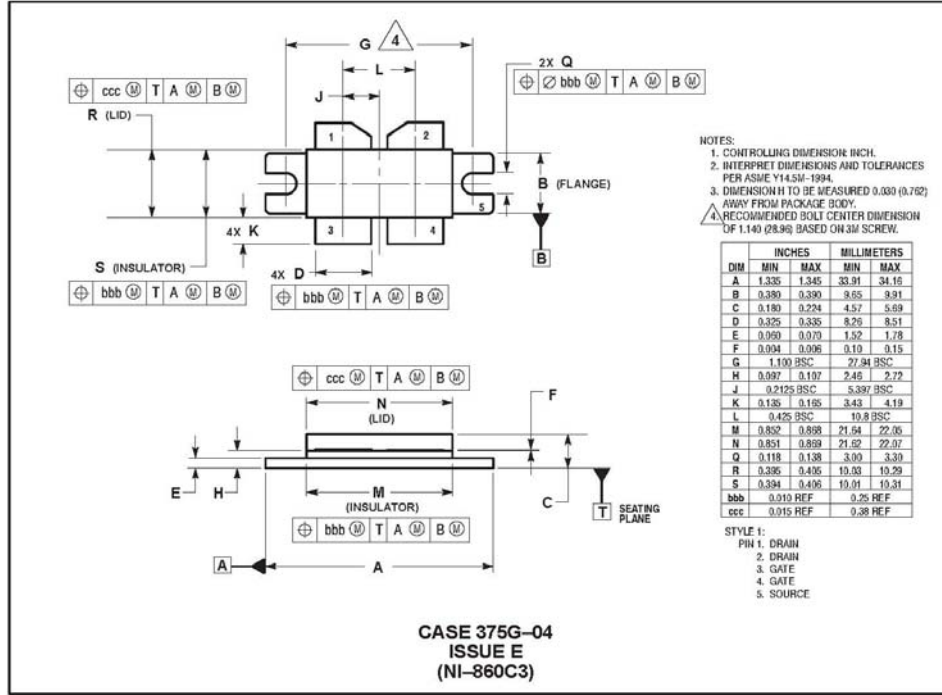


Figure 5. 470–860 MHz Broadband Series Equivalent Input and Output Impedance

PACKAGE DIMENSIONS



Motorola reserves the right to make changes without further notice to any products herein. Motorola makes no warranty, representation or guarantee regarding the suitability of its products for any particular purpose, nor does Motorola assume any liability arising out of the application or use of any product or circuit, and specifically disclaims any and all liability, including without limitation consequential or incidental damages. "Typical" parameters which may be provided in Motorola data sheets and/or specifications can and do vary in different applications and actual performance may vary over time. All operating parameters, including "Typicals" must be validated for each customer application by customer's technical experts. Motorola does not convey any license under its patent rights nor the rights of others. Motorola products are not designed, intended, or authorized for use as components in systems intended for surgical implant into the body, or other applications intended to support or sustain life, or for any other application in which the failure of the Motorola product could create a situation where personal injury or death may occur. Should Buyer purchase or use Motorola products for any such unintended or unauthorized application, Buyer shall indemnify and hold Motorola and its officers, employees, subsidiaries, affiliates, and distributors harmless against all claims, costs, damages, and expenses, and reasonable attorney fees arising out of, directly or indirectly, any claim of personal injury or death associated with such unintended or unauthorized use, even if such claim alleges that Motorola was negligent regarding the design or manufacture of the part. Motorola, Inc. Motorola, Inc. is an Equal Opportunity/Affirmative Action Employer. MOTOROLA and the M logo are registered in the US Patent & Trademark Office. All other product or service names are the property of their respective owners.

© Motorola, Inc. 2002.

How to reach us:

USA/EUROPE/Locations Not Listed: Motorola Literature Distribution; P.O. Box 5405, Denver, Colorado 80217. 1-303-675-2140 or 1-800-441-2447

JAPAN: Motorola Japan Ltd.; SPS, Technical Information Center, 3-20-1, Minami-Azabu, Minato-ku, Tokyo 106-8573 Japan. 81-3-3440-3569

ASIA/PACIFIC: Motorola Semiconductors H.K. Ltd.; Silicon Harbour Centre, 2 Dai King Street, Tai Po Industrial Estate, Tai Po, N.T., Hong Kong. 852-26668334

Technical Information Center: 1-800-521-6274

HOME PAGE: <http://www.motorola.com/semiconductors/>



MRF377 ENGINEERING PROTOTYPE DATA SHEET

APPENDIX C

K-TECH TELECOMMUNICATIONS VSB-ENC-200

DATA SHEET

Internal IF Specifications

Parameter	Specification	Comments
Center Frequency	44.0 MHz	
Pilot Location	Right hand side	
Phase Noise	-105 dBc @ 20 KHz	
SNR	37 dB	Typical
Impedance	50 ohms	
Power	-18 dBm	nominal
Spurs	Better than -50 dBc	
Band Attenuation	-50 dBc @ +/- 3 MHz	
Connector	BNC	
IF Testpoint	-20 dB	coupled

Precorrection

Parameter	Specification	Comments
Linear	+/- 125 nS	typical
Non-Linear	3 dB	typical

External 10 MHz Reference

Parameter	Specification	Comments
10 MHz IN		
Connector	BNC	
Impedance	50 ohms	
Voltage	HCMOS	
Stability	+/- 0.5 ppm	
10 MHz OUT		
Connector	BNC	When not using an external 10 MHz reference the 10 MHz IN and 10 MHz OUT should be connected together
Impedance	50 ohms	

Ordering Information

Part Number	Description
VSB-ENC-200 opt 325 / 200	8-VSB Modulator with Linear and Non-Linear Precorrection, RF Output notes: RF channel must be specified

Additional Information at KTech Web Site: www.ktechtelecom.com

For Pricing and Delivery information: sales@ktechtelecom.com

KTech Telecommunications, Inc.
 DTV Broadcast Products
 21540 Prairie St., Unit B
 Chatsworth, CA 91311
 Phone (818) 773-0333
 Fax (818) 773-8330

APPENDIX D
MINICIRCUITS ZHL-3010
DATA SHEET

AMPLIFIERS

Coaxial

MEDIUM HIGH POWER 50 kHz to 8 GHz



ZVE



ZHL-case T34



ZHL-case S32



ZHL-42

up to 1W (+30 dBm) output

MODEL NO.	FREQ. (MHz)	GAIN (dB)		MAXIMUM POWER (dBm)		DYNAMIC RANGE		VSWR Max.		DC POWER		CASE STYLE	PRICE \$ ea. Qty. (1-9)
		Min.	Flatness Typ. Max.	Output (1 dB Comp.) Min.	Input (no damage)	NF (dB) Typ.	IP3 (dBm) Typ.	In	Out	Volt (V)	Current (A)		
ZVE-8G	2000-8000	30	±2.0	+30*	+20	4	+40	2.1	2.1	12	1.2	BNS33	1095.00
ZHL-1A	2-500	16	±1.0	+28	+20	11	+38	2.1	2.1	2.4	0.60	S32	229.00
ZHL-2	10-1000	16	±1.0	+29	+15	9	+38	2.1	2.1	2.4	0.60	T34	349.00
ZHL-2-B	10-1000	27	±1.0	+29	+5	10	+38	2.1	2.1	2.4	0.60	T34	525.00
ZHL-211	800-950	20	±0.4	+29	+15	8	+38	1.8:1	1.8:1	2.4	0.60	T34	295.00
ZHL-2-12	10-1200	24	±1.0	+29*	+10	4*	+38	2.1	2.1	2.4	0.75	T34	625.00
ZHL-3A	0.4-150	24	±1.0	+29.5	+10	11	+38	2.1	2.1	2.4	0.60	S32	229.00
ZHL-32A	0.05-130	25	±1.0	+29	+10	10	+38	2.1	2.1	2.4	0.60	S32	229.00
ZHL-42	700-4200	30	±1.0*	+28	+5	10	+38	2.5:1	2.5:1	1.6	0.88	U36	895.00
ZHL-4240	700-4200	40	±1.5*	+28	-5	8	+38	2.5:1	2.5:1	1.6	0.90	U36	1395.00
ZHL-42W	10-4200	30	±1.5*	+28**	0	8**	+38	2.5:1	2.5:1	1.6	0.88	U36	1095.00
ZHL-4240W	10-4200	40	±1.5*	+28**	-5	8**	+38	2.5:1	2.5:1	1.6	0.90	U36	1495.00

- * ±28.5 dBm maximum at 1000-1200 MHz
- ** ±27 dBm at 10-700 MHz
- *** Below 100 MHz NF increases to 15 dB at 10 MHz
- ▲ Below 100 MHz NF increases to 16 dB at 10 MHz
- ⚡ Measured at 25°C
- ☆ At +25°C, +30 dBm typ. at 54°C amb.



ZRL

low noise, high IP3

MODEL NO.	FREQ. (MHz)	GAIN (dB)		MAXIMUM POWER (dBm)		DYNAMIC RANGE		VSWR Max.		DC POWER		CASE STYLE	PRICE \$ ea. Qty. (1-9)		
		Typ.	Min. Flatness Typ. Max.	Output (1 dB Comp.) Min.	Input (no damage)	NF (dB) Typ.	IP3 (dBm) Typ.	In	Out	Volt (V)	Current (A)				
ZHL-450-75	5-450	—	9.3	—	±0.7	+26	+20	3.5*	+48	2.5:1	1.6:1	12	0.525	S32	149.95
ZHL-1010-75	50-1000	—	9.5	—	±0.7	+26	+20	3.5	+47	1.5:1	1.5:1	12	0.525	S32	149.95
ZHL-1010	50-1000	—	9.5	—	±0.6	+26	+22	3.5	+46	2.0:1	2.0:1	12	0.525	S32	149.95
ZHL-2010	50-1000	—	20	—	±0.8	+26	+11	3.7	+46	2.0:1	2.0:1	12	0.90	S32	169.95
ZHL-3010	50-1000	—	30	—	±1.0	+26	-3	5.5	+46	2.5:1	2.0:1	12	1.0	S32	179.95
ZRL-400	150-400	30	27	±0.5	±1.0	+23.5	+10	2.5	+42	1.25:1	1.35:1	12	0.575	FJ893	119.95
	175-300	30	28	±0.25	±0.5	+23.5	+10	2.4	+42	1.20:1	1.30:1	12	0.575		
ZRL-700	250-700	29	27	±0.5	±1.0	+23.5	+10	2.0	+46	1.20:1	1.10:1	12	0.575	FJ893	119.95
	300-500	29	27.5	±0.3	±0.7	+23.5	+10	2.0	+46	1.10:1	1.05:1	12	0.575		
ZRL-1150LN	650-1400	32	27	±0.5	±1.0	+22	+10	0.8	+40	1.20:1	1.25:1	12	0.500	FJ893	119.95
	685-1000	29	25	±2.0	—	+22	+10	1.1	+30	1.25:1	1.20:1	12	0.500		
ZRL-1200	650-1200	27.5	25	±0.6	±1.0	+23.5	+10	2.0	+46	1.20:1	1.25:1	12	0.575	FJ893	119.95
	800-950	28	26	±0.4	±0.8	+23.5	+10	2.0	+46	1.20:1	1.20:1	12	0.575		
ZRL-2150	950-2150	25	22.5	±1.1	±1.8	+17.5	+10	1.5	+33	1.30:1	1.20:1	12	0.300	FJ893	119.95
	1500-2000	25	23	±0.9	±1.5	+22	+10	1.3	+34	1.30:1	1.20:1	12	0.300		
ZRL-2300	1400-2300	23.5	21	±0.7	±1.0	+23	+10	2.5	+42	1.20:1	1.16:1	12	0.575	FJ893	119.95
	1650-2150	24	22	±0.5	±0.8	+23	+10	2.3	+42	1.20:1	1.16:1	12	0.575		
ZRL-2400LN	1000-2400	31	28	±1.6	±2.0	+21	+10	1.2	+45	1.50:1	1.35:1	12	0.500	FJ893	139.95
	1000-1400	27	24	±1.8	±2.2	+23	+10	1.0	+44	1.15:1	1.25:1	12	0.500		
	1800-1900	25	23	±1.0	±2.0	+23	+10	1.2	+45	1.20:1	1.30:1	12	0.500		
ZRL-3500	700-1600	26	21	±2.2	±3.2	+21	+10	2.2	+43	1.40:1	1.30:1	12	0.575	FJ893	139.95
	1600-2600	21	16	±2.4	±3.5	+21	+10	2.4	+45	1.40:1	1.35:1	12	0.575		
	2600-3500	16	11	±2.4	±3.3	+21	+10	3.2	+45	1.30:1	1.30:1	12	0.575		

- ♦ NF gradually increases from 3.5 dB at 50 MHz to 10 dB typ. at 10 MHz

APPENDIX E
ARTICHILL REFRIGERATED LIQUID CHILLER
DATA SHEET



"P" Series Chillers 5.0 Nominal Tons

STANDARD SPECIFICATION

Cooling Capacity:	
Btu/H.....	55,700*
Nominal Tons.....	5.0
Fluid Leaving Temperature.....	45° F/7° C
Ambient Temperature.....	95° F/35° C
Reservoir Capacity (Gallons).....	50
Pump Motor HP.....	1.5
Pump Rated Capacity:	
GPM.....	15
@ PSI.....	42
Plumbing Connections In & Out.....	1"
Approx. Shipping Weight (lb.).....	650
Approx. Operating Weight (lb.).....	1000

* Capacity based on water; use of propylene or ethylene based glycols will decrease chiller capacity. Consult factory for capacity at various glycol concentrations and temperatures.

STANDARD FEATURES

Internal Bypass Valve The chiller includes a manual bypass valve which allows the optimum flow through the evaporator regardless of system flow. Reasonable system flow fluctuations do not adversely affect chiller performance.

Water Piping All copper insulated lines to prevent condensation. Valves and unions are provided for ease of component isolation and service.

Evaporator Chiller sizes 1-5 tons use a coaxial type evaporator. Sizes 6 tons and above use a compact shell and tube type evaporator with a removable end for service and maintenance.

Electrical Single point power connection to electrical panel is suitable for outdoor use; control circuit is 24 volts.

Refrigeration Single circuit HCFC R-22 system with all copper refrigeration lines; liquid line sight glass and moisture indicator; filter dryer; and externally equalized thermal expansion valve.

Air Cooled or Water Cooled Condenser Air cooled coil of seamless rifled copper tubing with mechanically bonded aluminum fins; TEAO, all weather fan motor(s). Water cooled condenser uses coaxial type evaporator with convoluted copper inner tube and steel outer jacket.

Indicators Inlet and outlet fluid temperature indicators and pump pressure gauge.

Cabinets Epoxy coated, welded steel frame with a high quality enclosure fabricated from aluminum for maximum durability in all atmospheres and superior white painted finish appearance; easy open access panels to facilitate service access.

Controls

- Control circuit on/off switches for service convenience
- Compressor anti-short cycle time delay
- Water flow safety switch
- Standard unit includes fan cycling control to regulate refrigeration head pressure
- Manual reset high and auto reset low refrigeration pressure safeties
- Water cooled version includes condenser water regulating valve

Compressor 100% suction gas cooled hermetic compressor with crankcase heaters, and internal thermal motor overload protection.

Pump Stainless steel centrifugal

Reservoir Vented, carbon steel construction with a highly durable, powder coated finish to resist corrosion. Tank includes a liquid level sight glass with isolation valves, manual tank fill, and a low level cut-out to prevent pump operation in low level conditions. Tank is insulated with 1/2" closed cell insulation.

AVAILABLE OPTIONS

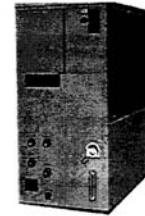
- Automatic City Water Switchover
- Sealed system with stainless steel reservoir
- Special cabinets materials and sizes
- Castors for portability
- Alternate voltages available
- Configurations for other power requirements
- Automatic emergency alarms with contacts for remote interface
- Redundant systems with automatic controls
- California seismic code calculations
- Hot gas bypass for capacity control
- Hot gas head pressure control for -20° F or -40° F ambient

200 Park Avenue • P.O. Box 717 • Newberry, SC 29108 • Phone: 803-321-1891 • Fax: 803-321-1898
Sales Toll Free: 800-849-7778 • E-Mail: chiller@arctichill.com • Visit Us At: www.arctichill.com

P-4006E 2/01

Air Cooled, Vertical Cabinet, Indoor or Outdoor Package Chiller

PACVPV0050S3 208/230/60/3
 PACVPV0050S4 460/60/3



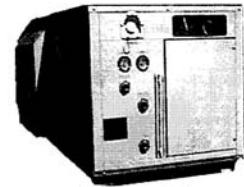
60"L x 32"W x 78" H

Electrical Data

Voltage	Code	Compressor		Pump		Fans (2)		Total RLA	Min Ckt	Max Fuse
		LRA	RLA	HP	RLA	HP	RLA			
208/230/60/3	673	118	16.5	1.5	5.6	1/2	7.0	31.1	36	50
460/60/3	673	71	10.0	1.5	2.8	1/2	3.8	18.6	22	30

Air Cooled, Horizontal Cabinet, Outdoor Package Chiller

PACHPH0050S3 208/230/60/3
 PACHPH0050S4 460/60/3



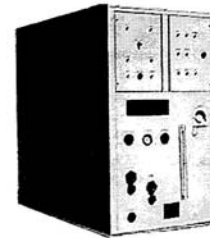
88"L x 40"W x 40"H

Electrical Data

Voltage	Code	Compressor		Pump		Fans (2)		Total RLA	Min Ckt	Max Fuse
		LRA	RLA	HP	RLA	HP	RLA			
208/230/60/3	673	118	16.5	1.5	5.6	1/2	7.0	31.1	36	50
460/60/3	673	71	10.0	1.5	2.8	1/2	3.8	18.6	22	30

Air Cooled, Indoor Chiller, with Outdoor Remote Condenser

PACRPV0050S3 208/230/60/3
 PACRPV0050S4 460/60/3



Chiller: *48"L x 32"W x 61"H
 **54"L x 32"W x 61"H
 Approx. Operating Wt.: 875 lbs.

Condenser: 52"L x 28"W x 36"H
 Approx. Operating Wt.: 125 lbs.

Indoor Chiller Electrical Data

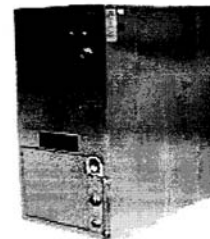
Voltage	Code	Compressor		Pump		Total RLA	Min Ckt	Max Fuse
		LRA	RLA	HP	RLA			
208/230/60/3	673	118	16.5	1.5	5.6	24.1	29	40
460/60/3	673	71	10.0	1.5	2.8	14.8	18	25

Remote Condenser Electrical Data

Voltage	Fans (2)		Total RLA	Min Ckt	Max Fuse
	HP	RLA			
208/230/60/1	1/2	7.0	7.0	10	15
460/60/1	1/2	3.8	3.8	5	10

Water Cooled, Indoor Package Chiller

PWCCPV0050S3 208/230/60/3
 PWCCPV0050S4 460/60/3



*40"L x 32"W x 62"H

Electrical Data

Voltage	Code	Compressor		Pump		Total RLA	Min Ckt	Max Fuse
		LRA	RLA	HP	RLA			
208/230/60/3	673	118	16.5	1.5	5.6	24.1	29	40
460/60/3	673	71	10.0	1.5	2.8	14.8	18	25

* Dimensions are outside dimensions of cabinet. See cabinet submittal drawings for extensions from cabinet such as mounting supports, louvers, etc. NOTE: Due to AretiChill's ongoing commitment to quality, specifications, ratings, sizes, and dimensions are subject to change without notice and without incurring liability.
 **With dual lead/lag pumps.

APPENDIX F
ANAREN 3A325 BALUN
DATA SHEET

Anaren

Xinger®



Model 3A325

Balun Transformers

Surface Mount Components

Description

The 3A325 is a low profile balanced to unbalanced transformer in an easy to use surface mount package covering TV broadcast applications. The 3A325 has an unbalanced port impedance of 50Ω and balanced port impedances of 25Ω to ground with 50Ω balance between outputs. This eases the matching of the push-pull amplifier's power transistors which have low impedance levels. The output ports have equal amplitude (-3dB) with 180° phase differential.

Features

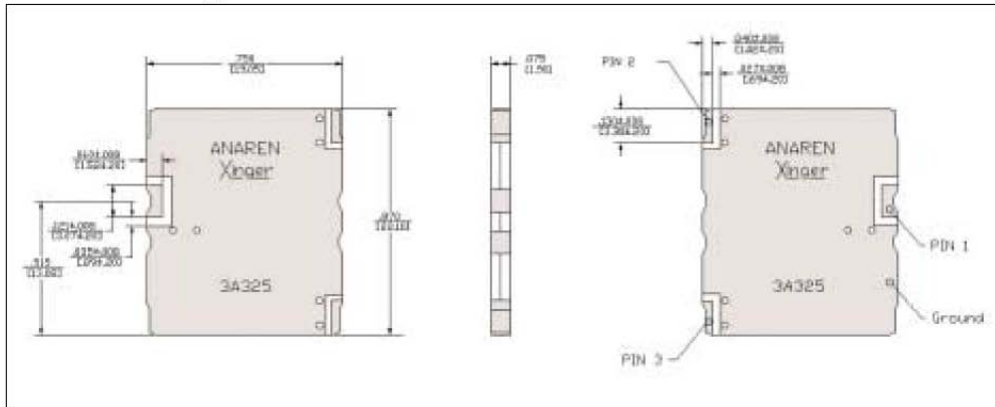
- 470 - 860 MHz
- 25Ω Balanced Port Impedance
- Low Insertion Loss
- High Power
- Input to Output DC Isolation
- Surface Mountable
- Tape And Reel
- Convenient Package

Electrical Specifications

Frequency MHz	Port Impedance Unbalanced	Port Impedance Balanced to Ground
470 - 860	50Ω	25Ω
Return Loss dB Min	Amplitude Bal. dB (p-p)	Phase Balance degrees
10	0.40	180 ± 5.0
Insertion Loss dB Max	θ _{JC} °C/diss. Watt	Power Watts Ave/CW
0.35	4.4	275

Specifications subject to change without notice.

Outline Drawing



Available on Tape and Reel for Pick and Place Manufacturing.

Sales Desk USA: Voice: (800) 544-2414 Fax: (315) 432-9121
 Sales Desk Europe: Voice: (+44) 23 92 232392 Fax: (+44) 23 92 251369

Anaren
 What'll we think of next?™

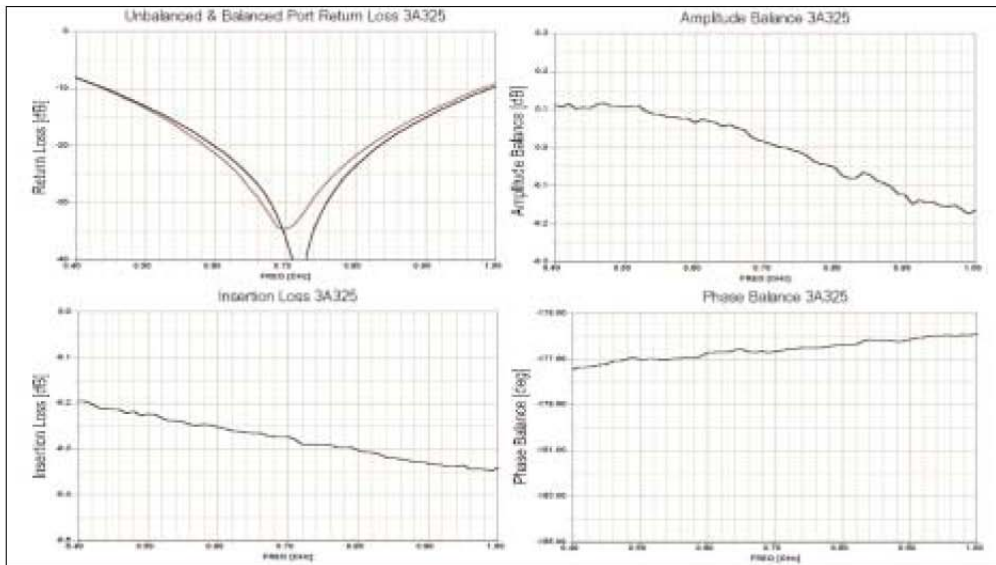
22.11

Model 3A325

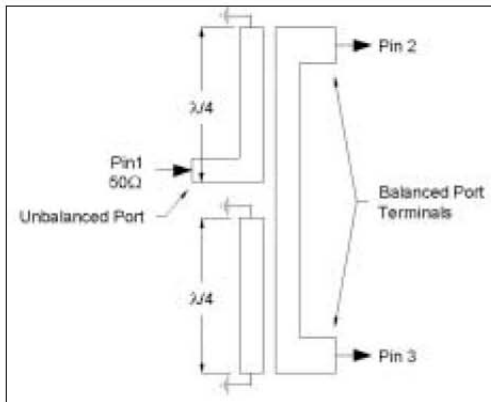
Anaren

Xinger®

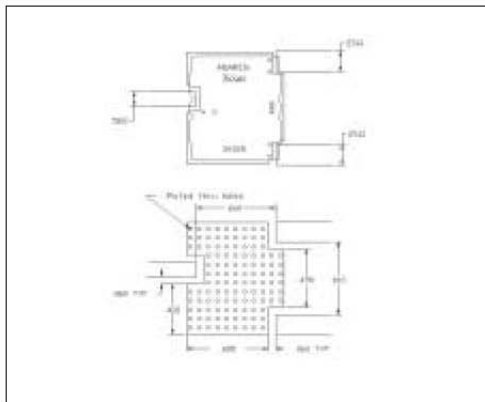
Typical Performance



Pin Configuration



Mounting Footprint



Available on Tape and Reel for Pick and Place Manufacturing.



2.2.12

Anaren
What'll we think of next?™

Sales Desk USA: Voice: (800) 544-2414 Fax: (315) 432-9121
Sales Desk Europe: Voice: (+44) 23 92 232392 Fax: (+44) 23 92 251369